ABSTRACT

SMITH, SCOTT ALAN. Inductively Coupled Plasma Etching of III-N Semiconductors. (Under the direction of Robert F. Davis)

The principal focus of this research was the employment of an in-house designed and constructed inductively coupled plasma (ICP) system for integrated studies pertaining to the etching rates and etching selectivity among AlN, GaN, and $Al_xGa_{1-x}N$. An (ICP) system was chosen because of its high plasma density and low cost relative to other high-density plasma etching systems. The etch rates were studied as a function of ICP power, pressure, DC bias, and gas composition. The use of a mixture of 2 sccm BCl_3 and 18 sccm Cl_2 resulted in a maximum etch rate of 2.2 μm/min for GaN as well as nearly vertical sidewalls with proper masking. A selectivity value, i.e. the ratio of the etch rates between two materials, as high as 48 was achieved between GaN and AlN with the addition of low concentrations of O_2 to a Cl_2/Ar chemistry. The use of another selectivity technique, namely, low DC biases resulted in a maximum selectivity of 38. The mechanisms responsible for the GaN etching were determined by monitoring both the ion density with a Langmuir probe and the relative Cl radical density with an optical emission spectrometer. Increasing the ion density resulted in a non-linear increase in the etch rates; increasing the Cl radical density had a minimal affect on etch rate.

INDUCTIVELY COUPLED PLASMA ETCHING OF III-N SEMICONDUCTORS

by

Scott Alan Smith

A dissertation submitted to the Graduate Faculty of
North Carolina State University
in partial fulfillment of the
requirements for the Degree of
Doctor of Philosophy

MATERIALS SCIENCE AND ENGINEERING

Raleigh

1999

APPROVED BY:

_____ _____

_____ _____
Chair of Advisory Committee

BIOGRAPHY

Scott Alan Smith was born on February 26, 1969 in Springfield, Massachusetts to Mr. and Mrs. Alan J. Smith. Raised in the Springfield Massachusetts area, he graduated from West Springfield High School in 1987. Immediately after graduation he worked as an electrician for three years before beginning college. In 1995 he graduated from Western New England College with a Bachelor of Science in Electrical Engineering. Prior to beginning his senior year at Western New England College he wed the former Lynn Marie Gwara in York, South Carolina. He has since pursued a Doctor of Philosophy degree from North Carolina State University under the direction of Dr. Robert F. Davis.

ACKNOWLEDGEMENTS

I would like to express my gratitude to all of the people who helped me in my efforts to receive a doctorate degree from North Carolina State University.

First I would like to thank my advisor, Dr. Robert Davis, for his encouragement and guidance throughout this process. His giving me the freedom to conduct my research as I liked helped me to grow as a researcher and as a person. I would also like to thank Dr. Robert Nemanich, Dr. Zlatko Sitar, and Dr. Griff Bilbro for their contributions as members of my advisory committee. Special thanks also go to Mrs. Jan Jackson for her assistance throughout the last four years.

I am very grateful to Dr. Colin Wolden for all of his valuable help and insight with my project. The help received from Dr. R. Claude Woods from the University of Wisconsin on the design of the system is very much appreciated.

I would like to thank the Air Force for acceptance into the PALACE Knight program. I believe this program is one of the best opportunities for students who aspire to work in a research environment. From the PALACE Knight office I would like to thank Ms. Betty Fergusen. From my group at Wright Patterson AFB I would like to thank Dr. William Lampert and Maj. Paul Hesse for all of their help and support over the past 2 years.

I would like to thank all of the good friends I have made in our group during my time here. In particular I would like to thank Robert James, Andrew Banks, Kieran Tracy, Pradeep Rajagopal, Scott Roberson, Michael Bremser, and Kenneth Järrendahl.

I wish to thanks my parents, Mr. and Mrs. Alan J. Smith, for all of their support. Finally, I would like to thank my wife, Lynn, whose love, patience, and understanding made this whole process much easier.

TABLE OF CONTENTS

LIST OF TABLES

LIST OF FIGURES

ETCHING OVERVIEW

LITERATURE REVIEW

SYSTEM DESCRIPTION

PAPER I

PAPER II

PAPER III

PAPER IV

PAPER V

PAPER VI

APPENDIX 2

CHAPTER 1 INTRODUCTION

Gallium nitride (GaN) is a wide bandgap semiconductor with potential and realized commercial applications in the areas of high-power and high-frequency microelectronic devices operable at room temperature and moderate (to 400 ºC) temperatures, and short wavelength optoelectronic devices [1-4]. Alloying GaN with InN and AlN provides the potential for tuning the bandgap between 1.9 and 6.2 eV. This is necessary for producing devices such as $Al_xGa_{1-x}N$ based HEMT structures or optoelectronic devices with light output between orange and ultraviolet.

Etching removes material from surfaces; it is a critical step in the fabrication of all microelectronic devices. Characteristics of the etching process that are typically investigated include etch rate, anisotropy (directionality of etch), selectivity (etch rate of one material compared to another), and damage (electronic and physical). Anisotropy is generally determined by viewing the material with a scanning electron microscope (SEM), and selectivity is determined by examining the individual etch rates of the two materials either visually in a microscope or via a profilometer. Electronic damage can be characterized by measuring the change in conductivity after etching or applying Schottky contacts and measuring the change in the reverse leakage current. Physical damage is usually determined by measuring the change in the roughness of the surface after etching.

Wet and dry processes have been employed to etch the III-N compounds. Wet etching of these materials has, to date, resulted in slow, isotropic etch characteristics which are undesirable in semiconductor processing [5]. The slow etch rates can be attributed to the chemical stability of these materials, and the lack of directionality is a characteristic of the particular wet etching process employed. Since wet etching is purely a chemical process, the amount of damage imparted to the material is typically very low. This characteristic is very desirable for semiconductor processing; however, disposal of the etchant chemistries has become a major problem in many cases.

Plasma etching has proven to be the preferred method for etching the III-N materials [6-8]. The chemical reactivity of a plasma combined with the damage inducing ion bombardment results in etch rates considerably higher than can be attained using wet

etching. In plasma etching, the etch profiles are typically highly directional, i.e., the process is anisotropic. Anisotropy is defined as the vertical etch rate divided by the horizontal etch rate. This can be very important when the critical dimensions of the devices become very small (<1μm), or when etching a mirror face for a cavity laser.

Selectivity is the ratio of the etch rates of two different materials. It can also be accomplished using plasma etching. Patterning a sample requires minimal erosion of the mask and considerable erosion (etching) of the sample; thus, high selectivity between the two materials is required. Selectivity may also be necessary between two different materials in a multilayer device, and in some devices, to stop the etching as soon as a particular layer is removed. Without selectivity, this may be difficult using only etch rate information due to variations in the thickness and/or etch rate in different sections of the sample.

Electrical damage is an undesirable characteristic of plasma etching. The inelastic impingement of ions onto a surface creates damage in the form of roughness, dangling bonds, and induced defects. The degree of damage is primarily caused by the use of a DC bias on the sample. In a high-density plasma such as that produced by either an inductively coupled plasma (ICP) or an electron cyclotron resonance (ECR) plasma system this damage can be minimized with the use of a separately controlled DC bias. In a high-density system, a low DC bias can be used while still achieving acceptable etch rates.

The four primary types of plasma etching that have been employed are reactive ion etching (RIE), magnetron ion etching (MIE), ECR, and ICP. The last three are considered high-density plasmas while RIE is low density. There is approximately one order of magnitude difference in ion density between the high and low-density sources. Both the RIE and the MIE employ capacitively coupled plasmas with the difference being the magnetic confinement of the plasma in the latter. Magnetic confinement increases the plasma density by confining the electrons and ions to a smaller volume. Neither of these techniques has a DC bias that is separately controlled, i.e., it is dependent upon the applied plasma power. The DC bias refers to the time-averaged cathode potential to which the ions respond. The ions are too massive to respond to the

high frequencies of the RF source. The ECR and ICP are both high-density sources that are capable of having a separately controlled DC bias, which means the plasma density and the energy of the ions striking the surface of the sample can be independently controlled.

Diagnostic tools including optical emission spectrometers (OES) and Langmuir probes are vital to the determination of the mechanisms that are responsible for etching. The OES identifies plasma species by their optical emission. This photonic emission is caused by the release of energy resulting from the transition of an excited electron to a lower energy state or by the recombination of an electron and ion. Use of this technique allows one to deduce relative concentrations of certain species in the plasma by monitoring a specific emission line from a rare gas such as xenon and one from the species of interest. The primary functions of the Langmuir probe are to determine electron densities, ion densities, plasma potentials, and electron energy distribution functions. Since plasmas are very complex in nature, these diagnostic tools are crucial to the determination of the underlying chemical mechanisms. Varying the etching parameters including power, pressure, DC bias, and gas concentrations while monitoring the ion density and relative reactive species provides a good indication of which properties of the plasma are responsible for the etching.

The OES is an excellent tool for plasma analysis. It can also be used for more practical purposes. Diagnostic endpoint detection is necessary when selectivity is low between two materials or when the layer having the surface on which it is desired to stop the etching is so thin that etch rate data will not suffice. By monitoring an OES line that represents a specific material, it is possible to watch the deflection of this signal to determine when a specific layer has been removed or has begun to etch.

The principal objectives of the present research were (i) the determination and optimization of the efficiencies of two different plasma chemistries, namely, Cl_2/Ar and BCl_3/Cl_2 for the etching of GaN, (ii) the achievement of etching selectivity between GaN and AlN, and (iii) the study of the operative plasma chemistries. Chapter 3 is a brief overview of the practical aspects of etching, the types of plasma sources used for the III-Nitrides, and some proposed etching mechanisms. Chapter 4 outlines the design and

construction of the ICP etching system. Chapter 5 discusses both the characterization of the etch rate using Cl_2 and Ar as the source gases and the selectivity between GaN, AlN, and $Al_xGa_{1-x}N$. Chapter 6 describes a method of attaining selectivity between GaN and AlN by adding O_2 to the plasma chemistry. Chapter 7 discusses the optimization of GaN etching in a Cl_2/Ar plasma employing design of experiments (DOE) software. Chapter 8 covers the same types of experiments discussed in chapter 7 except that Cl_2/BCl_3 are the source gases. Chapter 9 concerns the diagnostics of the Cl_2/Ar and Cl_2/BCl_3 plasma chemistries. Studies were performed using a Langmuir probe and an optical emission spectrometer. The OES was also used for endpoint detection, as discussed in chapter 10. All etch rates quoted herein imply an experimental variability of $\pm$ 5%.

1. R. F. Davis, Proc. IEEE **79**, 702 (1991).

2. H. Morkoç, G. B. Gao, M. E. Lin, B. Suerdlov, and M. Burns, J. Appl. Phys. **76**, 1363 (1994).

3. H. Morkoç, Mat. Sci. & Engr. B **43**, 137 (1997).

4. S. N. Mohammad and H. Morkoç, Progress in Quantum Electronics **20**, 361 (1996).

5. S. J. Pearton, C. R. Abernathy, F. Ren, J. R. Lothian, P. W. Wisk, and A. Katz, J. Vac. Sci. Technol. A **11**, 1772 (1993).

6. H. P. Gillis, D. A. Choutov, and K. P. Martin, J. Minerals, Metals & Mat **48**, 50 (1996).

7. R. J. Shul, G. A. Vawter, C. G. Willison, M. M. Bridges, J. W. Lee, S. J. Pearton, and C. R. Abernathy, Solid-State Electr. **42**, 2259 (1998).

8. C. R. Eddy, MRS Internet J. Nitride Semicond. Res. **4s1**, G10.5 (1999).

CHAPTER 2 ETCHING OVERVIEW

Plasma etching is the primary method for removal of material for many semiconductor material systems. There are many characteristics of plasma etching that must be considered when designing an etching system, or performing the experiments. Discussed below are some of these characteristics of plasma etching for practical applications, the different plasma sources that are employed, and some of the mechanisms that are thought to be responsible for the etching.

Three important characteristics of plasma etching from a practical viewpoint are selectivity, anisotropy, and etch rate. Selectivity is the ratio of the etch rates of two dissimilar materials. High selectivities are desirable in device processing when the etching must stop at or immediately after the interface between the two materials. An example of this would be to etch through the GaN capping layer and stop at the $Al_xGa_{1-x}N$ active layer in a III-N based high electron mobility transistor. In many cases selectivity between two materials is determined by the plasma chemistry employed.

Anisotropic etching implies the unidirectional removal of material. As the technology advances, and the critical dimensions of devices decreases, the need for vertical sidewalls increases. To achieve the 0.2μm wide by 4 μm deep trench illustrated in Figure 1, the process must be highly anisotropic. The degree of slope in the sidewalls is a function both of the anisotropy of the system and slope in the chemically etched mask. If the mask has any slope in the sidewall, and sufficient erosion of the mask occurs, the sloped sidewall will translate into the etched material, as shown in Figure 2 for GaN etched using a photoresist mask. In most cases this sloped sidewall would be unacceptable for device applications.

The plasma source used in the etching system can make a significant difference in the etch rates, anisotropy, selectivity, and damage. There are three primary plasma sources used in plasma etching, namely, capacitively coupled, electron cyclotron resonance (ECR), and inductively coupled plasma (ICP). The capacitively coupled source generates a low density of plasma electrons; the ECR and ICP sources generate a high density of plasma electrons, which is typically 1-2 orders of magnitude higher than the capacitively

coupled source. The typical ECR and ICP etching systems utilize a capacitively coupled source in addition to the ECR or ICP source. Figure 3 shows a schematic of an ICP system that employs a capacitively coupled source. The high-density source is used to generate the bulk plasma, while the capacitively coupled source is used to create the DC bias on the sample holder so that the ions are accelerated to the sample surface. Figure 4 is from an experiment performed by Coburn and Winters [1] that shows the necessity of the ion bombardment in the etching process. Using only the reactive gas or only the ion beam resulted in slow etch rates. However, when these were combined, the etch rate was significantly enhanced. Possible reasons for this phenomenon are discussed on the next page.

Capacitively coupled sources are typically driven by 13.56 MHz RF sources, as illustrated in Figure 5. The RF power is connected to an insulated plate on which the sample rests. The ground side is connected to the chamber, and sometimes, to a plate parallel to the sample. Figure 5 shows the second parallel plate, however, frequently the chamber is used as the ground. The pressure range in this type of plasma is typically 10-100 mTorr. The plasma is sustained by the oscillatory response of the mobile plasma electrons within the cloud of positive ions to the electric field generated by the RF source. The ions are continually generated through collisions between the neutral atoms and the oscillating electrons. The ions are too massive to respond to the RF field; thus, they respond only to the time-averaged electric fields that are directed toward the electrode. Strong time-averaged electric fields exist in the sheath region, i.e., the thin region above the powered electrode that contains primarily ions. Thus, ion bombardment of the electrode and sample occurs.

Inductively coupled sources, unlike capacitive sources, do not have an electrode in the plasma. The power is coupled through a dielectric window. This type of coupling is a much more efficient method of transferring power to the electrons and, consequently of increasing the plasma density. The ICP source consists of a 13.56 MHz RF source connected to a copper coil. The coil configuration can either be cylindrical or planar, depending on the geometry of the system. The copper coil basically acts as an inductor. A planar ICP configuration can be seen in Figure 6. Multipole permanent magnets can be

placed around the outside of the chamber to increase plasma density through plasma confinement and to also increase plasma uniformity across the diameter of the sample [2]. Application of the RF power to the coil creates a time varying magnetic field within the chamber. Associated with the magnetic fields is a time-varying electric field. The electrons oscillate with this electric field, collide with neutral atoms and forming the excited species and ions. The pressure regime for this process is typically between 1 and 50 mTorr.

Electron cyclotron resonance discharges are generally driven by a 2.45 GHz microwave source. A typical ECR configuration is illustrated schematically in Figure 7. The pressure regime for this type of discharge is typically between 1 and 10 mTorr. Unlike capacitive and inductive discharges, ECR discharges require the use of electromagnets to form an axially varying DC magnetic field in the chamber. The plasma is created when the microwave power, which is axially injected through a dielectric window, propagates a right hand circularly polarized wave along the magnetic field lines to a resonance zone where the wave energy is absorbed by the electrons. These electrons, in turn, collide with the neutral atoms to form ions and excited species in a manner similar to that in the ICP and capacitive sources.

It is widely accepted that both ions and radicals play equally important roles in ion assisted plasma etching. The radicals are necessary to form the volatile species; however, the exact role of the ions has not been resolved. Several explanations have been put forth regarding this issue [3]. There are three main steps that occur in the etching process: (1) diffusion of reactive species to and chemisorption from the sample surface, (2) formation of volatile product molecules and, (3) desorption of these molecules. The role(s) of the ions in these process steps is not known. The ions may bombard the surface creating damage and increasing the reaction probability of the arriving reactive species. As such, the second step noted above would become the rate-limiting factor. The incident ions may assist in the desorption of the reaction product via of sputtering. This assumes step three is the rate-limiting factor. The third possible mechanism, proposed by Coburn [3], begins with the chemisorption of the reactive species onto the surface. The formation

and desorption of the volatile reaction products occurs subsequently upon arrival of the impinging ion. This mechanism also implies that step two is the rate limiting step.

1. J. W. Coburn, H. F. Winters, J. Vac. Sci. Technol. A **16**, 391 (1979).

2. M. A. Lieberman and A. J. Lichtenberg, *Principals of Plasma Discharges and Materials Processing*, John Wiley and Sons, Inc., New York (1994).

3. J. W. Coburn, J. Vac. Sci. Technol. A **12**, 1417 (1994).

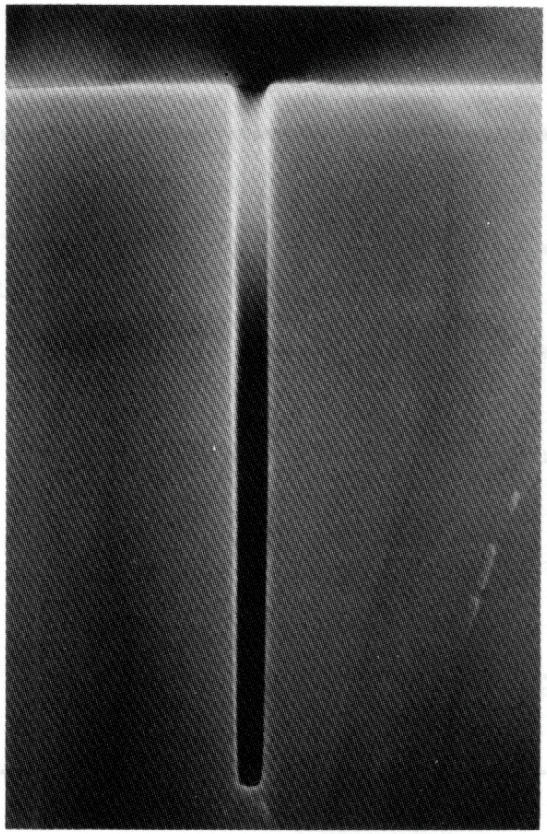

Figure 1. Scanning electron micrograph of an example of highly anisotropic plasma etching in silicon. The trench is 0.2 μm wide by 4 μm deep. (From Ref. 2)

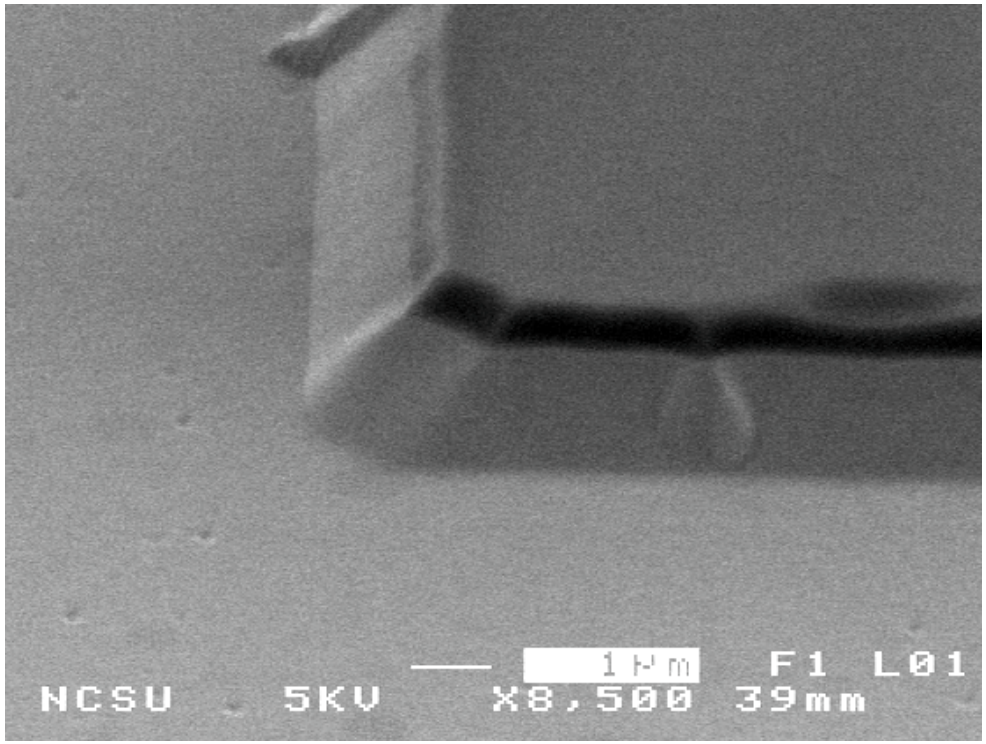

Figure 2. Scanning electron micrograph of GaN etched with an imperfect photoresist mask in an ICP etching system. The dark layer on the top is the photoresist.

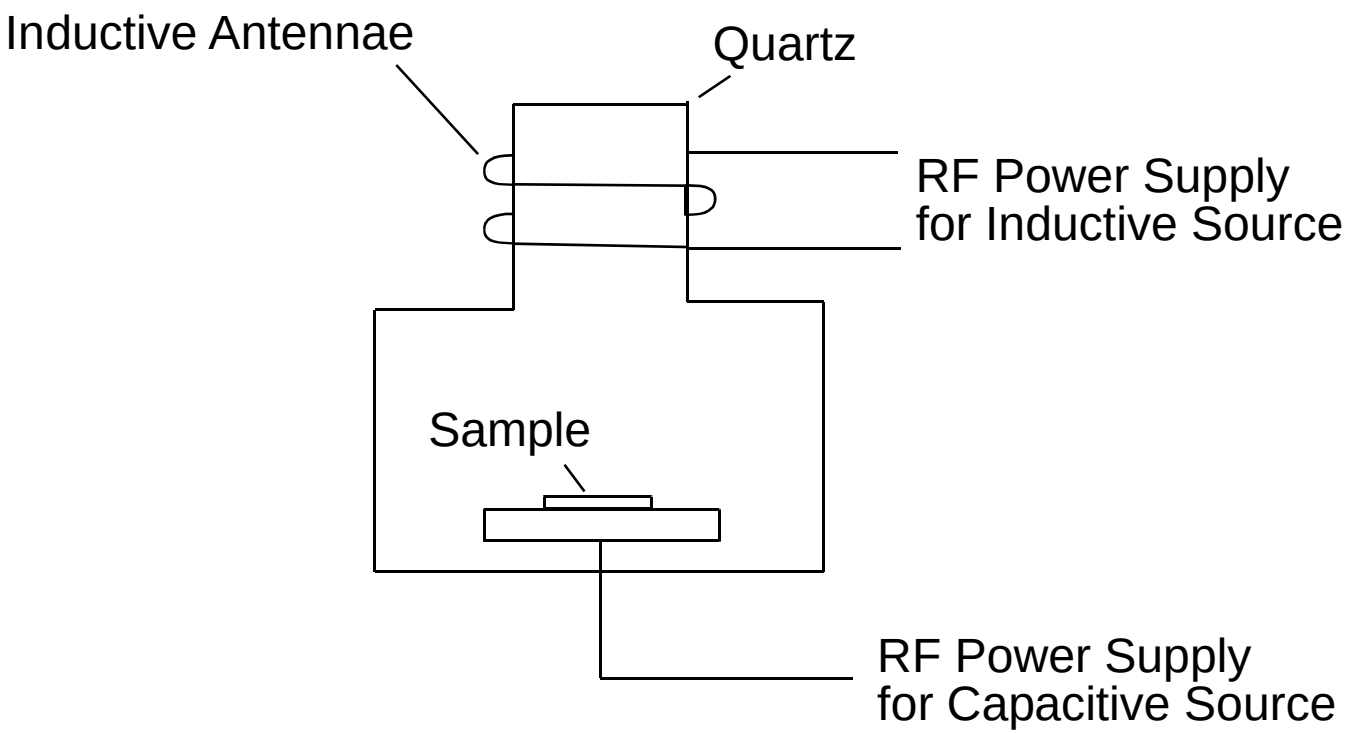

Figure 3. Schematic of an inductively coupled plasma system showing the capacitively coupled source used to induce a DC bias for ion bombardment.

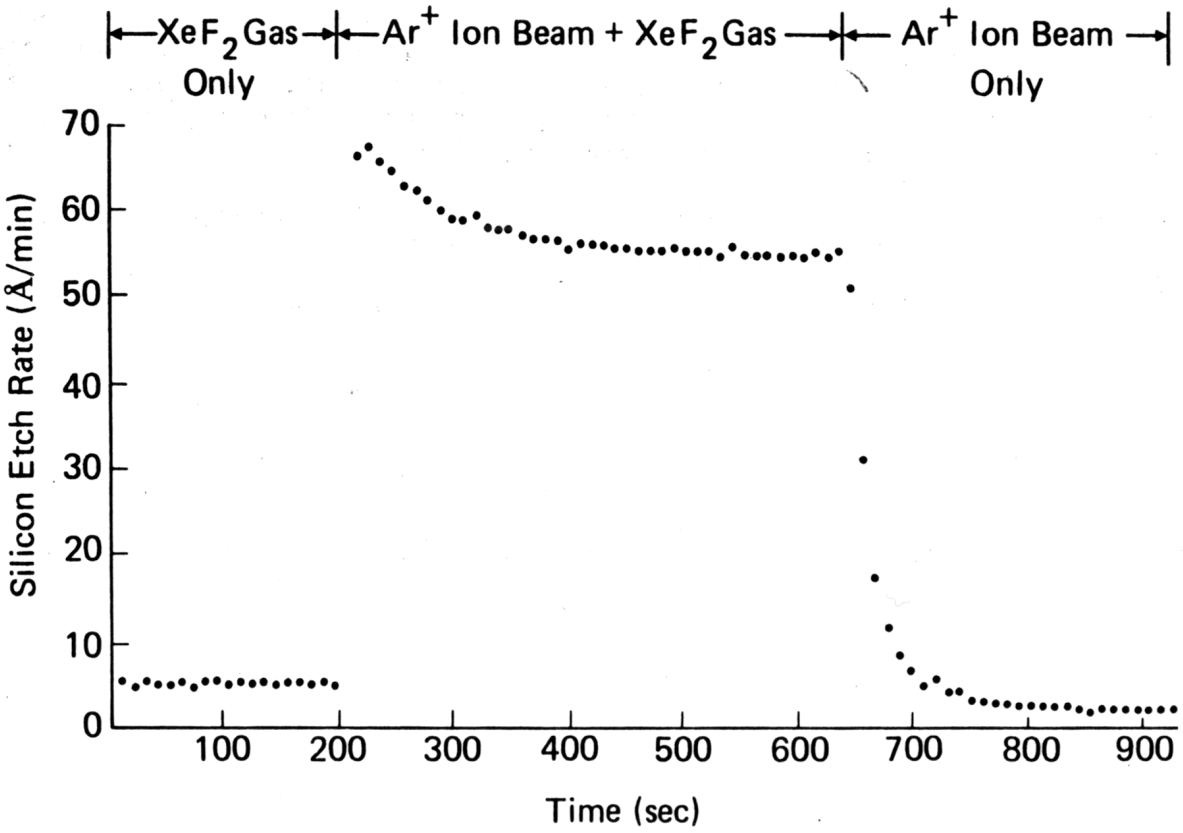

Figure 4. Plot showing the necessity of ion bombardment to the plasma etching process (From Ref. 1).

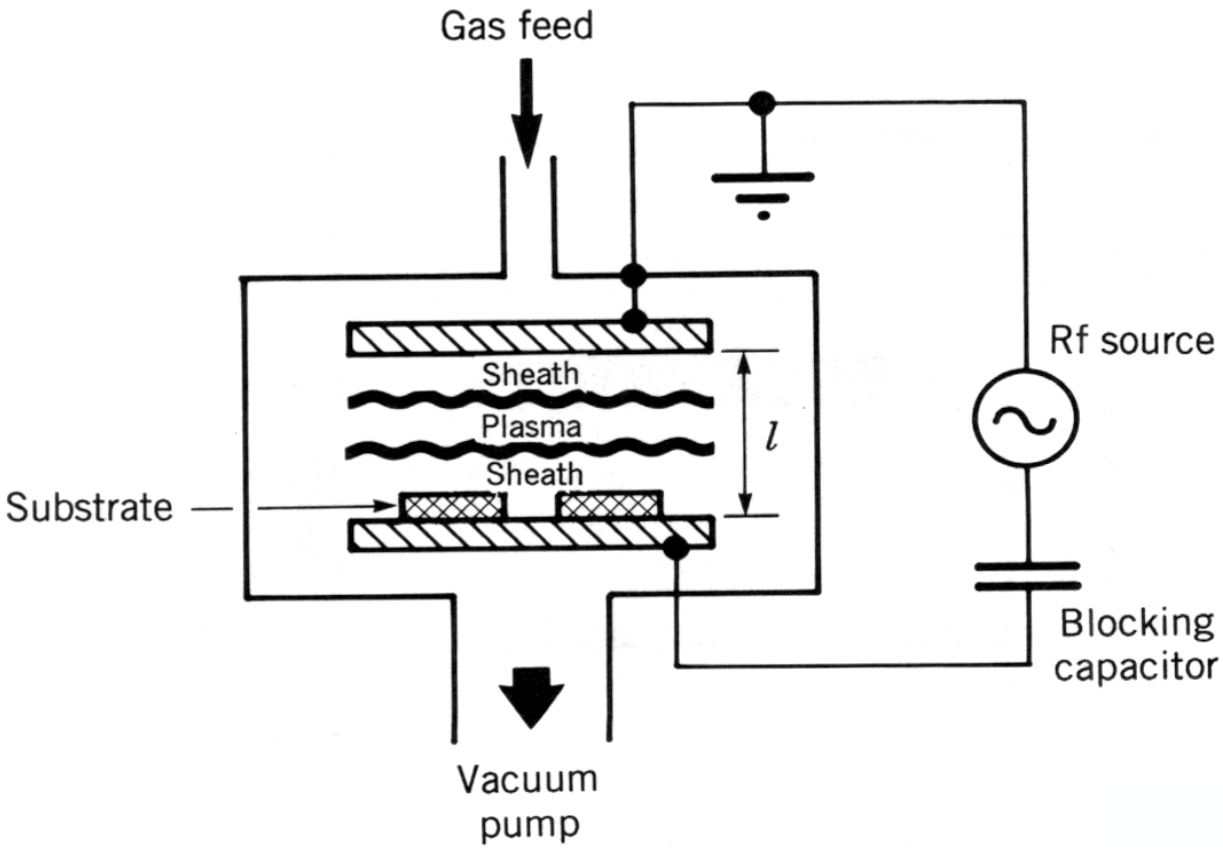

Figure 5. Schematic of a capacitively coupled plasma etching system. (From Ref. 2)

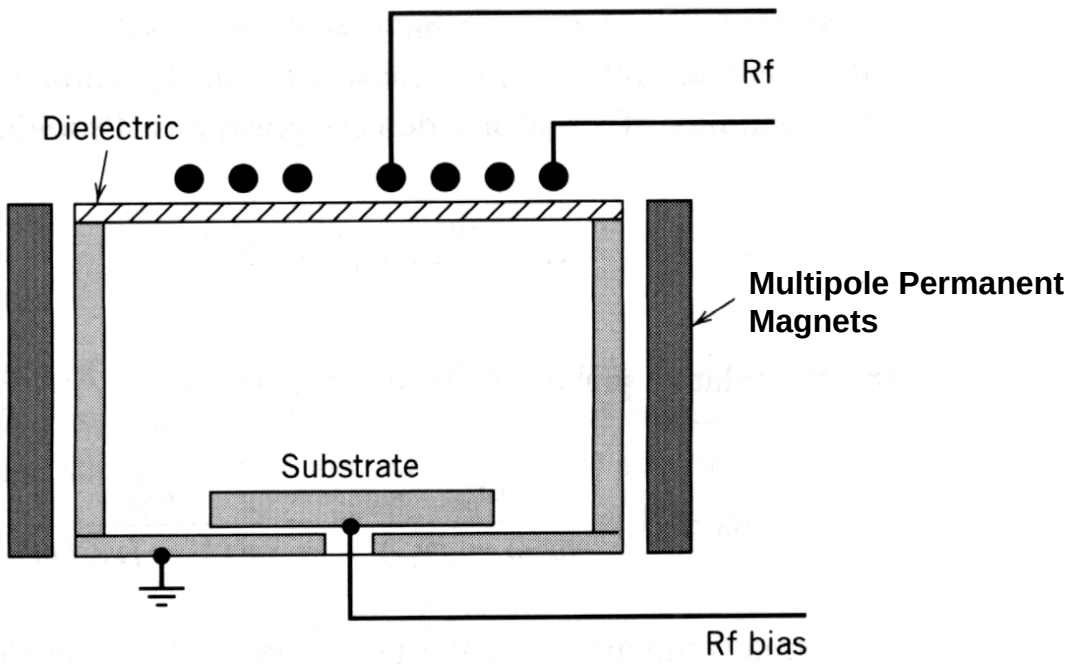

Figure 6. Schematic of a planar ICP etching system. (From Ref. 2)

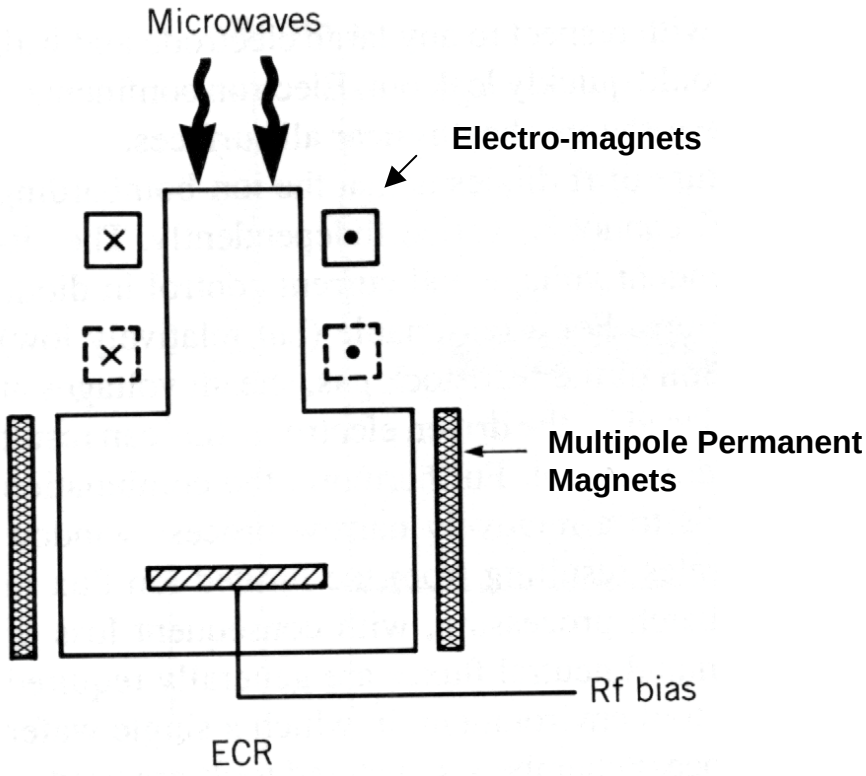

Figure 7. Schematic of an ECR etching system. (From Ref. 2)

CHAPTER 3 LITERATURE REVIEW

One of the earlier etching studies of GaN, within this latest period of research in the III-Nitrides, was reported by Tanaka *et al.* [1] in 1991 using reactive-fast-atom beam etching (R-FABE). Their approach utilized a reactive beam of energetic neutral chlorine molecules and a typical acceleration energy of 1.5 keV which corresponded to etch rates of approximately 1200 Å/min. Numerous papers have been subsequently published by several groups of investigators concerning the etching of GaN and other related III-N materials. Reviews of their work have been published by Gillis et al [2], Zolper and Shul [3], and Eddy [4]. Of the four primary plasma etching types, ECR and RIE have the most widespread use. Only high density etching systems will be discussed herein, since they pertain directly to this research.

In 1993, Pearton *et al.* [5] published their first of many journal articles on ECR etching of GaN, AlN, InN, and ternary alloys of these three materials. They etched GaN and AlN using CCl_2F_2/Ar, BCl_3/Ar, and CH_4/H_2/Ar as the source gases. All three gas combinations gave similar results for etching GaN as a function of the RF bias. The AlN etch rate was similar to that of GaN for the BCl_3/Ar and CH_4/H_2/Ar gases; however, the etch rate of the former was considerably slower when the CCl_2F_2/Ar gas combination was employed. This latter result was attributed to the formation of an AlF_3 passivation layer during etching. The highest etch rates for both GaN and AlN were approximately 200 Å/min. The slow rates were due primarily to the low (200 W) ECR power that was used.

The above etch rates were subsequently improved by Pearton *et al.* [6,7] using different plasma chemistries. By switching from the above-mentioned gases to a Cl_2/H_2 chemistry, the etch rates increased from 200 Å/min to approximately 600 Å/min for the same parameters. The increase in etch rate was attributed to more efficient removal of the nitrogen via the formation of NH_x. The actual mechanism by which the nitrogen is removed has yet to be shown diagnostically. Increasing the microwave power from 200 to 1000 W increased the etch rates by a factor of five. Pearton *et al.* [6] stated that this increase in etch rate was due to an increase in the densities of reactive chlorine and atomic hydrogen. While these densities will increase with microwave power, the

increase in etch rate could also be due to an increase in the ion density. The amount of reactive chlorine and atomic hydrogen that is needed for the process may saturate at low microwave powers leaving ion density as the rate-limiting factor.

Shul *et al.* [8] have also used an ECR system to etch GaN. They investigated the effect of substrate temperature on the etch rate using $Cl_2/H_2/CH_4/Ar$ and $Cl_2/H_2/Ar$ as the source gases. The etch rate of GaN increased about 14% from 30 to 170 °C using the CH_4-containing chemistry. Omitting the CH_4 allowed an increased in the etch rate of approximately 33% over the same temperature range. Figure 1 shows the etch rate dependence on temperature for GaN and AlN with the use of the aforementioned source gases [8]. The discernable dependence on temperature of the GaN indicates that desorption of the volatile species may be a rate limiting factor under certain conditions. The gas combination containing CH_4 showed a higher etch rate which was attributed to either the formation of a group III-methyl etch product or an etch mechanism which is enhanced by the addition of CH_4. The actual contribution by the CH_4 will be unknown until plasma diagnostics are performed.

A parametric study of the effect of the independent variation of pressure, RF power, and ECR power was performed by Shul *et al.* [9] using $Cl_2/H_2/CH_4/Ar$ as the feed gases. Interestingly, the investigators chose to vary the RF power rather than the DC bias. It is the DC bias, i.e., the energy of the bombarding ions, that affects the etch rates and not the RF power directly. The DC bias will tend to vary for a fixed RF power when varying the plasma density via the ECR power or the pressure. Thus, the true effects of the ECR power or pressure are difficult to discern from the effects of the changing DC bias. Etch mechanisms were postulated from the results of this study, but their results are in question due to the above stated problem. If the DC bias were fixed as opposed to the RF power, more information could be determined regarding the effects of the ECR power, pressure, and DC bias on the etch rates. In any case, etch rates of 2,850 Å/min were achieved using the parameters of 350 W ECR power, 2 mTorr pressure, and 275 W RF power.

Hydrogen has typically been used for more efficient removal of the nitrogen species in the form of NH_x, which, in turn, should increase the etch rates. The source gases in the

published studies discussed to this point have contained H_2. However, Vartuli *et al.* [10] performed a study of the effects using only Cl_2 and Ar for the etching of GaN. Only the RF power was varied. Etch rates of nearly 7000 Å/min were achieved using a mixture of 33.33 volume % Cl_2 and 66.66 volume % Ar at flow rates of 5 and 10 sccm, respectively. The parameters used to obtain this etch rate were 100 W ECR power, 1.5 mTorr pressure, and 450 W RF power. A study of the effects of mixing H_2 in various concentrations with Cl_2 has not been performed at this writing. The effects of H_2 may not be as significant as were once postulated [5-7, 8, 9].

Lee *et al.* [11] have furthered the understanding of the effects of temperature on the etch rates of GaN reported by Shul *et al.* [8]. The feed gas mixture was BCl_3/N_2 to avoid the complications of polymer formation by the methane-containing gas employed by the latter investigators. Sample temperature had a minimal affect on the etch rate. There appears to be some rate limiting step produced by the Cl_2-based chemistries that does not exist in BCl_3-based chemistries.

Iodine- and bromine-based chemistries have also been used to etch the III-N materials [12-14]. The compounds employed were HI, HBr, and ICl. The etch rates for GaN using HI were approximately 20% faster than they were for a Cl_2/H_2 mixture under the same operating conditions. The vapor pressure of $GaCl_3$ is higher than that of GaI_3 [15]. Thus, the measured higher etch rate for the HI source gas over the Cl_2/H_2 mixture could be due to the lower ionization potential of I relative to Cl which would result in a higher ion density. No explanation for the difference in etch rate was given in the literature [12-14]. Using HBr for the source gas resulted in slightly slower etch rates than were achieved using Cl_2/H_2 mixture. The difference was attributed to the lower vapor pressure of $GaCl_3$ compared to $GaBr_3$. This may contribute to the difference, but the higher vapor pressure of $GaCl_3$ compared to GaI_3 did not explain why the etch rates were faster for HI than they were for Cl_2/H_2 mixture. The difference in ionization potentials between Br and Cl (11.81 eV and 12.97 eV, respectively) also does not explain the difference in rates. Possible explanations could be either that GaBr is more difficult to form than GaCl or that HBr has a higher dissociation energy than Cl_2 resulting in lower concentrations of reactive species in the plasma containing the HBr.

The highest etch rates using ECR were achieved using ICl as the source gas [7]. Etch rates of 1.3 μ/min were achieved at an ECR power of 1000 W and a pressure of 1.5 mTorr. The DC bias was not reported. Thus, ICl appears to be a very potent source gas due to it's low dissociation energy (211.3 kJ/mol) and it's low ionization potential (10.088 eV). Diagnostic results have not been reported for the ICl chemistry, but it appears that it would have a higher density of Cl radicals and a higher ion density than one would expect from using Cl_2 as the source gas.

A Cl_2/CH_4-based chemistry has also been used to etch GaN [15]. The CH_4 was used to facilitate removal of the nitrogen via the formation of NH_x. However, as noted above, the significance of the hydrogen in this regard and the mechanism by which the nitrogen is removed is still in question. An etch rate of 1350 Å/min was achieved using 400 W of ECR power, -140 V DC bias, and 1 mTorr pressure. The resultant sidewall was considerably sloped due to erosion of the photoresist mask. Decreasing the DC bias to -95 V resulted in a nearly vertical sidewall indicating the resist degraded much slower at this bias.

Successful magnetron reactive ion etching has been performed by McLane *et al.* [16,17]. Etch rates to 3500 Å/min were achieved using BCl_3 as the source gas at a DC bias of -100 V. Etch rates were measured as functions of applied power and pressure. These rates increased with increasing power which, in turn, was believed to have caused an increased generation of Cl radicals. This explanation may not be correct due to the importance of ion density in the etching of GaN. Variation of the pressure between 1 and 10 mTorr resulted in a maximum etch rate at 7 mTorr.

Inductively coupled plasma (ICP) etching has had much attention recently. Shul *et al.* [18] first published on the ICP etching of GaN using $Cl_2/H_2/Ar$ as the source gases. This initial parametric study was conducted as a function of ICP power, RF power (DC bias), and pressure. Unless otherwise noted, the parameters were 22.5 sccm Cl_2, 2.5 sccm H_2, 5 sccm Ar, 1 mTorr pressure, 500 W ICP power, and 150 W rf power. This value of RF power corresponded to a DC bias of -190 V at the above stated parameters. The value of the DC bias changed with changing ICP power and pressure. Figure 2 shows the etch rates as a function of the ICP power. The maximum in the etch rate was obtained at 500

W; it then declined through 1000 W. The DC bias changed from -285 V to -130 V over this range. This explains the decrease in etch rate. The actual effect of ICP power on etch rates cannot be determined from Figure 2 due to the changing DC bias.

Figure 3 shows the etch rate as a function of pressure. In this case, the DC bias changed from -180 V to -375 V over the range examined due to a fixed RF power. The increase in etch rate from 1 to 5 mTorr was attributed to the increased formation of reactive species, suggesting a reactant limited regime at the lower pressures. This may not be true, since the ion density is unknown over this range, and the DC bias is increasing. Either or both of these could contribute to the etch rate instead of the increasing density of the reactive species. Above 5 mTorr the etch rate decreased slightly through 11 mTorr. It was speculated that this was due to either lower ion density, or sputter desorption of reactive species prior to reaction due to the higher DC biases, or redeposition on the etch surface. The sputter desorption of the reactive species before reaction is likely not the case, since, as will be discussed next, the increase in etch rate as the RF power was varied from 70 to 400 W is nearly linear. Figure 4 shows the effect of RF power (DC bias) on the etch rate. If the higher DC biases promoted sputter desorption of the reactive species, the etch rates would not have increased, as shown in Figure 4. The etching would have been purely physical sputtering resulting in lower etch rates than are shown in this figure.

Until recently, combinations of Cl_2, H_2, and Ar have been the predominant source gases for etching GaN. Lee *et al.* [19] have shown that the addition of a slight amount of BCl_3 to the Cl_2 increased the etch rate considerably. Figure 5 shows the dependence of Cl_2 concentration with additions of either Ar or BCl_3. The addition of 10% BCl_3 approximately doubled the etch rate for both pressure ranges. The addition of 10% Ar also increased the etch rates, but not as dramatically as the BCl_3. Increasing the concentration of either additive in the Cl_2 beyond 10% decreased the etch rates significantly.

The effect of changing the Cl_2 concentration with the addition of Ar or BCl_3 was also examined with a Langmuir probe and an optical emission spectrometer [19]. As expected, the ion density increased with increasing Ar concentration. Atomic chlorine

has a lower ionization potential than Ar; however, more of the Ar will ionize because it is a one step process. The ionization of Cl requires the initial dissociation of Cl_2, thus, making it is a two step process.

Figure 6 shows the ion current density (Langmuir probe), Cl^+ density (OES), Cl density (OES), and the density of BCl (OES) as a function of the BCl_3 concentration, as reported by Lee *et. al.* [19]. The densities of the Cl^+, BCl, and Cl radicals were not actually measured. The emission intensity for a specific species is a function of both the density of that species and the electron energy distribution function, the latter of which may change with gas concentration. Without using actinometry techniques, it is difficult to determine the effects of the BCl_3 concentration on these two characteristics of the plasma. This figure does show that the ion density decreased as the BCl_3 concentration increased. The etch rate curves in Figure 5 for the BCl_3/Cl_2 chemistry were attributed to the change in Cl radical density shown in Figure 6. However, one does not really know the relative Cl radical density. Thus, this conclusion may not be valid.

Shul *et al.* [20-21] have also published papers on the etching of GaN and AlN in an ICP system using BCl_3/Cl_2 as the source gases. Examined were the selectivity between these materials and their etch rates while varying the gas concentrations, ICP power, DC bias, and pressure. The optimum gas concentration was determined by varying the Cl_2 concentration from 0 to 100 % in steps of 20 % and found to be 80 % Cl_2 and 20 % BCl_3. The maximum etch rate of GaN was 8000 Å/min using the above gas concentration, 500 W ICP power, 2 mTorr pressure, and –375 V DC bias. A maximum selectivity of 6.3 was determined between the GaN and AlN.

1. H. Tanaka, F. Shimokawa, T. Sasaki, and T. Matsuoka, Optoelectronics-Devices and Technologies **6**, 150 (1991).

2. H. P. Gillis, D. A. Choutov, and K. P. Martin, J. Minerals, Metals & Mat **48**, 50 (1996).

3. J. C. Zolper and R. J. Shul, MRS Bulletin **22**, 36 (1997).

4. C. R. Edy, MRS Internet J. Nitride Semicond. Res. **4S1**, G10.5 (1999).

5. S. J. Pearton, C. R. Abernathy, F. Ren, J. R. Lothian, P. W. Wisk, and A. Katz, J. Vac. Sci. Technol. A **11**, 1772 (1993).

6. S. J. Pearton, C. R. Abernathy, F. Ren, J. R. Lothian, P. W. Wisk, A. Katz, and C. Constantine, Semicond. Sci. Technol. **8**, 310 (1993).

7. S. J. Pearton, C. R. Abernathy, and F. Ren, Appl. Phys. Lett. **64,** 2294 (1994).

8. R. J. Shul, S. P. Kilcoyne, M. Hagerott, J. E. Parmeter, C. B. Vartuli, C. R. Abernathy, and S. J. Pearton, Appl. Phys. Lett. **66,** 1761 (1995).

9. R. J. Shul, A. J. Howard, S. J. Pearton, C. R. Abernathy, C. B. Vartuli, P. A. Barnes, and M. J. Bozack, J. Vac. Sci. Technol. B **13**, 2016 (1995).

10. C. B. Vartuli, J. D. MacKenzie, J. W. Lee, C. R. Abernathy, S. J. Pearton, and R. J. Shul, Appl. Phys. Lett. **80,** 3705 (1996).

11. J. W. Lee, J. Hong, J. D. MacKenzie, C. R. Abernathy, and S. J. Pearton, J. Elec. Mat. **26**, 290 (1997).

12. S. J. Pearton, C. R. Abernathy, and C. B. Vartuli, Electron. Lett. **30**, 1985 (1994).

13. C. B. Vartuli, S. J. Pearton, C. R. Abernathy, R. J. Shul, A. J. Howard, S. P. Kilcoyne, J. E. Parmeter, and M. Hagerott-Crawford, J. Vac. Sci. Technol. A **14**, 1011 (1996).

14. C. B. Vartuli, S. J. Pearton, J. W. Lee, J. Hong, T. D. Mackenzie, C. R. Abernathy, and R. J. Shul, Appl. Phys. Lett. **69** (10), 1426 (1996).

15. B. Humphreys, M. Govett, MRS Internet J. Nitride Semicond. Res. **1**, 28 (1996).

16. G. F. McLane, L. Casas, S. J. Pearton, and C. R. Abernathy, Appl. Phys. Lett. **66,** 3328 (1995).

17. G. F. McLane, L. Casas, R. T. Lareau, D. W. Eckart, C. B. Vartuli, S. J. Pearton, and C. R. Abernathy, J. Vac. Sci. Technol. A **13**, 724 (1995).

18. R. J. Shul, G. B. McClellan, S. A. Casalnuovo, D. J. Rieger, S. J. Pearton, C. Constantine, C. Barratt, R. F. Karlicek, Jr., C. Tran, and M. Shurman, Appl. Phys. Lett. **69,** 1119 (1996).

19. Y. H. Lee, H. S. Kim, G. Y. Yeom, J. W. Lee, M. C. Yoo, and T. I. Kim, J. Vac. Sci. Technol. A **16**, 1478 (1998).

20. R. J. Shul, L. Zhang, C. G. Willison, J. Han, S. J. Pearton, J. Hong, C. R. Abernathy, and L. F. Lester, MRS Internet J. Nitride Semicond. Res. **4S1**, G8.1 (1999).

21. R. J. Shul, C. I. H. Ashby, C. G. Willison, L. Zhang, J. Han, M. M. Bridges, S. J. Pearton, J. Hong, C. R. Abernathy, and L. F. Lester, MRS Internet J. Nitride Semicond. Res. **4S1**, G8.1 (1999).

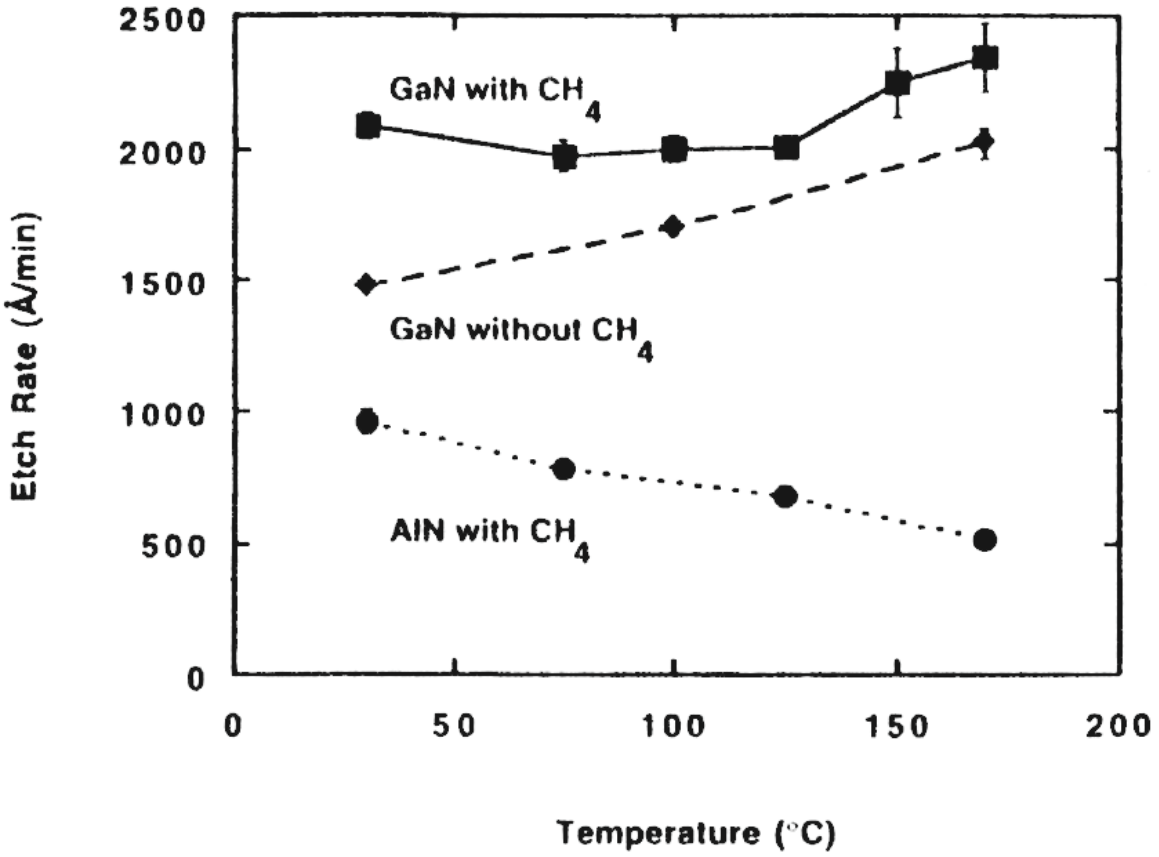

Figure 1. Etch rate dependence on temperature for GaN and AlN in $Cl_2/H_2/CH_4/Ar$ and $Cl_2/H_2/Ar$ source gases (R. J. Shul *et al*., 1995).

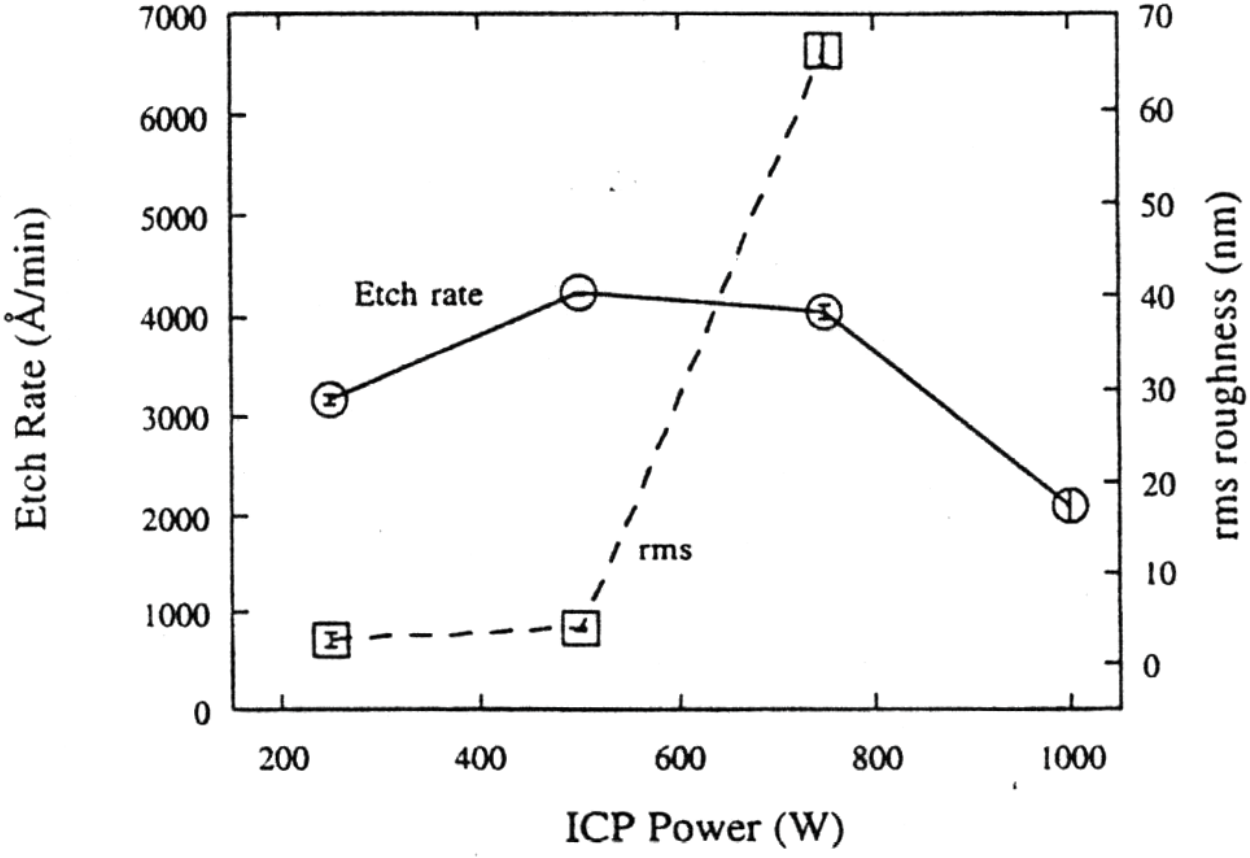

Figure 2. Etch rate of GaN in an ICP system as a function of ICP power (R. J. Shul *et al*., 1996).

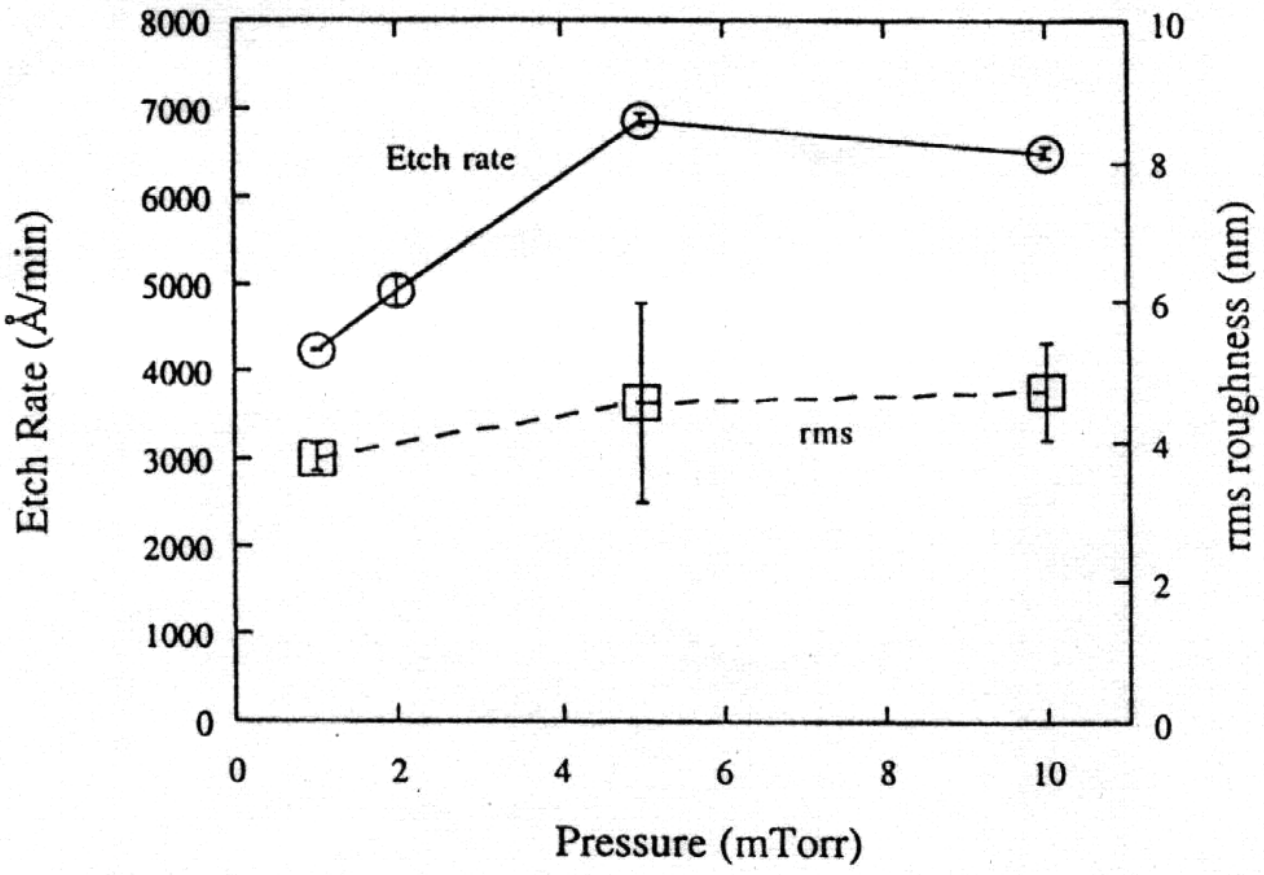

Figure 3. Etch rate of GaN as a function of pressure (R. J. Shul *et al*., 1995).

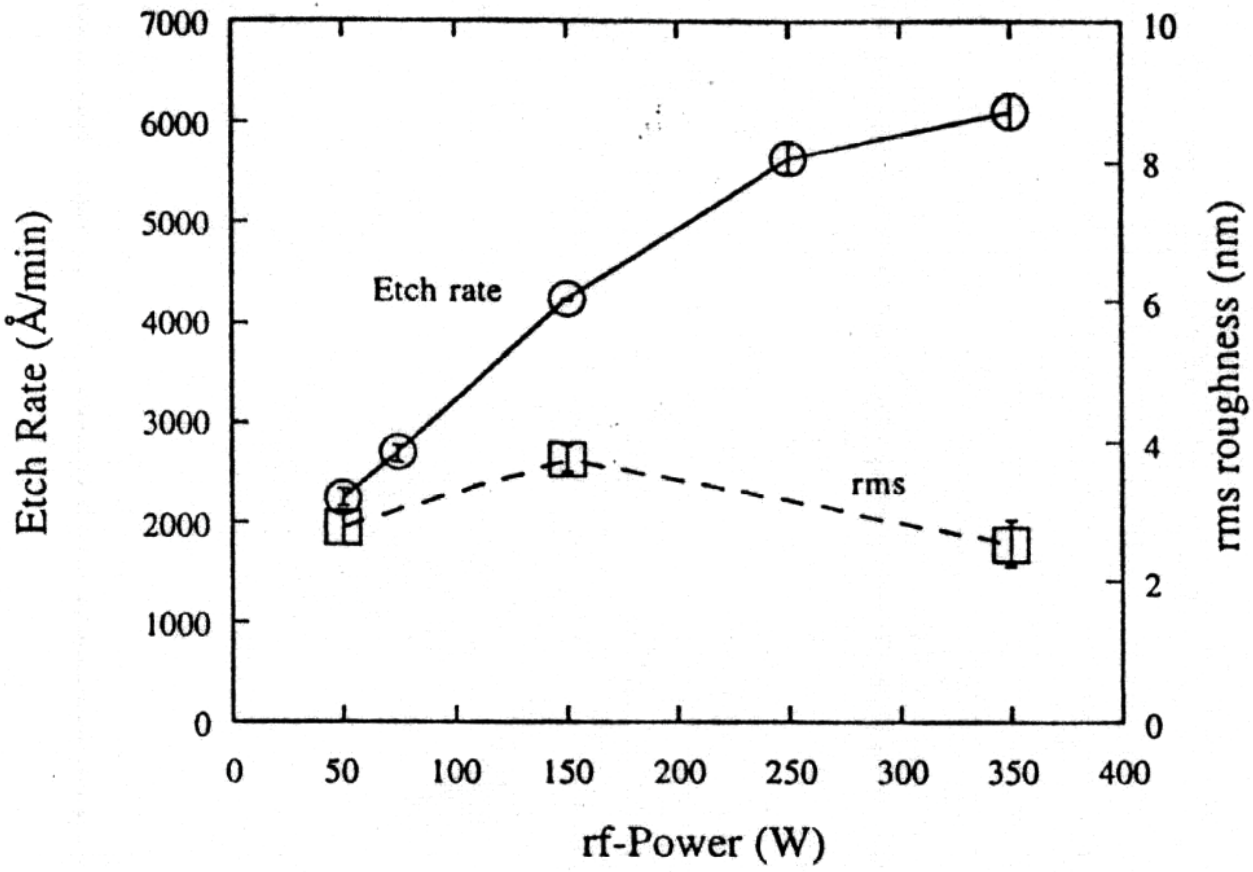

Figure 4. Etch rate of GaN as a function of RF power (R. J. Shul *et al*., 1995).

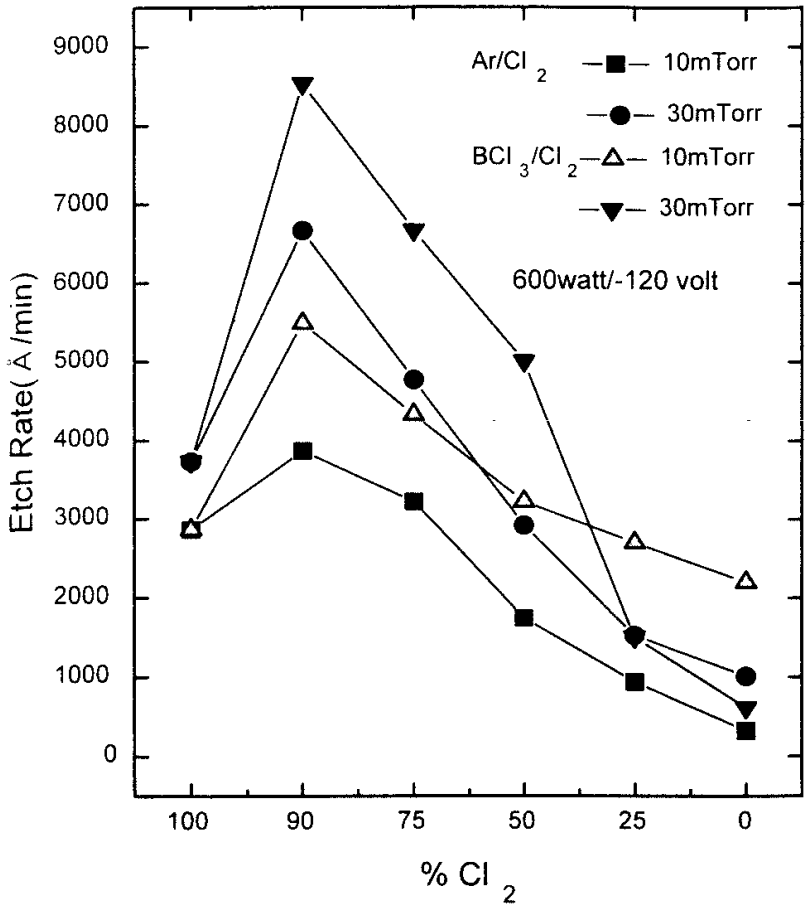

Figure 5. Etch rate of GaN as a function of the Cl_2 concentration in a mixture of either BCl_3 or Ar (Y. H. Lee *et al.*, 1998).

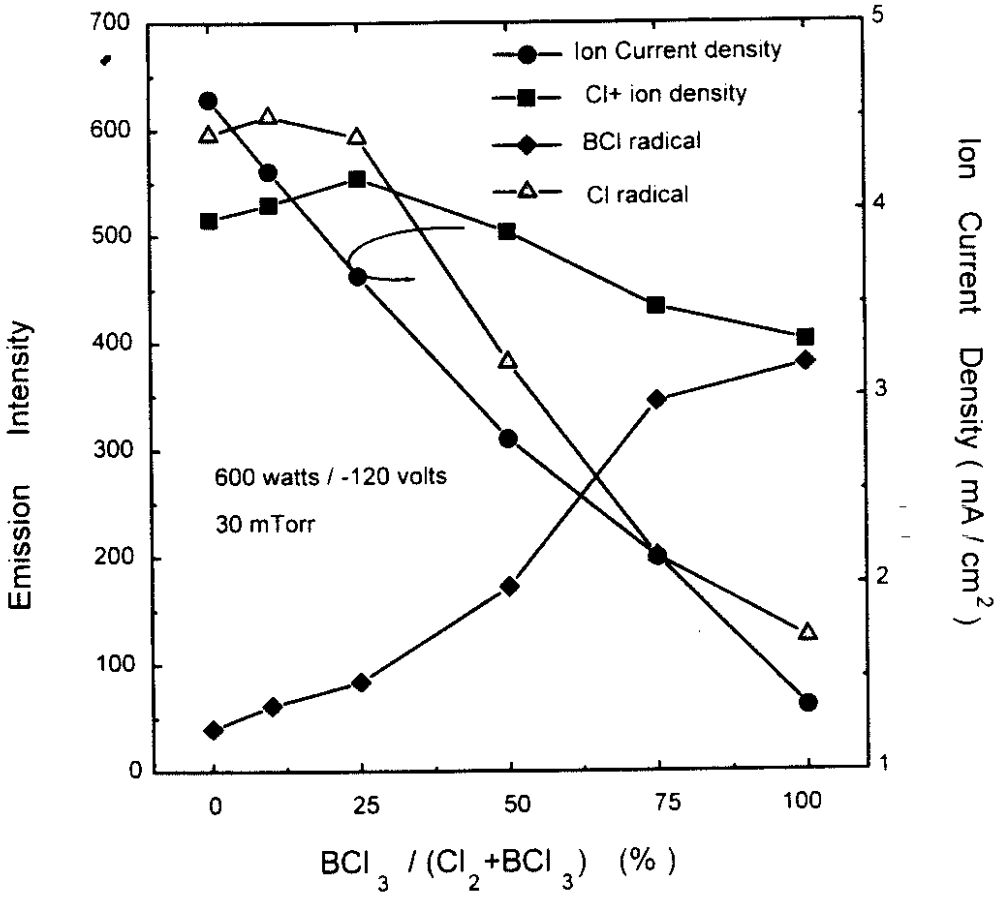

Figure 6. Ion current density, Cl^+ density, Cl density, and BCl density as a function of BCl_3 concentration in Cl_2 (Y. H. Lee *et al.*, 1998).

CHAPTER 4 SYSTEM DESCRIPTION

Introduction

The result of numerous experiments regarding the etching of GaN with an existing reactive ion etching (RIE) system showed the necessity for a new type of system having a much higher plasma density. The two techniques considered were electron cyclotron resonance (ECR) and inductively coupled plasma (ICP). Each had the same advantages over conventional RIE systems; however, the ICP was chosen because it is a more simple technology and more cost effective to implement.

Numerous journal articles regarding the design and operation of ICP etching systems were perused. The basic system design reported by Claude Woods [1] at the University of Wisconsin Engineering Research Center for Plasma-Aided Manufacturing as deemed suitable. The system was designed for diagnostic studies, which was appropriate for our planned research. The following sections describe in detail the various components of the system beginning with the overall system design including the wafer stage and inductive source. Next discussed are the design and configuration of the chamber, followed by the loadlock design, the pumping system and pressure control, the gas supply, and the RF power generators. Lastly, final comments on the system design are mentioned.

Overall System Design

The overall system design without the loadlock and stand is shown in Figure 1. The chamber is supported by an enclosed aluminum stand that is 78” long, 45” wide, and 48” high. The main chamber is the only part of Figure 1 that is above the surface of the stand. The latter houses all of the pumping equipment, the water cooling lines, one of the matching networks, and the mass flow controllers. Figure 2 shows the configuration of the chamber, loadlock, and stand.

Directly beneath the main chamber is a 10” Con-flat ‘T’ that is connected to the process turbomolecular pump at the horizontal port and a Thermionics motorized z-stage manipulator at the vertical port. The latter raises and lowers the wafer stage between the

process zone and the loadlock entry point. It was necessary to locate the loadlock entry point this low to accommodate the magnetic array around the perimeter of the chamber.

System Components

Wafer Stage

The wafer stage was the most challenging aspect of the system design. Figure 3 is an engineering drawing of the sample holder shown in Figure 1. The latter is electrically isolated from ground, cooled, and vacuum isolated from the rest of the chamber. The electrical isolation of an RF power source is more difficult than for a DC source. Initially the RF power was applied via copper cooling lines which entered the system through an insulated feedthrough at the bottom of the z-stage and terminated at the copper block represented by the crosshatched area in Figure 3. This configuration did not work, since the RF power also coupled to the tube which supported the stage. This problem was resolved by bringing the RF power through a shielded cable that terminated at the copper block.

The main body of the sample stage is essentially an ultra-torr fitting. Exposure of the interior of the sample stage to Cl_2 would result in the corrosion of the copper block. To surmount this potential problem the 3" diameter by 0.25" thick anodized aluminum sample transport plate shown in Figure 3 was mechanically clamped simultaneously to the copper cooling block and a viton O-ring via a threaded post attached to the disk. The male threads on this post connect to female threads on the end of a shaft connected to a rotary feedthrough. As this feedthrough is rotated, the disk is pulled against the copper block and a viton o-ring which seals the inside of the Cu stage against exposure to the Cl_2.

Inductive Source

The inductive source is a four turn, ≈8.5" diameter planar coil of 0.25" copper tubing. Figure 1 shows a cut away view and the configuration of this coil. The beginning and end of the coil are turned up 90^o and connected directly to the matching network which rests on the top of the chamber. The coil is water cooled to 16^o C. System Components

Chamber

The 16” diameter by 23” tall 304 stainless steel chamber was custom designed and fabricated to achieve our etching requirements. Additional ports and vacuum pumping capacity were provided for future expansion. Figure 4 shows a schematic of the chamber. Four of the ports are 1” by 10” rectangular viewports. Three of the viewports are made of Pyrex®; the fourth is made of fused silica. This last port is transparent to the required 200 nm which allows the use of an optical emission spectrometer (OES). The remaining ports consist of two 4”, six 2.75”, and one 6” diameter openings in the chamber. The two 4” ports are currently viewports, the 2.75” ports are used for a mass spectrometer and pressure gauges, and the 6” port is for the loadlock. Figure 5 is a top view of the chamber to show the locations of the various ports.

Surrounding the chamber is a magnetic bucket containing 24 azimuthally alternating magnetic poles that provide a nearly field-free region of approximately 24 cm in the center of the chamber. Each pole contains 10 Nd-Fe-B cylindrical magnets which are 1” long and 0.75” diameter. The separation of the poles against the chamber is approximately .85”.

Atop the chamber is a well that is recessed 3.375”, mounted on an 18” Conflat® flange, contains a 12.75” diameter by 0.75” thick quartz viewport, and is the location of the inductive source. Figure 6 shows a drawing of this well. The recession into the chamber facilitates the mounting of the inductive source and insures that the plane of the inductive source is located in the field of the magnetic bucket. The gas enters into the chamber through a gas shower ring that is connected to one of the 1.33” flanges on the top. In the initial design the gas was to be fed into all four flanges before entering the gas shower ring in four places around the chamber to assist the uniformity of the etching. Reconsideration of the low pressures used during etching revealed that one gas entry port was sufficient. This ring is located at the same level as the bottom of the quartz plate. The lip that holds the quartz plate is water cooled to prevent the degradation of the viton gasket due to the heat of the plasma.

Loadlock

As previously stated, a loadlock is connected to the 6" port on the chamber. A loadlock is necessary for this type of system, as exposure to H_2O vapor of a chamber containing Cl_2 or one which Cl_2 has adsorbed on the walls will result in the formation of HCl and corrosion of all the stainless steel components. Samples are transported from the loadlock to the chamber via a magnetically coupled transfer arm.

Pumping System

The pumping system for the main chamber consists of a 900 l/s Alcatel ATP900C turbomolecular pump that was designed for corrosive service. The modifications necessary to prevent corrosion consisted of the inclusion of ceramic coated blades and a nitrogen purge for the bearings. The pump is backed by a Leybold D65BCS mechanical pump with a 50 cfm throughput. The mechanical pump was also designed for corrosive service via the use of fomblin oil, a nitrogen purge, and an oil filtering system. The base pressure in the system is nominally $1*10^{-7}$ mTorr.

The loadlock pumping system is composed of an Alcatel 5150C turbomolecular pump with a Leybold D25BCS mechanical pump. The manufacturers quoted pumping speeds are 150 l/s and 10 cfm, respectively. This combination produces a nominal base pressure of $1*10^{-8}$ mTorr.

The chamber pressure is controlled my an MKS 153V-6 vein type throttle valve which is controlled through an MKS 146A controller that also monitors the chamber and loadlock pressures. Base pressures in the chamber and loadlock are measured with HPS Series 423 I-MAG cold cathode gauges, and the process pressure is measured with an MKS 1800 baratron gauge.

Gas Supply

The gases available for processing and experimentation are argon, nitrogen, xenon, oxygen, hydrogen, chlorine, and boron trichloride. A schematic of the gas delivery system is shown in Figure 7. The flow rates of these gases into the chamber are controlled via MKS 1459-C mass flow controllers. Since the xenon and nitrogen are not

used frequently, they shared the same gas lines and MKS 1459-C mass flow controller. The unused gas was disconnected from the gas line. The gas controller used is a MKS 647A.

RF Power Generators

As noted in section 3, high-density plasma etching systems typically consist of two RF generators; one for the plasma source and one to produce the DC bias on the substrate. The RF generator that produces the bulk plasma is a 2,000 W RF Power Products RF20S. The RF power is connected to the inductive antennae through an RF Power Products AM-20 automatic matching network, which is used to match the RF generator impedance to the plasma impedance. The RF source on the substrate is an RF Power Products RF5S, which is the same as the other source but only 500 W. The matching network is also similar but designed for the 500 W source.

Final Comments

Due to the relative simplicity of this system, the time from conception of the idea to the first experiment was approximately 6 months. The only intermediate problem was the RF coupling that occurred with the RF bias on the substrate. Rectification of this problem resulted in a relatively low maintenance system. As with any extremely corrosive environment, deterioration will occur over time. The pumping system will likely be the most affected. Every precaution has been taken to prolong the life of these components.

1. C. Lai, B. Brunmeier, and R. C. Woods, J. Vac. Sci. Technol. A **13**, 2086 (1995).

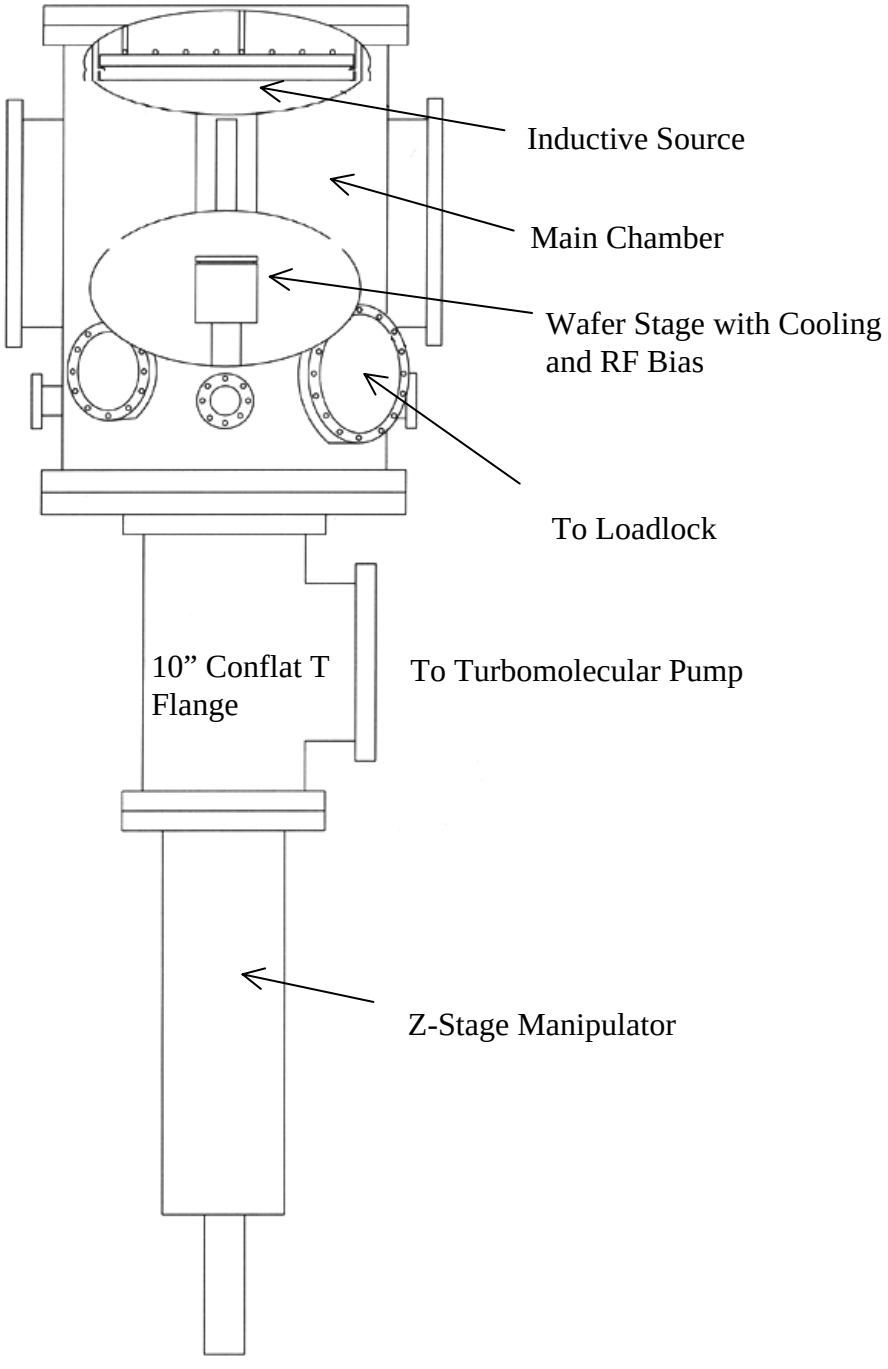

Figure 1. Drawing of overall system configuration without the loadlock.

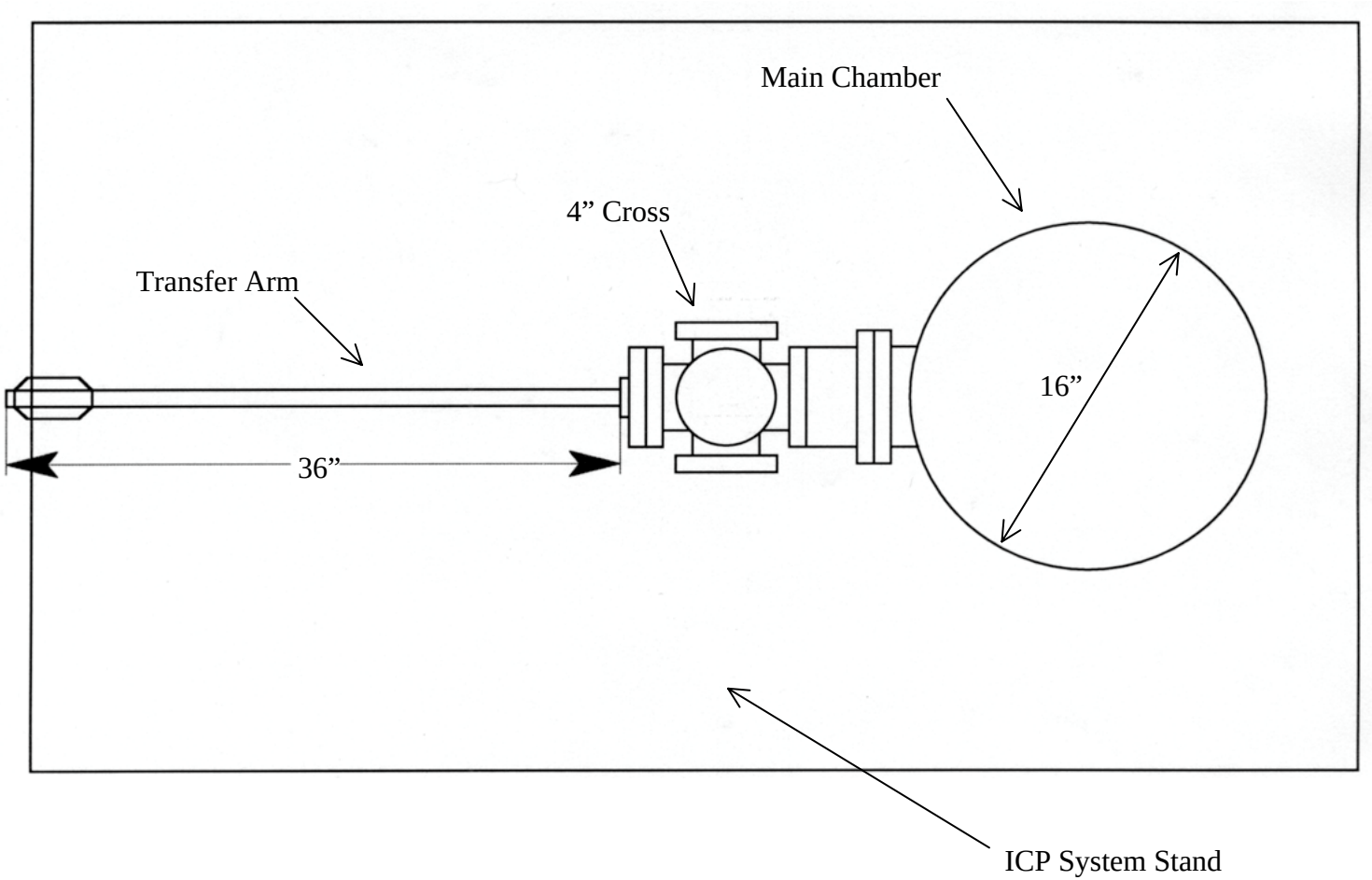

Figure 2. Plan view of configuration of chamber, loadlock, and stand. All dimensions are in inches.

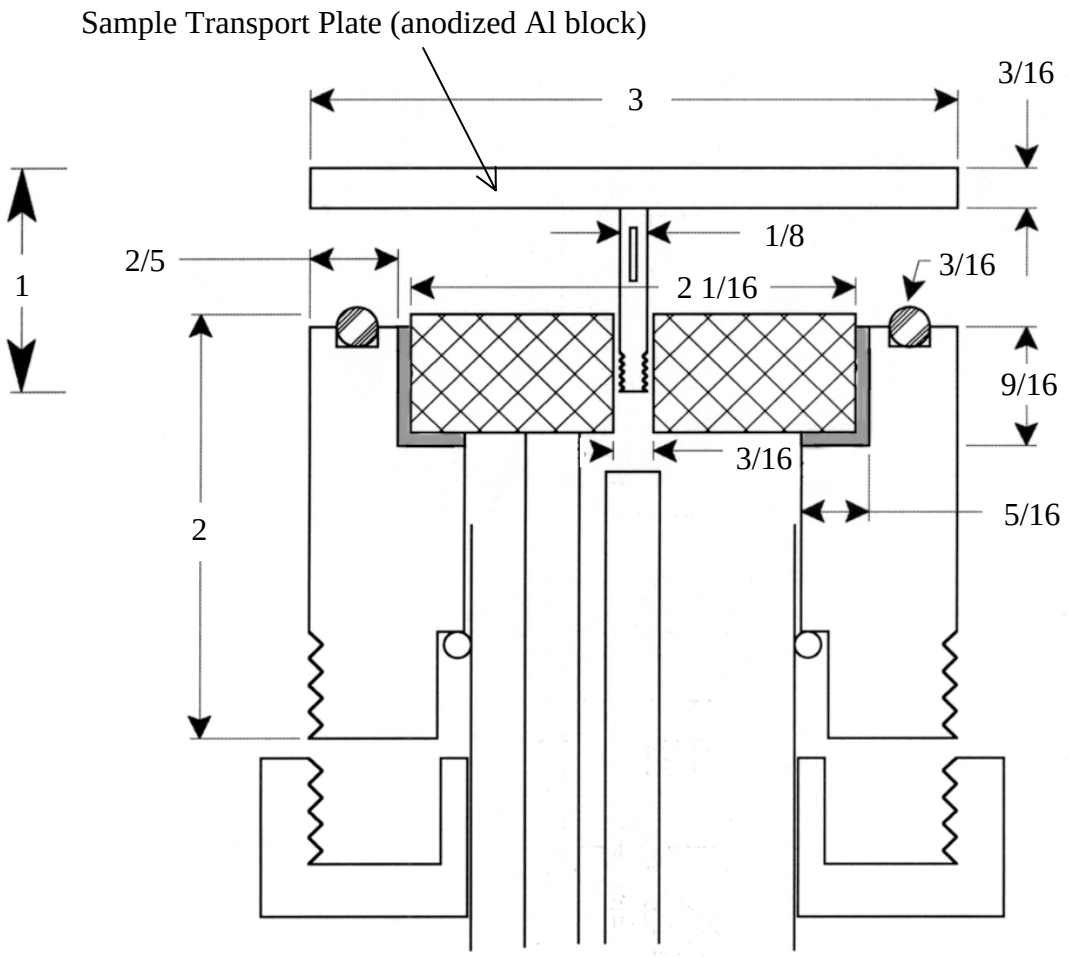

Figure 3. Cutaway view of the sample stage. The crosshatched area represents the water cooled copper block. All dimensions are in inches.

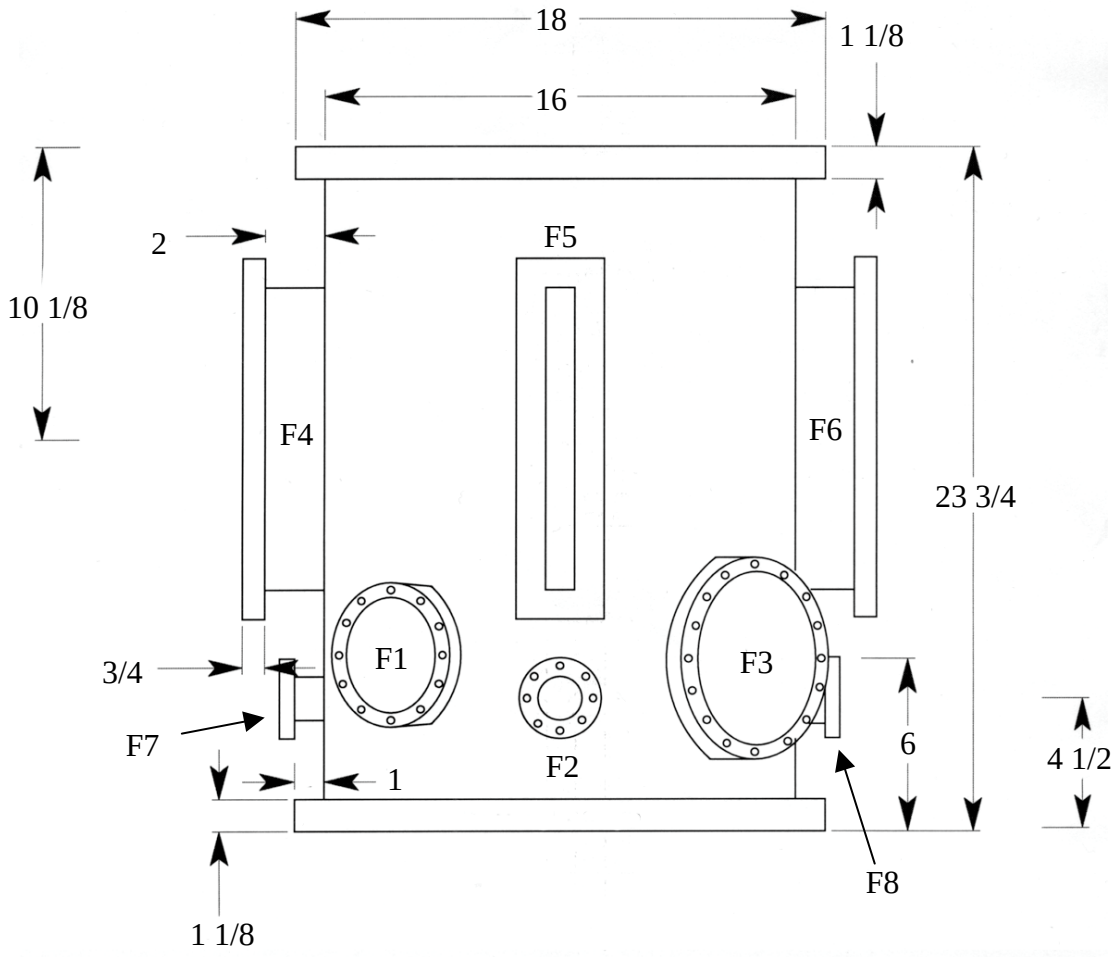

Figure 4. Schematic of custom designed main ICP etching chamber employed in this research. Ports F1, F4, and F6 contain Pyrex viewports, port F2 contains an RGA, port F3 is connected to the loadlock, port 5 contains a fused silica viewport and OES, and ports F7 -F8 are blanked off. All dimensions are in inches.

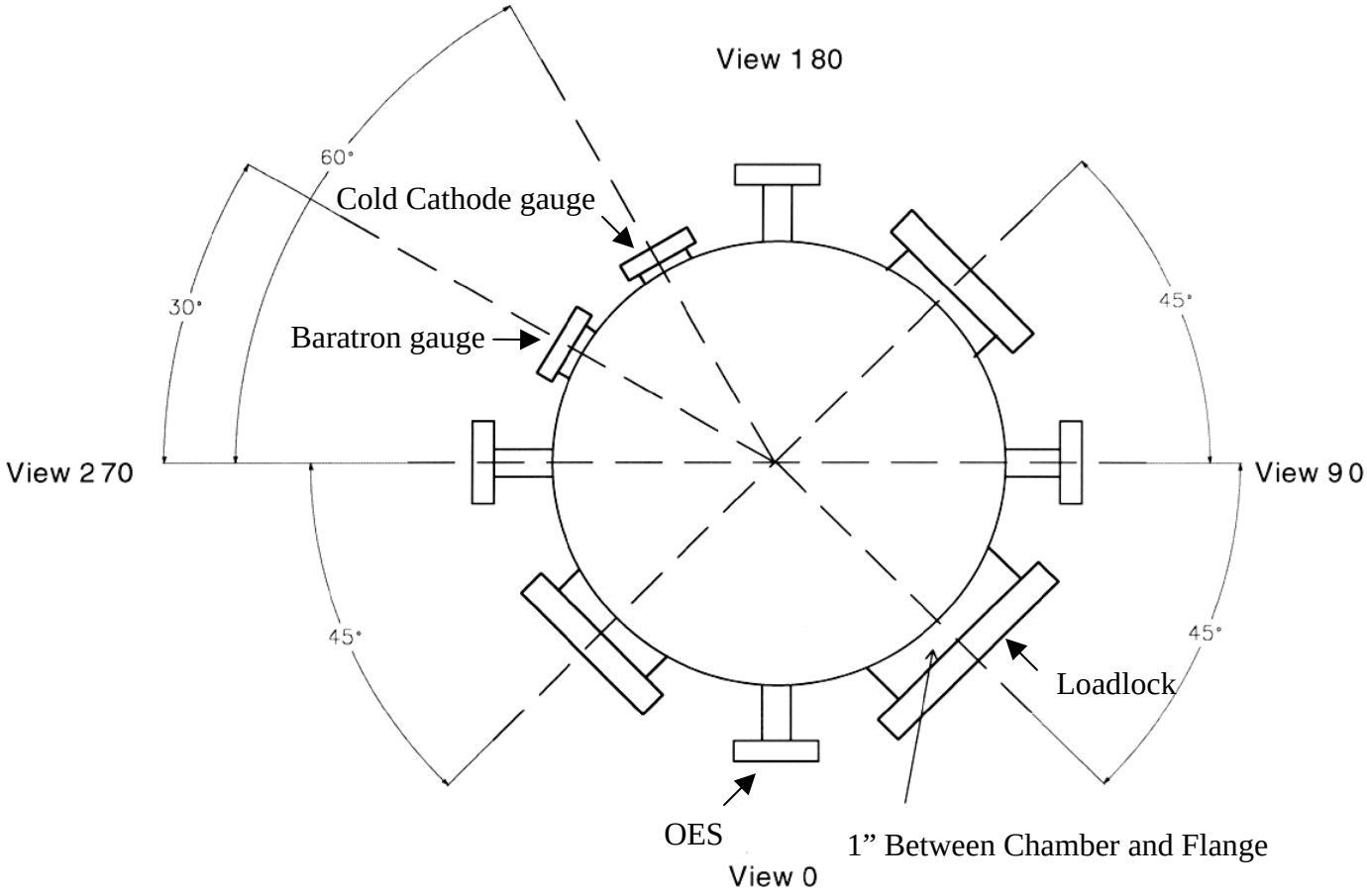

Figure 5. Top view of main chamber to show locations of the ports. Non-labeled ports are viewports. All dimensions are in inches.

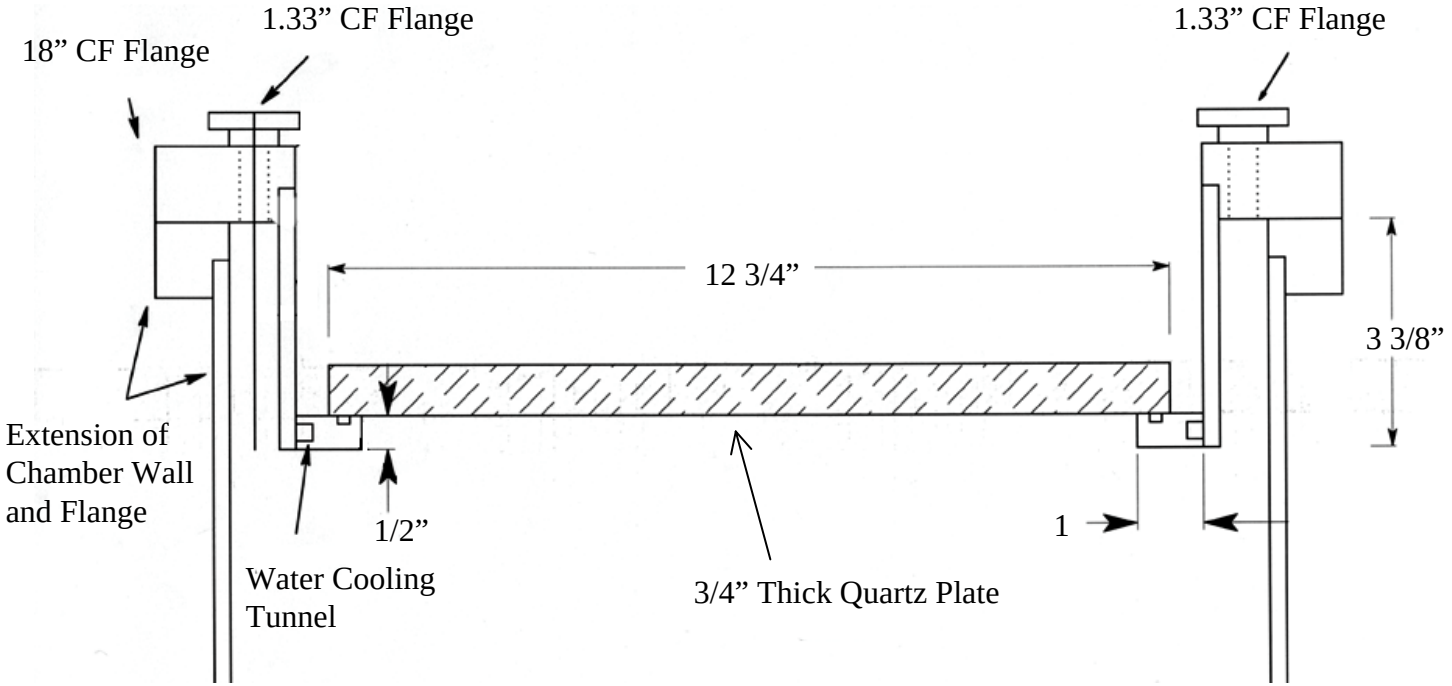

Figure 6. Schematic of vacuum well which is mounted atop the main chamber. Inductive source is located directly above the quartz plate. All dimensions are in inches.

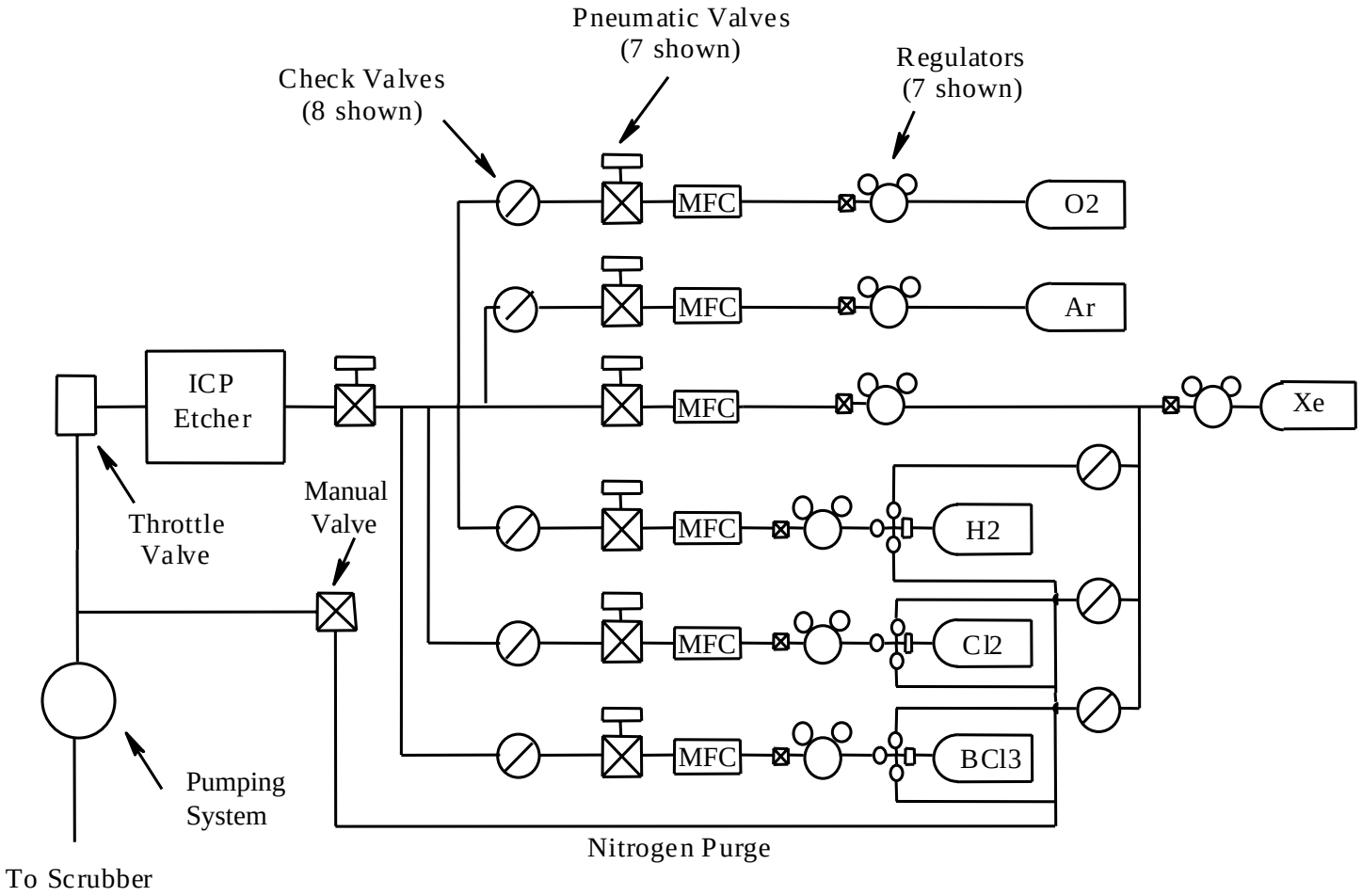

Figure 7. Schematic of the gas delivery system.

CHAPTER 5 PAPER I

High rate and selective etching of GaN, AlGaN, and AlN using an inductively coupled plasma

S. A. Smith[a)], C. A. Wolden, M. D. Bremser, A. D. Hanser, and R. F. Davis
Department of Materials Science and Engineering, North Carolina State University, Raleigh, North Carolina 27695-7919

W. V. Lampert
Materials Directorate, Air Force Research Laboratory, Wright Patterson Air Force Base, OH 45433-7750

The etching behavior of gallium nitride (GaN), aluminum gallium nitride ($Al_xGa_{1-x}N$), and aluminum nitride (AlN) has been systematically examined in an inductively coupled plasma (ICP) using Cl_2 and Ar as the reagents. Etch rates were strongly influenced by ICP power and DC bias, while relatively insensitive to pressure, flow rate, and gas composition. Maximum etch rates of 9,800 Å/min for GaN, 9,060 Å/min for $Al_{.28}Ga_{.72}N$, and 7,490 Å/min for AlN were attained. The etch profiles were highly anisotropic over the range of conditions studied. The DC bias had to exceed certain voltages before significant etch rates were obtained. These values were <-20 V for GaN, -40 V for $Al_{.28}Ga_{.72}N$, and >-50 V for AlN. As such, increasing selectivity for GaN over $Al_{.28}Ga_{.72}N$ and AlN was achieved at DC biases below -40 V. At -20 V, the GaN etch rates were 38 times greater than AlN and a factor of 10 greater than $Al_{.28}Ga_{.72}N$. These results demonstrate the importance of ion bombardment in the etching of these materials.

* Published in: *Applied Physics Letters* **71**, 3631 (1997)

The realized and future potential of GaN, AlN, and $Al_xGa_{1-x}N$ for short wavelength light emitters and detectors, and high-temperature and high-power electronics is considerable [1,2]. Etching anisotropic features is a crucial step in the fabrication of many of these devices. Wet chemical etching of GaN has to date produced only slow etch rates and isotropic etch profiles [3], both of which are undesirable for commercial applications. Dry etching is an attractive alternative from which one can achieve controlled degrees of anisotropy, high etch rates, material selectivity, low damage, and the ability to control an etch stop

The four primary dry techniques that have been employed to etch GaN are reactive ion etching (RIE), electron cyclotron resonance etching (ECR), magnetron reactive ion etching (MIE), and inductively coupled plasma etching (ICP) [4-6]. The slowest etch rates and the lowest degree of anisotropy were determined for RIE. This has been attributed to the low plasma densities and the higher operating pressures inherent in this technique. The other three process routes are high density, low pressure alternatives to the parallel plate reactor. To date, the use of ECR has produced the fastest GaN etch rates of 13,000 Å/min with an ICl chemistry [7]. Rates of 6,875 Å/min were attained with an ICP system and a $Cl_2/H_2/Ar$ mixture [8].

Chlorine-based gases such as BCl_3, $SiCl_4$, and Cl_2 are the primary reagents that have been employed to etch the III-Nitrides. Vartuli *et al.* have reported a dry technique that etches GaN selectively with respect to AlN and $Al_xGa_{1-x}N$ [9,10]. Selectivities of 10 between GaN and AlN, and 4 between GaN and $Al_{.31}Ga_{.69}N$ were reported. In this letter we report the results of a systematic study of ICP etching of III-Nitrides using a Cl_2/Ar chemistry. Selective etching of GaN relative to both AlN and $Al_{.28}Ga_{.72}N$ was achieved by controlling the DC bias. The dependence of the etch rate on both ICP power and DC bias are also reported for the three materials. Lastly, the anisotropic nature of the etch profiles is demonstrated.

The ICP system was a custom built, 41 cm diameter by 58 cm tall, loadlocked stainless steel chamber. The RF power was coupled through a 32.4 cm diameter quartz window at the top of the chamber. The inductive source was a planar, 4 turn, 23 cm diameter copper coil which was connected to a RF Power Products 2 kW RF generator

operating at 13.56 MHz via an autotuning matching network. Gas was fed into the chamber through a stainless steel shower ring positioned level with the bottom of the quartz window. A water-cooled wafer chuck was mounted on a motor driven vertical translation stage which had 30.5 cm of travel. This allowed samples to be transferred between the loadlock chamber and the processing zone. A second 500 W RF source was connected to the wafer chuck to apply a controllable DC bias to the substrate. The substrate cooling water was maintained at 16°C to prevent the baking of photoresist during etching. The chamber was evacuated by an Alcatel 900 l/s turbomolecular pump which attained a base pressure of 10^{-7} torr.

A magnetic bucket containing 240 Nd-Fe-B magnets was mounted on the outside perimeter of the chamber to increase the plasma density by confining the electrons to a central volume within the chamber. This reduced electron losses due to collisions with the chamber walls. The ions were also confined due to electrostatic coupling with the electrons. The former were not directly affected by the magnetic field [11].

The GaN, AlN, and $Al_{.28}Ga_{.72}N$ samples used for this study were epitaxially grown on 6H-SiC-(0001) substrates via metalorganic vapor phase epitaxy (MOVPE) using trimethylaluminum (TMA) and triethylgallium (TEG) as the Al and Ga sources, respectively, and NH_3 as the nitrogen source [12,13]. An ≈100nm AlN buffer layer was deposited on the SiC substrates prior to the growth of the GaN and the $Al_{.28}Ga_{.72}N$. Preparation of the samples for etching employed the sequence of applying a Ni coating, patterning with photoresist, and dipping into HNO_3 to etch away the Ni and into acetone to remove the photoresist. Just prior to entry into the etching system, the samples were dipped into 10% HF acid for 10 minutes to remove oxygen and carbon contaminants. Samples were attached to a 7.6 cm diameter anodized aluminum transport plate using vacuum grease which was mounted onto the wafer chuck. After entry into the system a base pressure of $\leq 5*10^{-7}$ torr was attained before the etching experiments were initiated.

The etch rates were determined by the step heights measured using a Dektak II profilometer. Anisotropy was determined by scanning electron microscopy (SEM). Other effects such as electrical damage, physical damage, and chemical contamination are currently being investigated.

The etching parameters studied and the ranges examined are summarized in Table I. The DC bias was varied instead of bias power since the former more directly determines the energy of the ions which strike the surface. The three samples were etched simultaneously to ensure accurate comparisons. It was determined that the gas phase concentration and total flow rate within the ranges shown in Table I had no significant impact on the etch rates (<20%). The etch rate was slightly more sensitive to pressure, varying 44% over the range investigated. A more extensive study of all parameters using optical emission spectrometry (OES) and mass spectrometry will be reported at a later date.

Figure 1 shows that the etch rates for the three materials as a function of ICP power for the three materials behaved similarly. The etch rates increased rapidly from 100 to 500W. Above 500 W the rate of increase was slightly attenuated, although no maximum was reached. Between 900 and 1100 W, the etch rates of the $Al_{.28}Ga_{.72}N$ closely matched those of the GaN. The observed increase in the etch rates with ICP power was likely due to increases in both the reactive chlorine concentration and the ion density. Additional diagnostics are necessary to distinguish between these two effects. The maximum etch rates achieved at an ICP power of 1100 W were 9,140 Å/min for the GaN, 9,060 Å/min for the $Al_{.28}Ga_{.72}N$, and 7,490 Å/min for the AlN.

The etch profiles were highly anisotropic over all conditions examined. Figure 2 shows a typical profile obtained under the base conditions (see Table I) using nickel as the etch mask. The vertical striations were transferred from imperfections in the mask edge. The etched surface was smooth and appeared to be free of physical damage such as pitting.

The DC bias had a very pronounced effect on the etch rates for all three materials, as shown in Figure 3. Again, the behavior was qualitatively similar for the three materials. Firstly, each material had a threshold voltage below which the etch rates were very low. These voltages were: <-20 V for GaN, ~-40 V for $Al_{.28}Ga_{.72}N$, and between -50 and -150 V for AlN. Above the threshold value the rates increased dramatically to -250 V at which point a plateau occurred for the three materials. Between -350 and -450 V the rates increased again, suggesting that an additional etching mechanism may be operative

at these high biases. The maximum rates achieved at a DC bias of -450 V were 9,800 Å/min for GaN, 8,670 Å/min for $Al_{.28}Ga_{.72}N$, and 6,700 Å/min for AlN.

The etch selectivity of GaN relative to AlN and $Al_xGa_{1-x}N$ is of significant interest for the fabrication of $Al_xGa_{1-x}N$ based heterostructure devices. One example is the etch penetration through a GaN capping layer to the $Al_xGa_{1-x}N$ recessed gate in a high electron mobility transistor. Etching of the latter material should be minimal. Selective etching was achieved at low DC biases. The data from Figure 3 was converted into selectivity and plotted in Figure 4 for GaN relative to $Al_{.28}Ga_{.72}N$ and AlN over the range of -(20-50 V). The selectivity is the ratio of the etch rate of GaN to the AlN or $Al_xGa_{1-x}N$. At -50 V, the selectivity between GaN and AlN was 8.5; whereas, it was only 1.2 between the GaN and $Al_{.28}Ga_{.72}N$. The greatest selectivities for GaN were found at a bias of -20 V, a factor of 38 over AlN and approximately 10 over $Al_{.28}Ga_{.72}N$. These differences in etch rates are consistent with the different bond energies between Ga-N and Al-N of 8.92 eV/atom and 11.52 eV/atom, respectfully [14]. A second factor is the lower volatility of $AlCl_x$ relative to $GaCl_x$. Since lower DC biases were used to attain the selective etching, there is a tradeoff between the selectivity and the total etch rate.

The strong dependence of the etch rate on DC bias indicates that ion bombardment plays a significant role in the etching of these materials. Ion bombardment can enhance etching via damaging the surface to make it more reactive, stimulating desorption of the etch products, and direct physical sputtering. The existence of a threshold bias indicates that breaking Ga-N or Al-N bonds by ion bombardment may be the rate-limiting step. It is presumed that ion damage increases the reactivity of these ordinarily inert materials. The ion-induced damage may be necessary to form the volatile $GaCl_x/AlCl_x$ etch products.

In summary, dry etching of GaN, AlN, and $Al_{.28}Ga_{.72}N$ have been investigated in an ICP system using Cl_2 and Ar as the process gases. The rates for all three materials depended strongly on both the ICP power and the DC bias. Maximum etch rates of 9,800 Å/min for the GaN, 9,060 Å/min for the $Al_{.28}Ga_{.72}N$, and 7,490 Å/min for the AlN were achieved which are the highest reported to date for this chemistry. Threshold biases of >-50V and -40V were required to induce significant etching for AlN and $Al_{.28}Ga_{.72}N$. No

threshold was found for GaN down to -20 V. As a result, selectivities of 38 between GaN and AlN and 10 between GaN and $Al_{.28}Ga_{.72}N$ were obtained at a DC bias of -20V. This is of potential interest for the fabrication of $Al_xGa_{1-x}N$ based heterostructure devices. Research is ongoing to quantify the effects of plasma induced damage and to better understand the underlying mechanisms.

This work was supported by the Office of Naval Research under contract No. N00014-96-1-0765. Colin A. Wolden acknowledges support as an NRC/ARO postdoctoral fellow. Scott A. Smith wishes to acknowledge R. Claude Woods for assistance in the design of the etching system and to the U.S. Air Force PALACE Knight program.

1. R.F. Davis, Proc. IEEE **79**, 702 (1991).

2. H. Morkoç, G.B. Gao, M.E. Lin, B. Suerdlov, and M. Burns, J. Appl. Phys. **76**, 1363 (1994).

3. S. J. Pearton, C. R. Abernathy, F. Ren, J. R. Lothian, P. W. Wisk, and A. Katz, J. Vac. Sci. Technol. A **11** (4), 1772 (1993).

4. R. J. Shul, S. P. Kilcoyne, M. Hagerott Crawford, J. E. Parmeter, C. B. Vartuli, C. R. Abernathy, and S. J. Pearton, Appl. Phys. Lett. **66** (14), 1761 (1995).

5. M. E. Lin, Z. F. Fan, Z. Ma, L. H. Allen, and H. Morkoç, Appl. Phys. Lett. **64** (7), 887 (1994).

6. G. F. McLane, T. Monahan, D. W. Eckart, S. J. Pearton, and C. R. Abernathy, J. Vac. Sci. Technol. A **14** (3), 1046 (1996).

7. C. B. Vartuli, S. J. Pearton, J. W. Lee, J. Hong, T. D. Mackenzie, C. R. Abernathy, and R. J. Shul, Appl. Phys. Lett. **69** (10), 1426 (1996).

8. R. J. Shul, G. B. McClellan, S. A. Casalnuovo, D. J. Rieger, S. J. Pearton, C. Constatine, C. Barratt, R. F. Karlicek Jr., C. Tran, and M. Schurman, Appl. Phys. Lett. **69** (8), 1119 (1996).

9. C. B. Vartuli, S. J. Pearton, J. W. Lee, A. Y. Polyakov, M. Shin, D. W. Greve, M. Skronowski, and R. J. Shul, Electrochem. Soc. **144** (6), 2146 (1997).

10. C. B. Vartuli, S. J. Pearton, J. D. Mackenzie, C. R. Abernathy, and R. J. Shul, Electrochem. Soc. **143** (10), L246 (1996).

11. E. R. Lory, Solid State Technology (Nov.), 117 (1984).

12. A. D. Hanser, C. A. Wolden, W. G. Perry, R. Therrien, and R. F. Davis, submitted to Journal of Electronic Materials .

13. M. D. Bremser, W. G. Perry, T. Zheleva, N. V. Edwards, O. H. Nam, N. Parikh, D. E. Aspnes, and R. F. Davis, MRS Internet J. Nitride Semicond. Res. **1**, 8 (1996).

14. R. J. Shul, R. D. Briggs, S. J. Pearton, C. B. Vartuli, C. R. Abernathy, J. W. Lee, C. Constantine, and C. Barratt, Mater. Res. Soc. Symp. Proc. **449**, 969 (1996).

Table I - The experimental parameters examined, their ranges, and the base conditions employed in this study.

Parameter	Range	Base Cond.
ICP Power	100-1100 W	500 W
DC Bias	20-450 (-V)	-150 V
Pressure	1-9 mtorr	5 mtorr
Total Flow Rate	10-30 sccm	25 sccm
Cl_2 Percentage	50-100%	80%
Ar Percentage	0-50%	20%

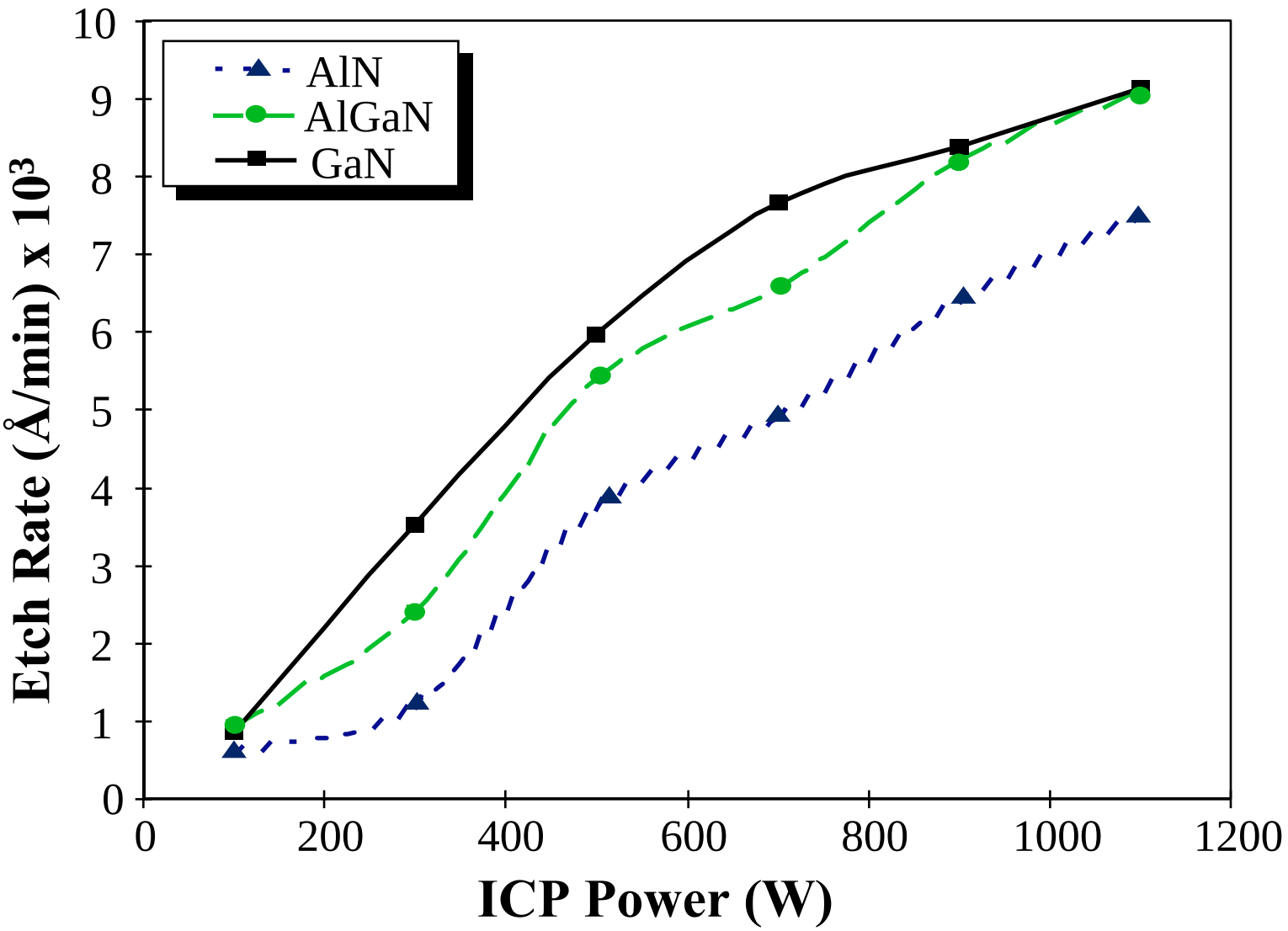

Figure 1. The etch rates of GaN, $Al_{.28}Ga_{.72}N$, and AlN as a function of ICP power.

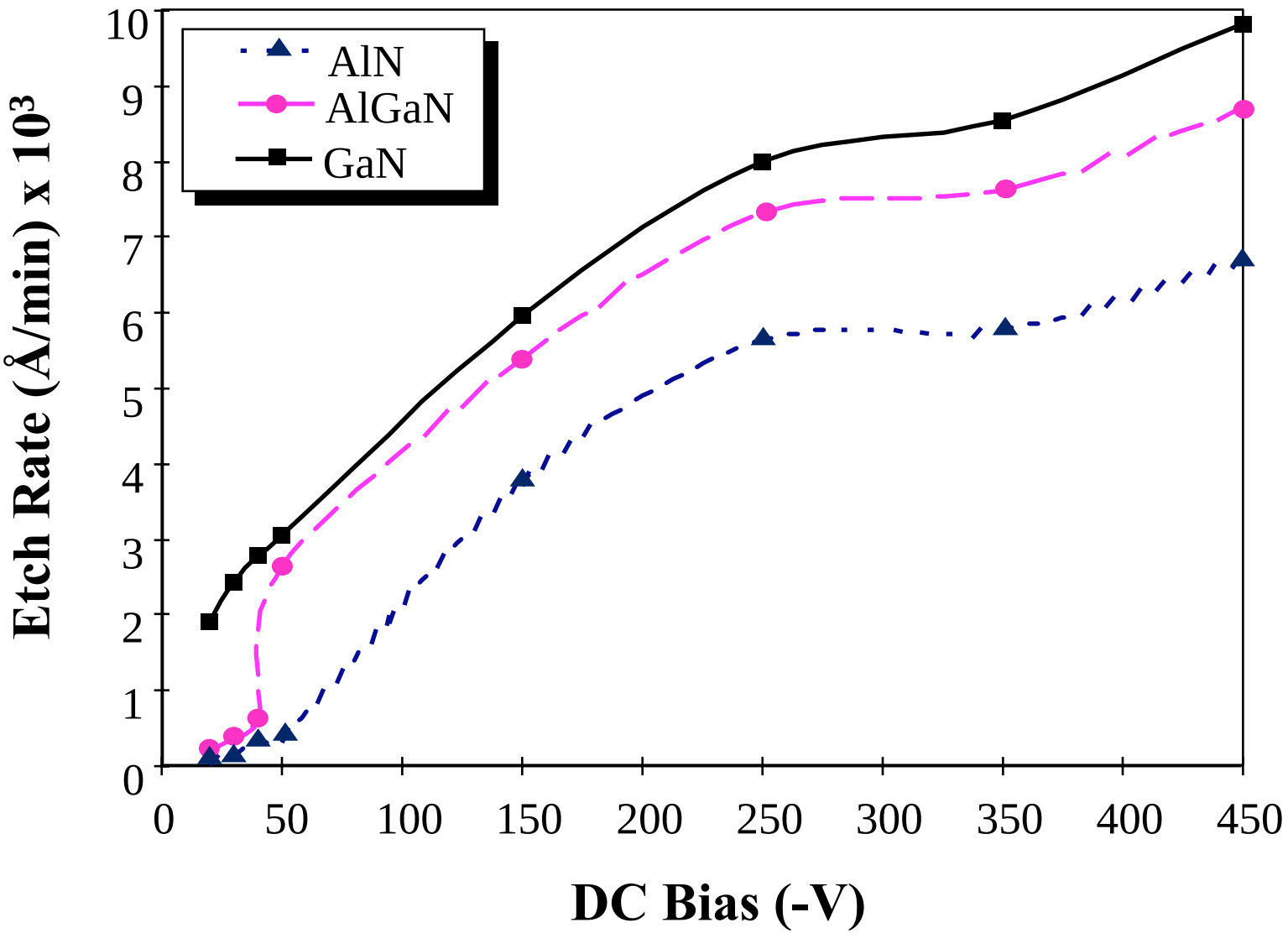

Figure 2. Typical etch profile using Ni as the etch mask under base conditions. Vertical striations were transferred from imperfections in the mask edge.

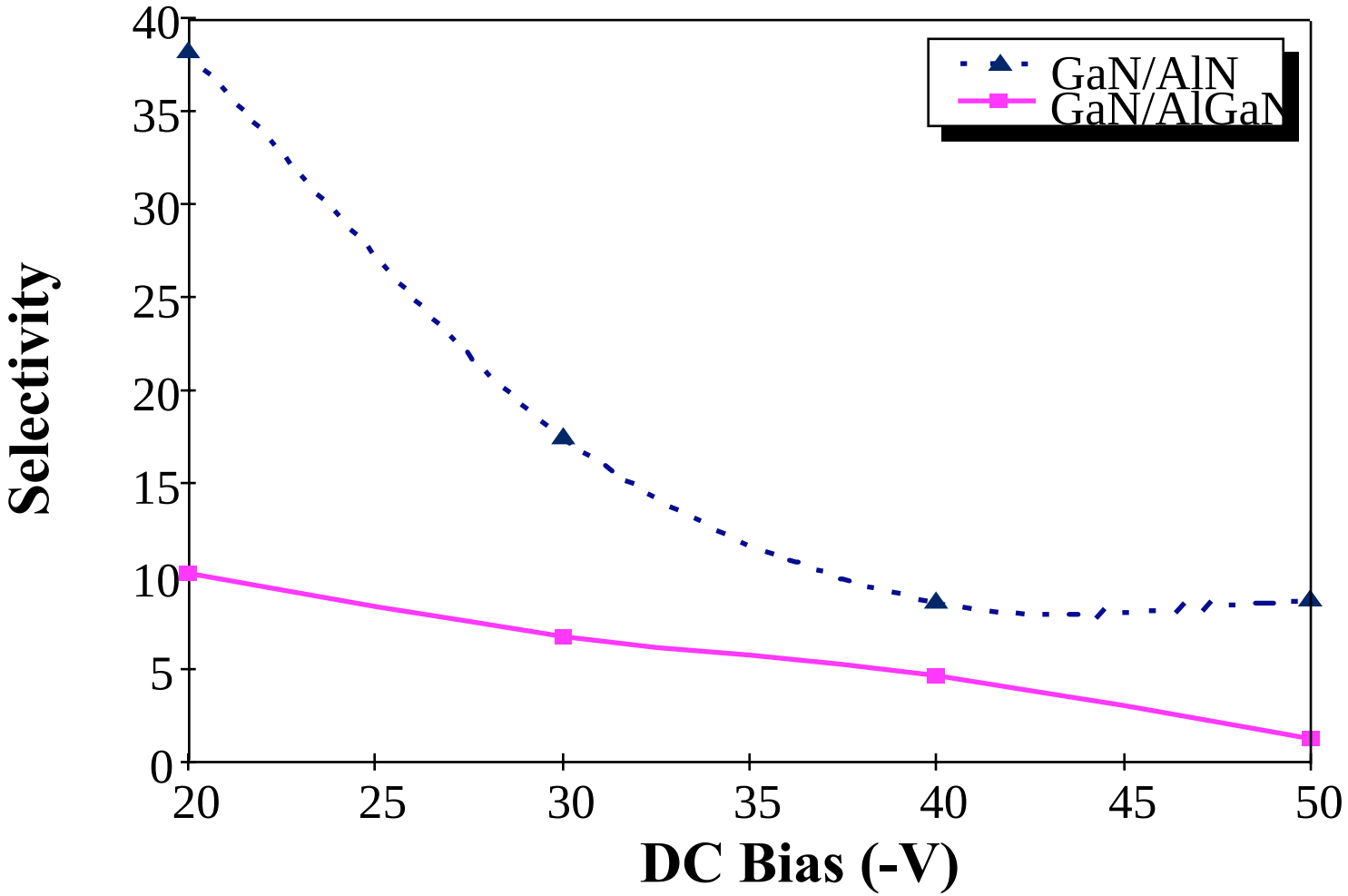

Figure 3. The etch rates of GaN, $Al_{.28}Ga_{.72}N$, and AlN as a function of DC bias.

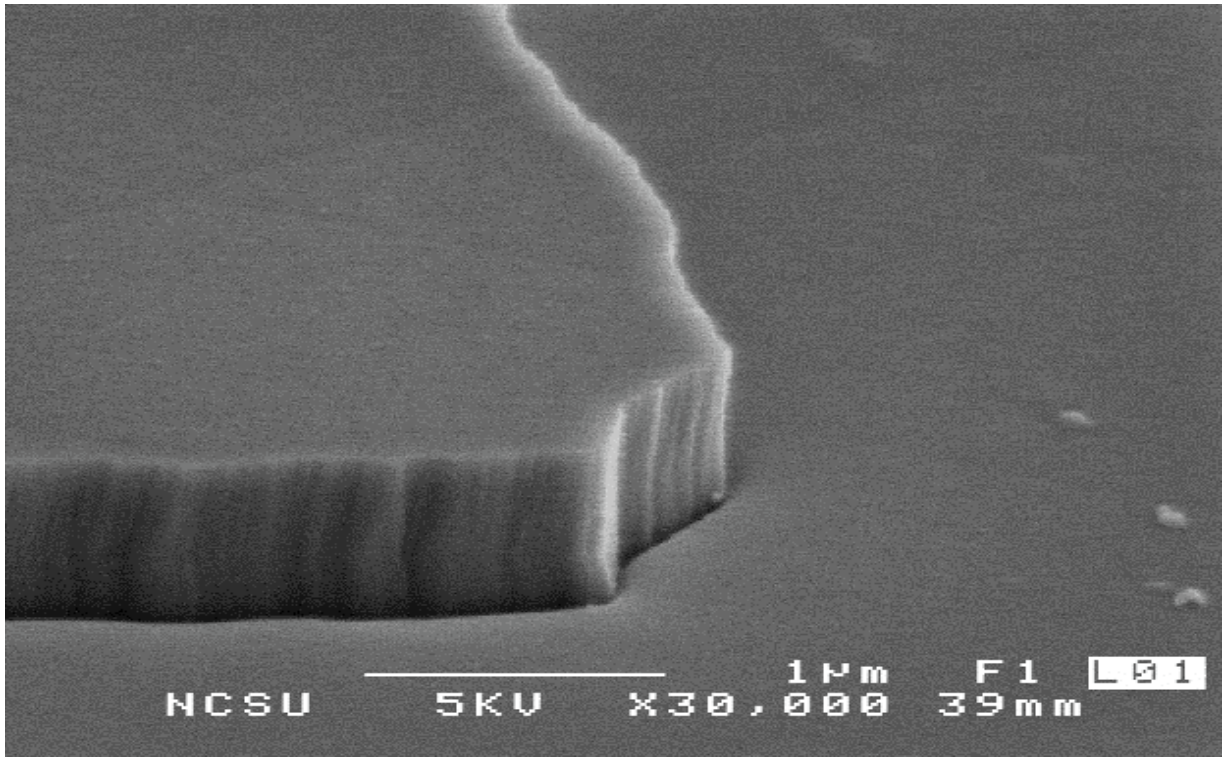

Figure 4. The selectivity of GaN relative to $Al_{.28}Ga_{.72}N$ and AlN as a function of DC bias. Values of selectivity were obtained from the GaN/AlN and GaN/ $Al_{.28}Ga_{.72}N$ etch rate ratios using the data for the individual etch rates shown in Figure 3.

CHAPTER 6 PAPER II

Selective and non-selective etching of GaN, AlGaN, and AlN using an inductively coupled plasma

S. A. Smith*, C. A. Wolden, M. D. Bremser, A. D. Hanser, and R. F. Davis
Department of Materials Science and Engineering, North Carolina State University, Raleigh, North Carolina 27695-7919

W. V. Lampert
Materials Directorate, Air Force Research Laboratory, Wright Patterson Air Force Base, OH 45433-7750

** Permanent address: Materials Directorate, Air Force Research Laboratory, Wright Patterson Air Force Base, OH 45433-7750*

The etching behavior of gallium nitride (GaN) has been systematically examined in an inductively coupled plasma (ICP) using Cl_2 and Ar as the reagents. Design of experiments (DOE) software was used to optimize the etch rate as well as determine any interactions between the parameters (ICP power, DC bias, and pressure). Interactions were found between the ICP power and pressure as well as the ICP power and DC bias. There were no interactions between the DC bias and pressure. Selective etching of GaN relative to AlN and $Al_{.28}Ga_{.72}N$ was achieved at low DC biases. At -20 V, the GaN etch rates were 38 times greater than AlN and a factor of 10 greater than $Al_{.28}Ga_{.72}N$.

Published in: 1997 *Proc. 22nd International Symposium on Compound Semicon.* 349-352

1. Introduction

The etching of GaN and the alloy $Al_xGa_{1-x}N$ has been a challenge for researchers due to the strong Ga-N and Al-N bonds as well as the chemical inertness of these materials. Different plasma sources, namely capacitively coupled, inductively coupled (ICP), and electron cyclotron resonance (ECR) have been employed to etch these materials. Capacitively coupled plasma sources such as that in reactive ion etchers (RIE) have produced low etch rates and non-vertical sidewalls etching these materials due in part to low plasma densities and high operating pressures.[1] High density plasma discharges such as (ECR) and (ICP) have distinct advantages over RIE systems in that they have higher plasma densities, lower operating pressures, and dc biases that are controlled separately from the plasma source. As a result, higher etch rates, vertical sidewalls, and lower etching induced damage occurs.

The etch selectivity of GaN relative to AlN and $Al_xGa_{1-x}N$ is of significant interest for the fabrication of $Al_xGa_{1-x}N$ based heterostructure devices. One example is the etch penetration through a GaN capping layer to the $Al_xGa_{1-x}N$ recessed gate in a high electron mobility transistor. Etching of the latter material should be minimal.

In this paper we report a systematic study of ICP etching of GaN as a function of DC bias, ICP power, and pressure using a Cl_2/Ar chemistry. To minimize the number of experiments, design of experiments (DOE) software was used to optimize the etch rates with respect to these parameters. Selectivity of GaN relative to AlN and $Al_xGa_{1-x}N$ is also discussed as a function of DC bias at low dc biases.

2. Experiment

2.1 System description

The ICP system was a custom built, 41 cm diameter by 58 cm tall, loadlocked stainless steel chamber. The RF power was coupled through a 32.4 cm diameter quartz window at the top of the chamber. The inductive source was a planar, 4 turn, 23 cm diameter copper coil which was connected to an RF Power Products 2 kW RF generator operating at 13.56 MHz via an autotuning matching network. Gas was fed into the chamber through a stainless steel shower ring positioned level with the bottom of the quartz window. A

water-cooled wafer chuck was mounted on a motor driven vertical translation stage which had 30.5 cm of travel. This allowed samples to be transferred between the loadlock chamber and the processing zone. A second 500 W RF source was connected to the wafer chuck to apply a controllable DC bias to the substrate. The substrate cooling water was maintained at 16°C to prevent the baking of photoresist during etching. The chamber was evacuated by an Alcatel 900 l/s turbomolecular pump which attained a base pressure of 10^{-7} torr.

A magnetic bucket containing 240 Nd-Fe-B magnets was mounted on the outside perimeter of the chamber to increase the plasma density by confining the electrons to a central volume within the chamber. This reduced electron losses due to collisions with the chamber walls. The ions were also confined due to electrostatic coupling with the electrons. The former were not directly affected by the magnetic field.[2]

2.2 Sample preparation

The GaN, AlN, and $Al_{.28}Ga_{.72}N$ samples used for this study were epitaxially grown on 6H-SiC-(0001) substrates via metalorganic vapor phase epitaxy (MOVPE) using trimethylaluminum (TMA) and triethylgallium (TEG) as the Al and Ga sources, respectively, and NH_3 as the nitrogen source.[3,4] An ≈100nm AlN buffer layer was deposited on the SiC substrates prior to the growth of the GaN and the $Al_{.28}Ga_{.72}N$. Preparation of the samples for etching employed the sequence of applying a Ni coating, patterning with photoresist, and dipping into HNO_3 to etch the Ni and into acetone to remove the photoresist. Just prior to entry into the etching system, the samples were dipped into HCl for 10 minutes to remove oxygen and carbon contaminants. Samples were attached to a 7.6 cm diameter anodized aluminum transport plate using vacuum grease which was mounted onto the wafer chuck. After entry into the system a base pressure of $\leq 5*10^{-7}$ torr was attained before the etching experiments were initiated.

3. Results

3.1 Etch rate optimization

For this study three parameters were optimized: the ICP power, DC bias, and pressure were varied, while the gas flows and concentrations were held constant at 20 sccm Cl_2 and 5 sccm Ar. The ranges for the 3 varied parameters were as follows: ICP power = 100-1100 W, DC bias = 50-450 V, and pressure = 1-11 mtorr. Previous experiments had shown that changing the gas flow rates and concentration minimally affected the etch rates (<20%). The etch depths were measured using a Dektak profilometer on at least three different points on each sample.

To determine the effects of interactions between parameters and their affect on etch rate and to optimize the etch rate SAS JMP statistical softwarewas employed which reduced the total number of experiments from 150 to 20. A central composite design was chosen as it uses five levels of each parameter and and accounts for any curvature in the response. Past experiments have shown that none of the parameters behave linearly with the etch rate. Table I shows the design matrix of the parameters which were varied and the resultant etch rates. As can be seen from this table, there are 15 different experiments with the center point repeated 6 times.

Figure 1 is a plot of contours of GaN etch rate derived from the data in Table I. In this type of plot, and in the case of Figure 1, one parameter (pressure) was varied while the other two are on the x (ICP power) and y (DC bias) axes. The individual contours are of equal response and have a step increase of 1000 Å/min between lines. This type of analysis can be very useful when a process window must be identified when there are multiple responses.

A plot of the interaction profiles between the different parameters are shown in Figure 2. The interaction plots between the DC bias and pressure reveal that there is no interdependence between them; whereas, the ICP power and pressure are highly dependent on each other. It was observed that the optimum pressure for etching increased with increasing ICP power. There is also a dependence between the DC bias and the ICP power.

The predictions by the DOE software were checked experimentally at 5 different points and can be seen in Figure 3. The parameters were as follows: (1) ICP=1100 W,

Bias=-428 V, Pressure=6 mtorr, (2) ICP=960 W, Bias=-174 V, Pressure=9 mtorr, (3) ICP=1750 W, Bias=-600 V, Pressure=12 mtorr, (4) ICP=370 W, Bias=135 V, Pressure=2 mtorr, (5) ICP=270 W, Bias=410 V, Pressure=4 mtorr. With the exception of sample 3, all of the points were within original input parameter ranges previously stated. Sample 3 was well outside of the original ranges; however, there was only a 8.6% difference between the actual and predicted etch rates. The highest error was found for sample 5 at 20%.

3.2 Selective etching

Selective etching of GaN relative to AlN and $Al_{.28}Ga_{.72}N$ was achieved at low DC biases. All materials were etched concurrently to insure an accurate comparison. The experimental parameters were 500 W ICP power, 5 mtorr pressure, and a -20 to -50 V variable DC bias. Figure 4 shows the selectivity of GaN as ratios of the etch rate of this material to that of AlN and $Al_{.28}Ga_{.72}N$. At -50 V, the selectivity between GaN and AlN was 8.5; whereas, it was only 1.2 between the GaN and $Al_{.28}Ga_{.72}N$. The greatest selectivities for GaN were found at a bias of -20 V, a factor of 38 over AlN and approximately 10 over $Al_{.28}Ga_{.72}N$. These differences in etch rates are consistent with the different bond energies between Ga-N and Al-N of 8.92 eV/atom and 11.52 eV/atom, respectively.[5] A second factor is the lower volatility of $AlCl_x$ relative to $GaCl_x$. Since lower DC biases were used to attain the selective etching, there is a tradeoff between the selectivity and the total etch rate.

3.3 Summary

Dry etching of GaN has been investigated in an ICP system produced in the authors' laboratories using Cl_2 and Ar as the process gases. Design of experiments software was used to both optimize the parameters and to determine the interactions between the different parameters. Interactions were observed between the ICP power and pressure as well as the ICP power and the DC bias. There was no interaction between the DC bias and the pressure. Selective etching of GaN relative to AlN and $Al_{.28}Ga_{.72}N$ was achieved at low DC biases. Selectivities of 38 between GaN and AlN and 10 between GaN and $Al_{.28}Ga_{.72}N$ were obtained at a DC bias of -20V. These results are of potential interest for

the fabrication of $Al_xGa_{1-x}N$ based heterostructure devices. Research is ongoing to quantify the effects of plasma induced damage and to better understand the underlying mechanisms.

This work was supported by the Office of Naval Research under contract No. N00014-96-1-0765. Colin A. Wolden acknowledges support as an NRC/ARO postdoctoral fellow. Scott A. Smith wishes to acknowledge Claude Woods from the University of Wisconsin for help in the design of the ICP system and U.S. Air Force PALACE Knight program.

1. M. E. Lin, Z. F. Fan, Z. Ma, L. H. Allen, and H. Morkoç, Appl. Phys. Lett. **64** (7), 887 (1994).

2. E. R. Lory, Solid State Technology (Nov.), 117 (1984).

3. M. D. Bremser, W. G. Perry, T. Zheleva, N. V. Edwards, O. H. Nam, N. Parikh, D. E. Aspnes, and R. F. Davis, MRS Internet J. Nitride Semicond. Res. **1**, 8 (1996).

4. A. D. Hanser, C. A. Wolden, W. G. Perry, R. Therrien, and R. F. Davis, (in preparation).

5. R. J. Shul, R. D. Briggs, S. J. Pearton, C. B. Vartuli, C. R. Abernathy, J. W. Lee, C. Constantine, and C. Barratt, Mater. Res. Soc. Symp. Proc. **449**, 969 (1996).

Table I - Design matrix for etch rate optimization of GaN thin films.

Run	ICP Power(W)	DC Bias(-V)	Pressure(mtorr)	Etch Rate(Å/min)
1	303	131	3	3730±40
2	303	131	9	1940±90
3	600	250	6	7760±80
4	303	369	3	6380±140
5	303	369	9	3960±60
6	600	250	6	7770±60
7	897	131	3	7050±100
8	897	131	9	7200±200
9	600	250	6	7790±90
10	897	369	3	10920±360
11	897	369	9	9520±380
12	600	250	6	7680±50
13	100	250	6	940±20
14	1100	250	6	11480±330
15	600	250	6	7840±80
16	600	50	6	2120±210
17	600	450	6	10630±250
18	600	250	6	7630±90
19	600	250	1	5020±140
20	600	250	11	5650±160

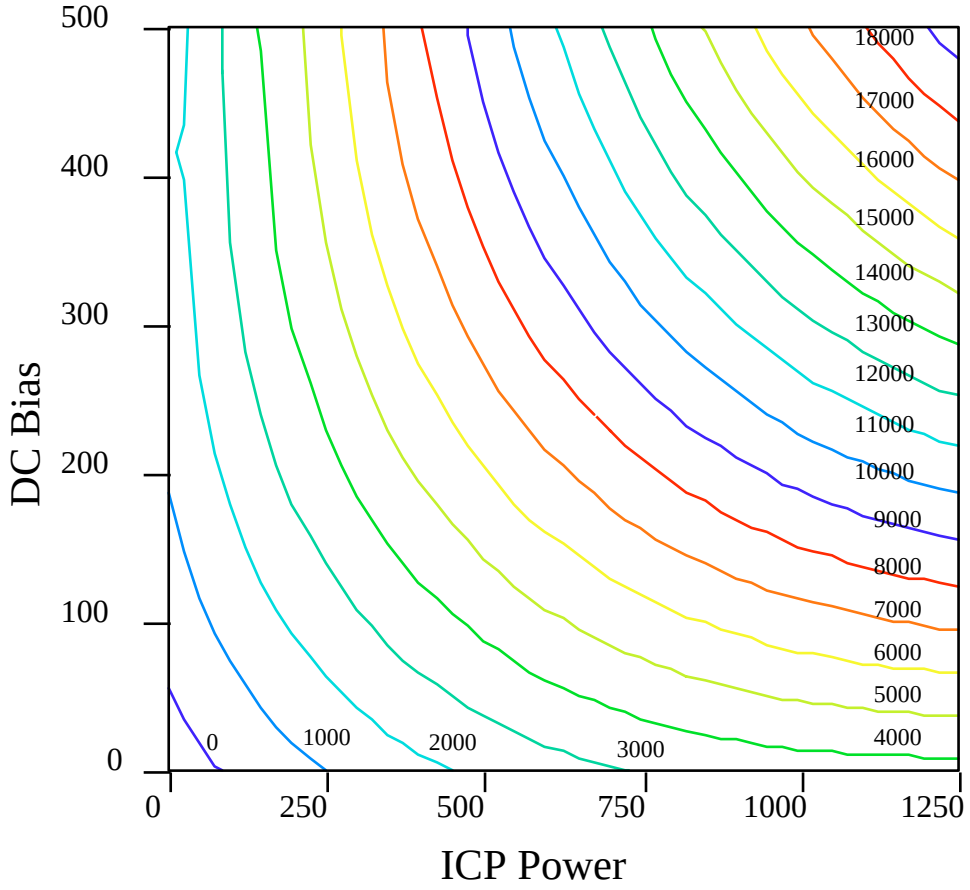

Figure 1. Contour plot derived from the data in Table I of etching rate of GaN as a function of ICP power and DC bias at 5 mTorr. The contours signify etch rate in Å/min.

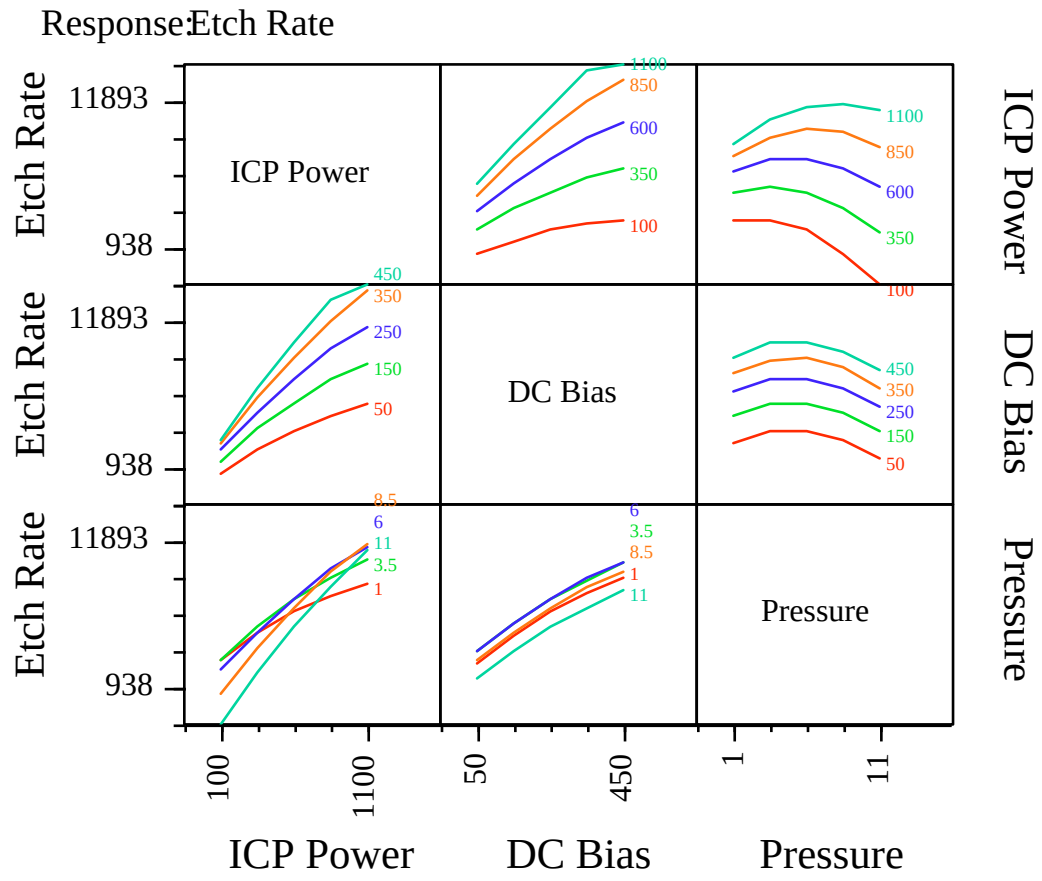

Figure 2. Interaction profiles that show the interdependence between ICP power, DC bias, and pressure on the etch rate of GaN.

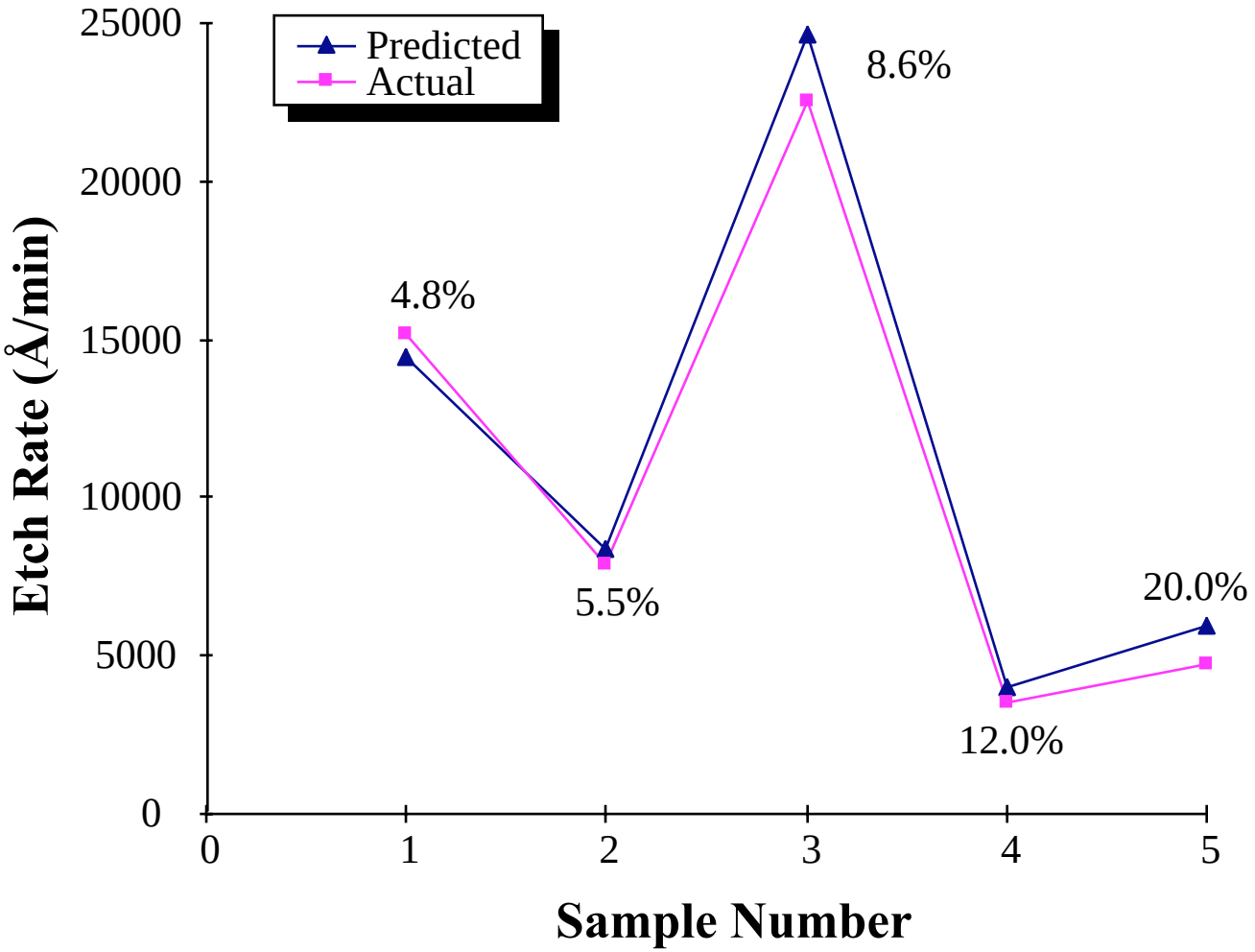

Figure 3. Comparison of experimental and predicted GaN etch rate from studies used to test the accuracy of the DOE model. See text for parameters.

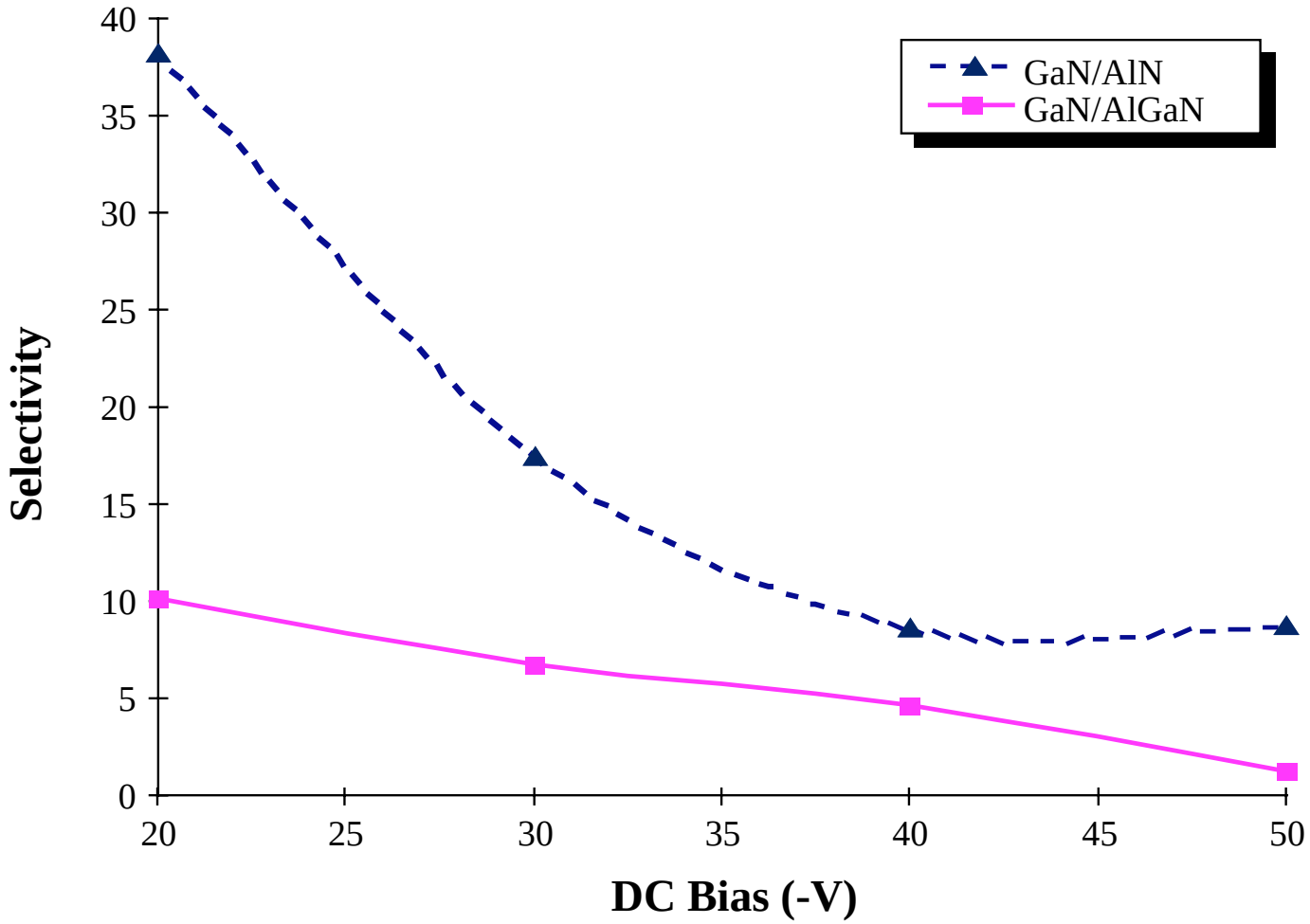

Figure 4. The selectivity of GaN relative to $Al_{.28}Ga_{.72}N$ and AlN as a function of DC bias. Values of selectivity were obtained from the GaN/AlN and GaN/ $Al_{.28}Ga_{.72}N$ etch rate ratios using the data for the individual etch rates shown in Figure 3.

CHAPTER 7 PAPER III

Selective etching of GaN over AlN using an inductively coupled plasma and an $O_2/Cl_2/Ar$ chemistry

S. A. Smith and W. V. Lampert
Materials and Manufacturing Directorate, Air Force Research Laboratory, Wright Patterson Air Force Base, OH 45433-7750

P. Rajagopal, A. D. Banks, D. Thomson, and R. F. Davis
Department of Materials Science and Engineering, North Carolina State University, Raleigh, North Carolina 27695-7919

An alternative method for achieving etching selectivity between GaN and AlN has been demonstrated. The etch rate of AlN was significantly decreased by the addition of a low concentration of O_2 to a Cl_2-Ar mixture in an inductively coupled plasma (ICP) etching system. The etch rate of GaN in the O_2-containing plasma was approximately 15% less than the plasma without the O_2 for the same parameters. The pressure and the ICP power were varied to achieve a maximum selectivity of 48 at a pressure of 10 mTorr, a DC bias of –150 V, and an ICP power of 500 W. The etch rates of GaN and AlN at these parameters were 4,800 Å/min and 100 Å/min, respectively.

INTRODUCTION

The application of growth techniques which substantially reduce the density of dislocations, e.g., lateral epitaxial overgrowth [1] and pendeo-epitaxy [2], should allow the potential for high performance optoelectronic and microelectronic devices to be realized [3]. The device processing procedure, including plasma etching, must also be of the highest caliber. Much of the attention in plasma etching research in the III-nitrides has been focused on etch rate optimization and etch profiles. Both of these aspects have advanced to the point of commercial viability. Etch rates ≥ 1 μm/min have been achieved using the mixtures ICl/Ar and BCl_3/Cl_2 [4,5]. With high resolution masking, highly anisotropic and smooth sidewalls can also be achieved. Other important properties of any plasma etching process are the degree of ion-induced damage (electrical and physical) and the selectivity of the etchants. Selectivity is important for applications such as the processing of high electron mobility transistors or any other heterojunction device where the etching must stop at a particular buried layer.

Selectivity in etching between GaN and AlN is the ratio of the etch rates of these two materials. Until recently the achievement of selectivity between GaN and AlN had minimal success in the nitride community. The ratios were either very low (≤10) or the GaN etch rates were low. Both should be moderately high for this property to be commercially useful. Vartuli *et al.* [5,6] demonstrated a selectivity of 10 between GaN and AlN using an electron cyclotron resonance etching system, but the etch rates were not stated. Smith *et al.*[7] achieved a selectivity of 38 between these two materials using ICP etching and low DC biases (< -50 V). The etch rate of GaN was approximately 2000 Å/min. This is the highest value reported while attaining high selectivity; however, for commercial purposes this rate should be increased.

The method employed by Smith *et al.*[7] relies on the fact that the etching is initiated at a lower bias for the GaN than for the AlN. This was attributed to the higher bond strength of AlN. In this present research a different method for attaining selectivity between GaN and AlN has been used, namely, the introduction of a small concentration of O_2 into the ICP system with the Cl_2 and Ar.

EXPERIMENTAL PROCEDURE

The GaN and AlN samples used for this study were epitaxially grown on 6H-SiC-(0001) substrates via metalorganic vapor phase epitaxy (MOVPE) using trimethylaluminum (TMA) and triethylgallium (TEG) as the Al and Ga sources, respectively, and NH_3 as the nitrogen source.[8,9] An ≈100nm monocrystalline AlN buffer layer was deposited on the SiC substrates prior to the growth of the GaN. Preparation of the samples for etching employed the sequence of applying a Ni coating, patterning with photoresist, dipping into HNO_3 to remove the Ni, and into acetone to remove the photoresist. Just prior to placement into the etching system, the samples were sequentially dipped into acetone, methanol, and 10% HCl acid for 10 minutes each to degrease and remove the carbon contaminants. Samples were attached to a 7.6 cm diameter anodized aluminum transport plate using vacuum grease which was mounted onto the wafer chuck. A base pressure of $\leq 5*10^{-7}$ Torr was attained prior to etching. The etch rates were determined by measuring the step heights using a Dektak II profilometer. The GaN and AlN samples were etched concurrently to insure accurate selectivity values.

The etch rate was determined as a function of pressure and ICP power. The DC bias was held constant at –150 V. A lower DC bias would have resulted in slow GaN etch rates, thus, defeating the purpose of this type of selectivity. Using higher biases would have increased the AlN etch rates too much, lowering the selectivity. The pressure was varied from 5 to 20 mTorr in steps of 5 mTorr. Once an optimum pressure for selectivity was determined, the ICP power was varied from 300 to 800 W. There were two similar chemistries used for these experiments, namely, a mixture (flow rate) of O_2 (2 sccm) and Cl_2 (18 sccm) with and without the addition of Ar (5 sccm). Though we previously determined that the addition of Ar did not significantly enhance the GaN etch rates in pure Cl_2 [7], it was added to increase the plasma density that was significantly decreased by the addition of O_2. This was verified through the use of a Langmuir probe.

RESULTS

Figure 1 shows a plot of the etch rates of GaN and AlN in the Cl_2-O_2 and Cl_2-O_2-Ar chemistries as a function of total pressure. At 5 mTorr, the etch rates were similar for both chemistries. At 10 mTorr, the GaN etch rate in the chemistry without the Ar decreased while the one with the Ar increased slightly. Beyond 10 mTorr, the GaN etch rates decreased considerably and in parallel for both chemistries. The AlN etch rates were eventually constant and similar throughout the entire pressure range for both chemistries. The AlN etch rates were extremely low (≤ 100 Å/min) at 10 mTorr and beyond, which was the basis of the selectivity studies.

Figure 2 shows the selectivity as a function of pressure for both chemistries. The addition of Ar increased the plasma density from $7.963*10^{16}/m^3$ to $1.050*10^{17}/m^3$, which increased both the GaN etch rate and the selectivity, but not the AlN etch rate. Thus, the ion density was not the rate limiting factor for the AlN. A maximum selectivity of 48 was determined at 10 mTorr with a GaN etch rate of 4,800 Å/min. Above 10 mTorr the selectivity dropped considerably due to the much lower GaN etch rates. At 20 mTorr for both chemistries no step in the AlN detected with the profilometer, but due to resolution constraints we assumed a step of 50 Å. An AlN etch rate of zero Å/min at this pressure would be inconsequential, since the GaN etch rates were so low. As previously stated, the benefit of this type of selectivity is to achieve high selectivities over AlN at high GaN etch rates.

The GaN and AlN etch rates as well as selectivity as a function of ICP power are shown in Figure 3. The DC bias and pressure were held constant at -150 V and 10 mTorr, respectively in the Cl_2-O_2-Ar mixture. Their values were chosen because they resulted in a selectivity of 48 for 500 W ICP power, as shown in Figure 2. The selectivity sharply increased from 10 to 48 as the ICP power was increased from 300 W to 500 W. Above 500 W the GaN etch rate did increase, but the AlN etch rate also increased, resulting in a decrease in the selectivity to 30.

DISCUSSION

The underlying principal behind this selectivity is the passivation of the AlN layer through the formation of a stable oxide layer. Since *in situ* surface analysis techniques were not available, the question remains as to what happened to the GaN surface that allowed it to continue to etch in the presence of oxygen. Possible scenarios are that (1) an oxide does not form on the GaN, (2) an oxide does form but it is continually sputtered off and does not prevent the reaction between the Ga and Cl, or (3) an oxide does form and it has an etch rate similar to that of the GaN. It is important to note the similarity of the GaN etch rates between the $Cl_2/O_2/Ar$ and Cl_2/Ar chemistries; the former etched approximately 15% slower than the latter for the same settings.

It is expected that combining this technique with the one developed by Smith *et al.*[7] employing low DC biases would result in extremely high selectivities, but at lower GaN etch rates. This may be a viable solution if there is the necessity to stop at extremely thin layers (<50 Å) after etching through a GaN layer. Selectivities of 10 between GaN and $Al_{.28}Ga_{.72}N$ were accomplished using the low DC bias method; thus, it is expected that higher selectivities will be attained by combining the two methods.

In summary, an alternative method for achieving ICP etching selectivity between GaN and AlN has been demonstrated. The addition of small concentrations of O_2 to a Cl_2-Ar chemistry passivates the AlN surface via the formation of aluminum oxide on the surface and significantly reduces the etch rate. The GaN etch rate was affected minimally by the addition of the O_2, thus, resulting in a high selectivity between the GaN and AlN. A maximum selectivity of 48 was achieved at a pressure of 10 mTorr, a DC bias of –150 V, and an ICP power of 500 W. The GaN etch rate at these parameters was 4,800 Å/min; the AlN etch rate was 100 Å/min. This technique should also work for $Al_xGa_{1-x}N$ but at reduced selectivities due to the lower Al concentration at the surface.

This work was supported by the Office of Naval Research under contract No. N00014-96-1-0765. Scott A. Smith wishes to acknowledge the U.S. Air Force PALACE Knight program.

1. T. Gehrke, K. J. Linthicum, D. B. Thomson, P. Rajagopal, A. D. Batchelor, and R. F. Davis, MRS Internet J. Nitride Semicond. Res. **4S1**, G3.2 (1999).

2. T. S. Zheleva, S. A. Smith, D. B. Thomson, K. J. Linthicum, P. Rajagopal, and R. F. Davis, J. Electron. Mater. **27**, 238 (1998).

3. C. B. Vartuli, S. J. Pearton, J. W. Lee, J. Hong, T. D. Mackenzie, C. R. Abernathy, and R. J. Shul, Appl. Phys. Lett. **69**, 1426 (1996).

4. S. A. Smith, W. V. Lampert, P. Rajagopal, D. Thomson, and R. F. Davis, to be published.

5. C. B. Vartuli, S. J. Pearton, J. W. Lee, A. Y. Polyakov, M. Shin, D. W. Greve, M. Skronowski, and R. J. Shul, Electrochem. Soc. **144**, 2146 (1997).

6. C. B. Vartuli, S. J. Pearton, J. D. Mackenzie, C. R. Abernathy, and R. J. Shul, Electrochem. Soc. **143**, L246 (1996).

7. S. A. Smith, C. A. Wolden, M. D. Bremser, A. D. Hanser, R. F. Davis, and W. V. Lampert, Appl. Phys. Lett. **71,** 3631 (1997).

8. A. D. Hanser, C. A. Wolden, and R. F. Davis, J. Electron. Mater. **27**, 238 (1998).

9. M. D. Bremser, W. G. Perry, T. Zheleva, N. V. Edwards, O. H. Nam, N. Parikh, D. E. Aspnes, and R. F. Davis, MRS Internet J. Nitride Semicond. Res. **1**, 8 (1996).

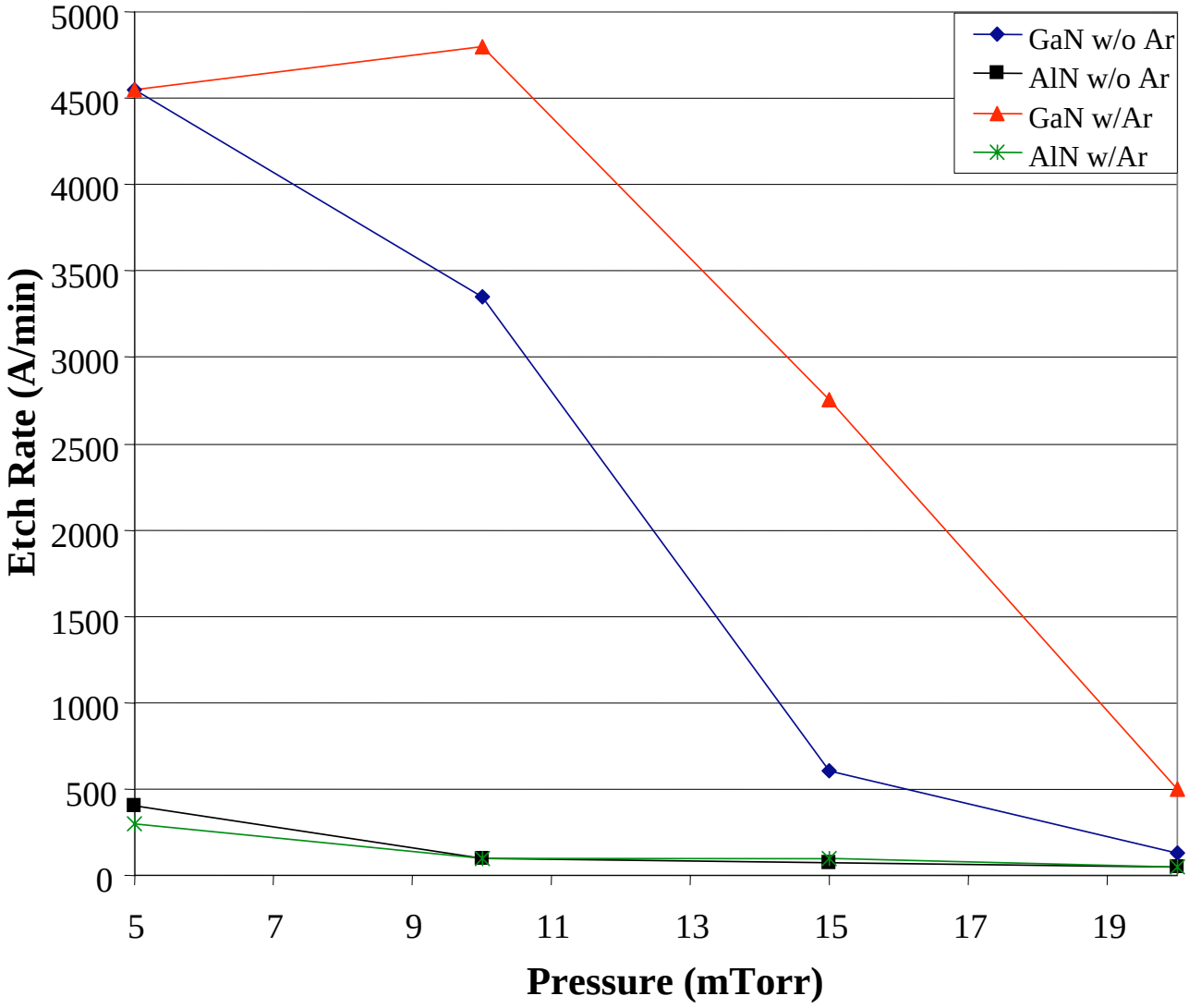

Figure 1. The etch rates of GaN and AlN as a function of pressure.

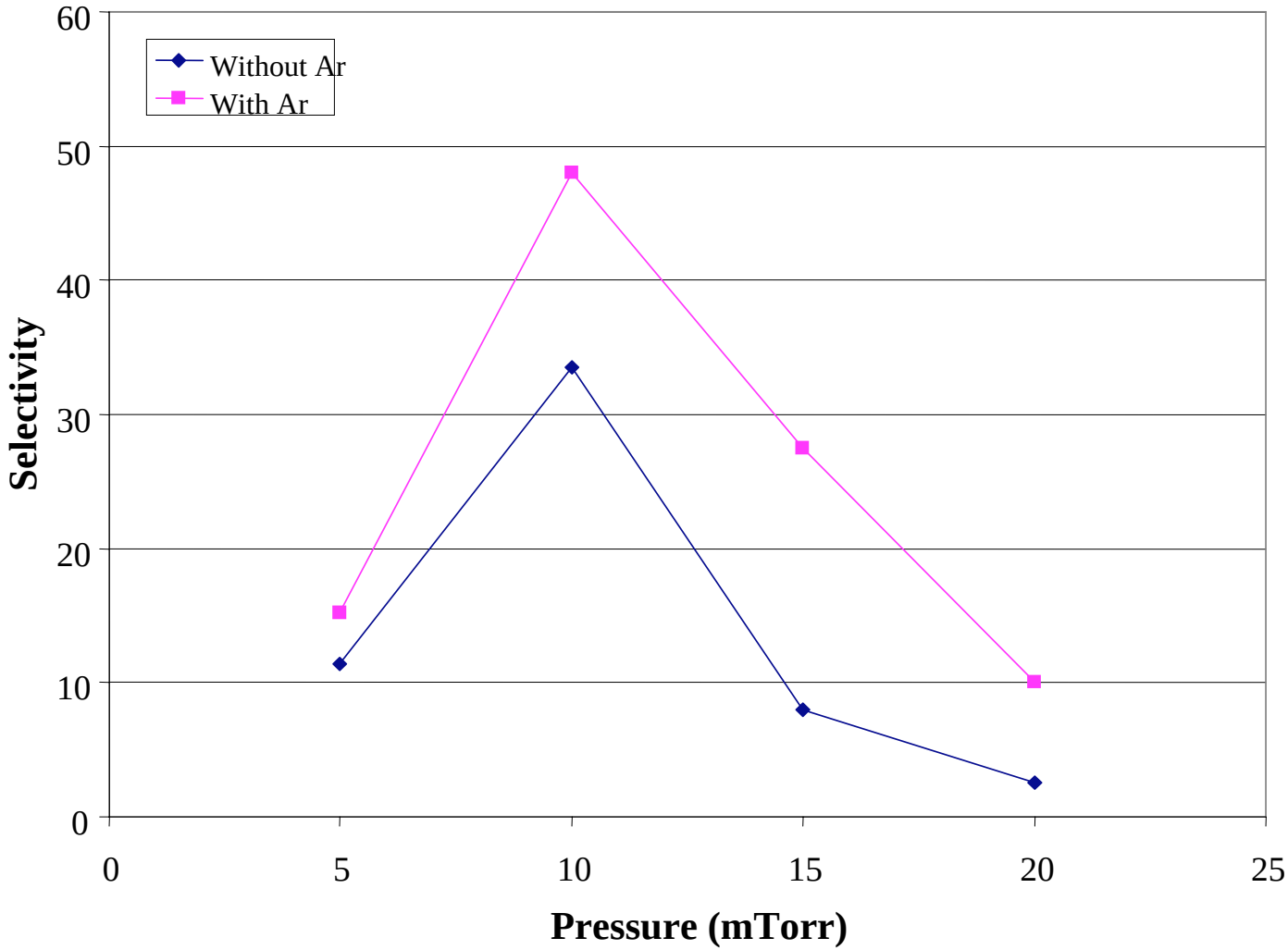

Figure 2. The selectivity of GaN over AlN as a function of pressure.

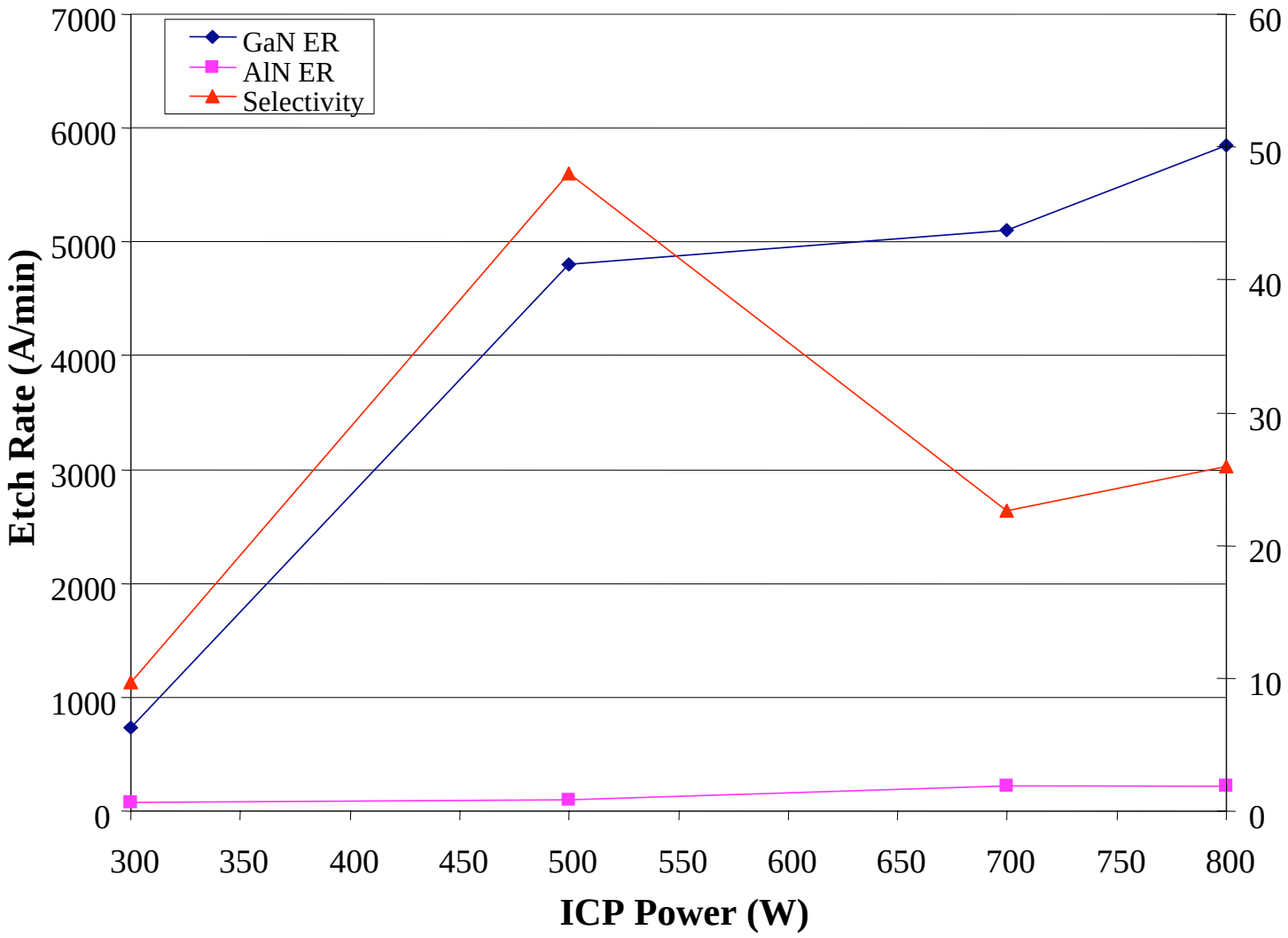

Figure 3. The etch rates of GaN and AlN, and the selectivity of GaN over AlN as a function of ICP power.

CHAPTER 8 PAPER IV

Etching optimization of GaN in an inductively coupled plasma containing BCl_3 and Cl_2

S. A. Smith and W. V. Lampert
Materials and Manufacturing Directorate, Air Force Research Laboratory, Wright Patterson Air Force Base, OH 45433-7750

P. Rajagopal, D. Thomson, and R. F. Davis
Department of Materials Science and Engineering, North Carolina State University, Raleigh, North Carolina 27695-7919

The etching behavior of gallium nitride (GaN) in an inductively coupled plasma (ICP) containing the process gas mixture of 10 % BCl_3 and 90 % Cl_2 has been investigated and optimized. Design of experiments (DOE) software was employed to determine both the optimum conditions for etching and the existence of any interactions between the etching parameters. The resultant DOE model, determined from the input parameter values and corresponding etch rates, was tested at five different points in the parameter space to ensure accuracy. The etch rates were highly dependent upon ICP power and DC bias and to a lesser extent upon system pressure. Parameter interactions were found between the ICP power and pressure and between the ICP power and the DC bias. For example, the maximum response of etch rate with respect to pressure changed as the ICP power changed. There was minimal interaction between the DC bias and the pressure. The error between the predicted etch rates and the actual etch rates ranged from 5% to 12%. A maximum etch rate of 16,700 Å/min was achieved.

The plasma etching of GaN has been accomplished by several research groups using various plasma technologies and chemistries [1-9]. The most successful research has been accomplished via the use of inductively coupled plasma (ICP) sources [9-10] and electron cyclotron resonance (ECR) sources [3-5]. Plasma densities for these sources are typically one order of magnitude higher than the capacitively coupled sources used in reactive ion etching (RIE). The ECR and ICP systems have distinct advantages over the capacitively coupled systems in that the etch rates are considerably higher and the sidewalls of the etched material are highly anisotropic due to the higher plasma density and the lower operating pressures, respectively. A major benefit of the ICP and ECR sources over the capacitively coupled sources is that the DC bias is controlled separately from the plasma source. This provides more control over the etching parameters.

The plasma chemistries used to etch GaN have been predominantly chlorine-based with the exception of the occasional use of iodine- [4], bromine- [2-4] and methane-based chemistries [1]. Etch rates to 1100 Å/min and 900 Å/min were achieved in an ECR system using $HI/H_2/Ar$ and $HBr/H_2/Ar$ chemistries, respectively. Methane-based chemistries have produced lower etch rates in the same system. Chlorine-based chemistries are the obvious choice due to the volatility of the group III chlorides. The combination of Cl_2 gas with H_2 and/or Ar has been the most commonly used. Etch rates to 9,800 Å/min for Cl_2/Ar have been achieved by the present authors [10]. The use of BCl_3 alone or with Ar has also been reported [8]. The etch rates of GaN achieved in the studies noted above are sufficiently high for practical applications; however, high plasma power and biases were employed due to the chemical stability of the GaN. The next logical step to increase the etch rates while lowering the power requirements was to alter the plasma chemistry. In this paper we report the results and conclusions of a study that employed design of experiments (DOE) software (SAS JMP) to (1) increase the etch rate of GaN under reduced ICP power and DC bias, (2) optimize the etching parameters for GaN using a gas mixture of BCl_3 and Cl_2 as the reagents, and (3) determine any interactions between these parameters with the fewest number of experiments. The performance of these studies without the software, assuming the three parameters ICP

power, DC bias, and pressure and 5 points per parameter, would have required 5^3, or 125 experiments. A parametric model was developed that fit the input data.

The GaN and AlN samples used for this study were epitaxially grown on on-axis 6H-SiC(0001) substrates via metalorganic vapor phase epitaxy (MOVPE) using trimethylaluminum (TMA) and triethylgallium (TEG) as the Al and Ga sources, respectively, and NH_3 as the nitrogen source [11-12]. An ≈100nm AlN buffer layer was deposited on the SiC substrates prior to the growth of the GaN. Preparation of the samples for etching employed the sequence of applying a Ni coating, patterning with photoresist, and dipping into HNO_3 to etch the Ni and into acetone to remove the photoresist. Prior to entry into the etching system, the samples were dipped into 50% HCl acid for 10 minutes to remove carbon contaminants. Samples were attached to a 7.6 cm diameter anodized aluminum transport plate using vacuum grease that was mounted onto the wafer chuck. A base pressure of $\leq 5*10^{-7}$ Torr was attained after entry into the system and before the etching experiments were initiated.

The parameters and the ranges investigated were ICP power, 100-1100 W; DC bias, 50-450 V; and pressure, 1-11 mTorr. The flow rates of BCl_3 and Cl_2 were held constant at 2 sccm and 18 sccm, respectively. A Dektak profilometer was used to measure the etch depths. Three measurements were taken per sample and averaged in the determination of the etch rates.

A central composite response surface design was used for these experiments. This design allows the fitting of a curved surface, which was the expected response. Five different points were examined for each parameter to account for any curvature in the response. Table I shows the design matrix used for these experiments. Six of the twenty experiments were repeated for determination of the experimental variability or random error.

Figure 1 shows a prediction profile. It allows one to change one of the three parameters to determine it's affect on the other parameters and the etch rate for the selected settings. Two profiles are shown, one atop the other, to illustrate this effect. The ICP power was the parameter changed. As can be seen in this figure, the settings were 300 and 900 W ICP power for the top and bottom plots, respectively, -250 V DC bias for

both, and 6 mTorr pressure for both. From Figures 1(b) and 1(e) it can be seen that the line shape of the DC bias does not change with the changing ICP power, though the curve is shifted up to higher etch rates as was expected. This indicates minimal interaction between the ICP power and the DC bias. The response of the pressure to this change of ICP power was significant, and can be seen in Figures 1(c) and 1(f). As with the DC bias, the curve shifted up to higher etch rates, but more importantly, the shape of the curve changed. The maximum in etch rate in Figure 1(c) was at approximately 2 mTorr; however, after the change in ICP power in Figure 1(d) the maximum shifted to 6 mTorr. This indicates that there is an interaction between the ICP power and pressure.

Figure 2 is the same type of plot as Figure 1 with the settings at typical settings that would be used in GaN processing. For the settings of 600 W ICP power, -150 V DC bias, and 2 mTorr, it is apparent in Figure 2(a) that a maximum in the etch rate would be achieved with an increase in the ICP power. The model predicted a maximum at 1500 W; however, as the error in the model is large outside the range of data input, the maximum could not be precisely determined. The etch rate exhibited a linear dependence on the DC bias, as shown in Figure 2(b). This indicates that the energy of the bombarding ions, whether manifested in damage to the surface or in ion assisted desorption, may be rate limiting. Increasing the total pressure, as in the case of Cl_2/Ar etching of GaN [10], resulted in a maximum in the etch rate, as shown in Figure 2(c), which is believed to have been caused by the opposing combination of decreasing ion density and increasing reactive radical density. The etch rates of GaN attained in this research were considerably higher than those achieved when using Cl_2/Ar as the plasma chemistry [10]. The reason for this is not known at this time; however, diagnostic techniques are currently being employed to determine the role of BCl_3 in the etching process.

Figure 3 is a contour plot of the GaN etch rate obtained from the application of the DOE model. In this plot, one parameter (pressure) was fixed while the other two were varied, as shown on the x (ICP power) and y (DC bias) axes. Since the DOE software creates a model based upon the data in Table I, etch rates higher than the highest shown in this table will be predicted. Related plots can be developed with any of the three

parameters fixed and the other two varied on the x- and y-axes. This analysis is very useful for the determination of a process window when there are multiple responses such as etch rate, selectivity, and damage.

The results of the study of parameter interactions for the BCl_3/Cl_2 chemistry are presented in Figure 3. The numbers to the right of each curve in a given set represent the plasma parameter that is labeled on the right ordinate and associated with the given set. These sets of curves show the change in the response of the parameters labeled on the bottom of the plots as a function of the change in the parameters labeled on the right. If there were no interactions between the parameters, all of the etch rate curves in a particular box would be parallel, such as in the DC bias (ordinate) vs. pressure (abscissa) curves in Figure 4. In contrast there is a marked interdependence between the ICP power (ordinate) and the pressure (abscissa), and also between the ICP power (ordinate) and the DC bias (abscissa). This is helpful, for example, in the determination of the optimum pressure for a particular ICP power. These results also show that the maxima in pressure (ordinate) increases as the ICP power (abscissa) increases.

To test the accuracy of the DOE model, five experiments were performed to compare the predicted etch rates to the actual etch rates. The results are presented in Table II. The ranges for the parameters were representative of the ranges used when creating the DOE model. The outer limits of the parameters were avoided, since most practical applications of the information would fall in the middle of the ranges. The error between the predicted and actual etch rates ranged from 5% to 12%. This is reasonable, since the rms error was 665 Å/min, and some of the values of the parameters are close to the upper or lower limits where the reliability of the model is lower. An example of the reduction in accuracy of the model outside the input ranges is a recipe that is currently used for device processing, namely ICP power = 300 W, DC bias = -20 V, and pressure = 2 mTorr. This recipe is used because it imparts low damage to the GaN surface. The predicted etch rate for these parameters was 2440 Å/min; the actual etch rate was 2000 Å/min. This is an error of 18 %.

The resultant sidewalls were nearly vertical with faint vertical striations, as shown in Figure 5. Nickel was used as the mask due to its high tolerance to chlorine-containing

plasmas. The rough dark layer on the top is a portion of this mask that was not fully removed with an HNO_3 dip. The dark band at the bottom of the mesa is the AlN buffer layer. The quality of the masking process appears to be the biggest factor affecting the quality of the etched sidewalls. Photoresist was previously used as the mask resulting in either sloped sidewalls or severe vertical striations.

In summary, ICP etching of GaN has been accomplished using BCl_3 and Cl_2 as the process gases. Design of experiments software was employed to optimize the etching parameters and to determine any interactions between the parameters. Three types of plots were derived from the input data, namely, interaction profiles; contour plots; and prediction profiles. From the interaction profiles, it was found that there were interactions between the ICP power and pressure as well as between the ICP power and the DC bias. The accuracy of the DOE model was tested by performing five etch runs with parameter values falling within the ranges examined in the DOE model. The amount of error ranged from 5% to 12%. Etch rates as high as 16,700 Å/min were achieved.

This work was supported by the Office of Naval Research under Contract No. N00014-96-1-0765 (C. Wood, monitor). Scott A. Smith wishes to acknowledge the U.S. Air Force PALACE Knight program.

1. S. J. Pearton, C. R. Abernathy, F. Ren, J. R. Lothian, P. W. Wisk, and A. Katz, J. Vac. Sci. Technol. A **11**, 1772 (1993).

2. S. J. Pearton, C. R. Abernathy, and F. Ren, Appl. Phys. Lett. **64,** 2294 (1994).

3. C. B. Vartuli, S. J. Pearton, C. R. Abernathy, R. J. Shul, A. J. Howard, S. P. Kilcoyne, J. E. Parmeter, and M. Hagerott-Crawford, J. Vac. Sci. Technol. A **14**, 1011 (1996).

4. C. B. Vartuli, S. J. Pearton, J. W. Lee, J. Hong, T. D. Mackenzie, C. R. Abernathy, and R. J. Shul, Appl. Phys. Lett. **69** (10), 1426 (1996).

5. R. J. Shul, S. P. Kilcoyne, M. Hagerott, J. E. Parmeter, C. B. Vartuli, C. R. Abernathy, and S. J. Pearton, Appl. Phys. Lett. **66,** 1761 (1995).

6. C. B. Vartuli, J. D. MacKenzie, J. W. Lee, C. R. Abernathy, S. J. Pearton, and R. J. Shul, Appl. Phys. Lett. **80,** 3705 (1996).

7. J. W. Lee, J. Hong, J. D. MacKenzie, C. R. Abernathy, and S. J. Pearton, J. Elec. Mat. **26**, 290 (1997).

8. G. F. McLane, L. Casas, S. J. Pearton, and C. R. Abernathy, Appl. Phys. Lett. **66,** 3328 (1995).

9. Y. H. Lee, H. S. Kim, G., G. Y. Yeom, J. W. Lee, M. C. Yoo, and T. I. Kim, J. Vac. Sci. Technol. A **16**, 1478 (1998).

10. S. A. Smith, C. A. Wolden, M. D. Bremser, A. D. Hanser, R. F. Davis, and W. V. Lampert, Appl. Phys. Lett. **71,** 3631 (1997).

11. A. D. Hanser, C. A. Wolden, and R. F. Davis, J. Electron. Mater. **27**, 238 (1998).

12. M. D. Bremser, W. G. Perry, T. Zheleva, N. V. Edwards, O. H. Nam, N. Parikh, D. E. Aspnes, and R. F. Davis, MRS Internet J. Nitride Semicond. Res. **1**, 8 (1996).

Table I - Design matrix used for etch rate optimization of GaN(0001) thin films.

Run	ICP Power (W)	**DC Bias** (-V)	**Total Pressure** (mTorr)	**Etch Rate** (Å/min)
1	303	131	3	5470±20
2	303	131	9	3490±30
3	600	250	6	11010±190
4	303	369	3	9450±240
5	303	369	9	5780±60
6	600	250	6	10700±70
7	897	131	3	11170±340
8	897	131	9	10210±180
9	600	250	6	10580±240
10	897	369	3	16040±150
11	897	369	9	15460±380
12	600	250	6	10650±220
13	100	250	6	2090±20
14	1100	250	6	16220±270
15	600	250	6	10590±200
16	600	50	6	5330±70
17	600	450	6	14700±150
18	600	250	6	10430±200
19	600	250	1	9960±90
20	600	250	11	7840±30

Table II – Accuracy tests for DOE model.

Run Number	ICP Power (W)	DC Bias (-V)	Pressure (mTorr)	Predicted (Å/min)	Actual (Å/min)	% Difference
1	400	250	7	7420	8330	12
2	700	100	4	8500	7850	8
3	650	325	9	11350	10800	5
4	1000	315	2	15840	16700	5
5	300	75	5	3530	4000	12

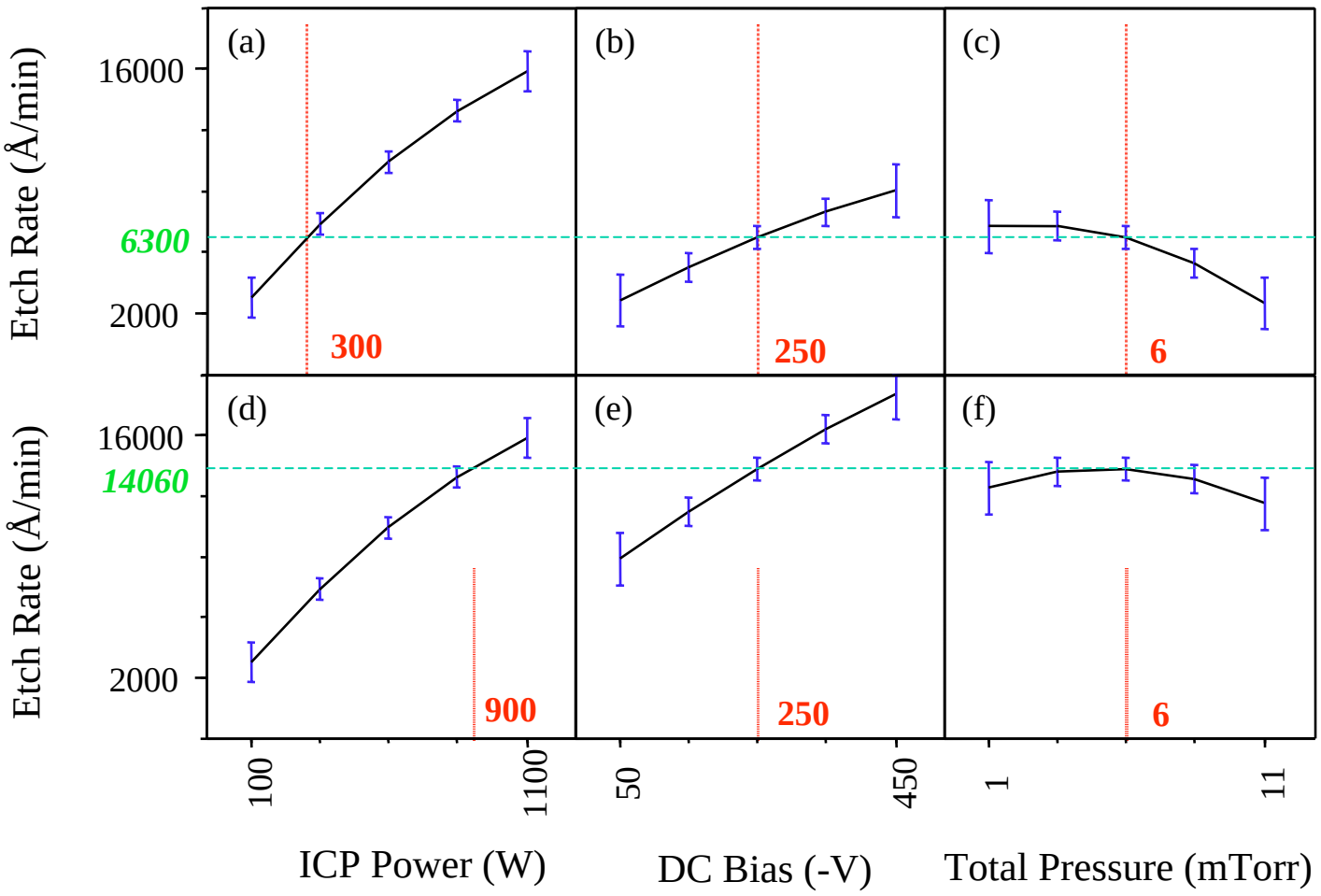

Figure 1. Prediction profile of GaN etch rates obtained from the application of the DOE model. The horizontal dashed lines represents the etch rates of 6300 and 14060 Å/min for the two sets of parameter values, and the vertical dotted lines correspond to the parameter values at the bottom.

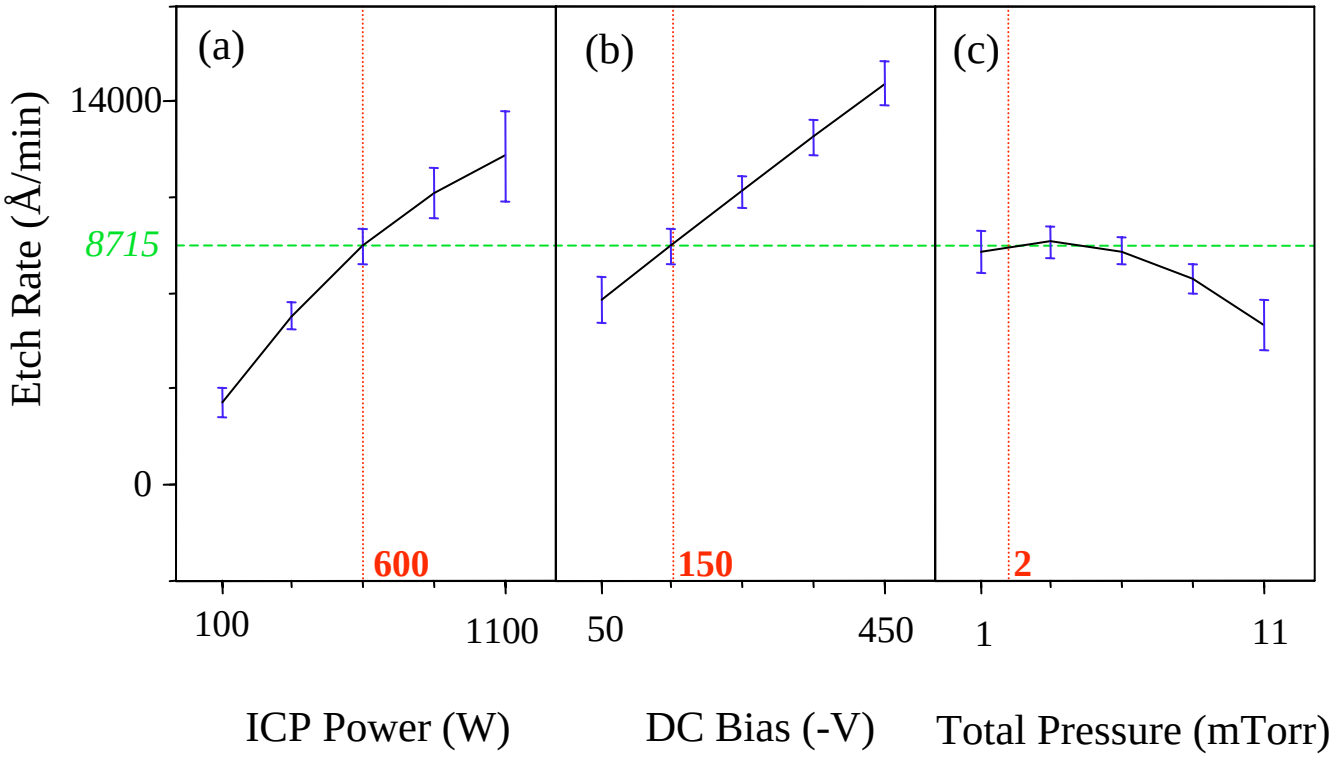

Figure 2. Prediction profile of GaN etch rates obtained from the application of the DOE model. The horizontal dashed line represents the etch rate of 8715 Å/min, and the three vertical dotted lines correspond to the parameter values at the bottom.

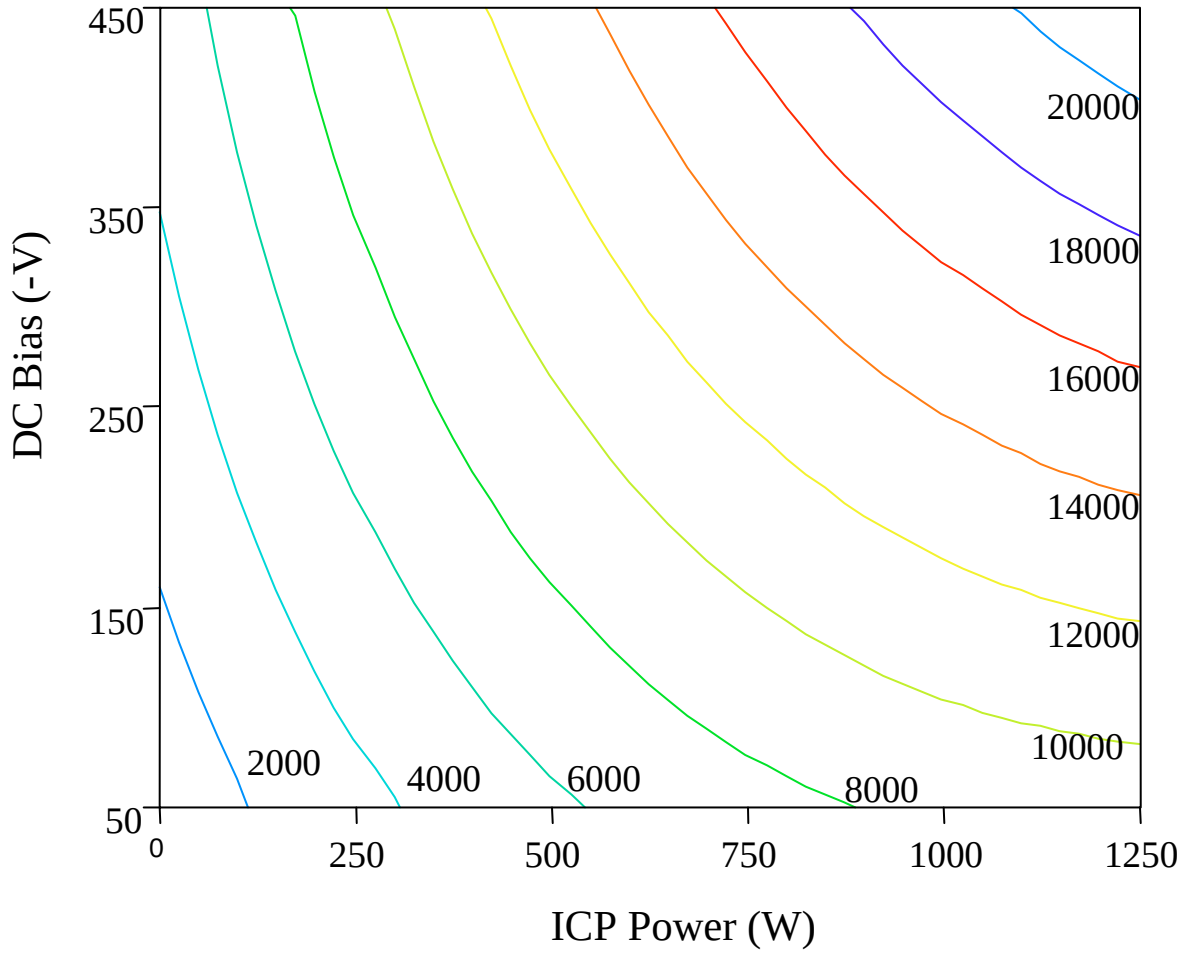

Figure 3. Contour plot obtained from the application of the DOE model. The x-axis represents the ICP power, and the y-axis represents the DC bias. Each given contour represents the indicated etch rate in Å/min for a process pressure of 2 mTorr.

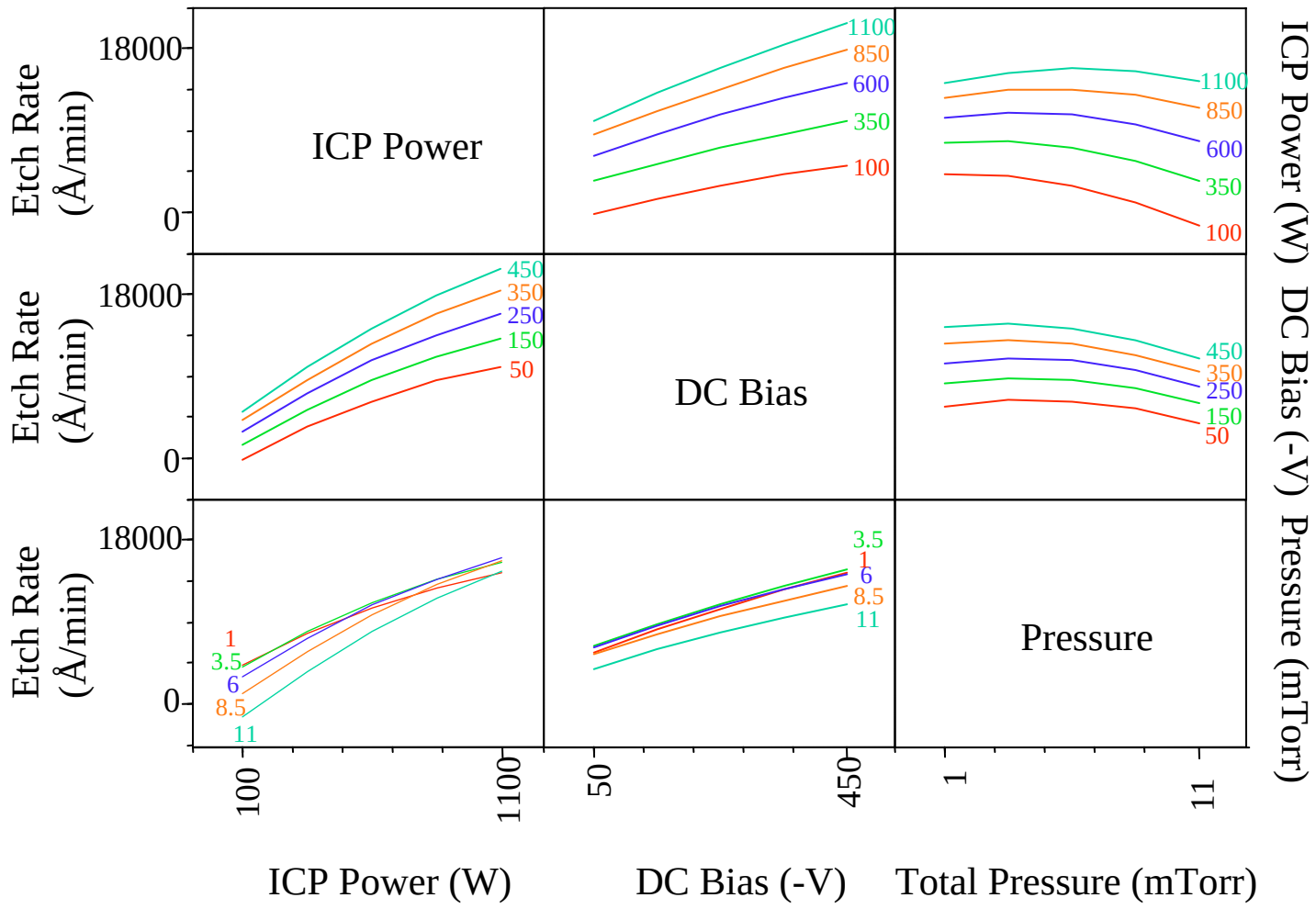

Figure 4. Interaction profiles that show the interdependence between ICP power, DC bias, and total pressure on the etch rate of GaN. The numbers given at the endpoints of the set of curves in each square are the values of the variable denoted on the ordinate on the right side of the figure; there is no scale associated with this ordinate.

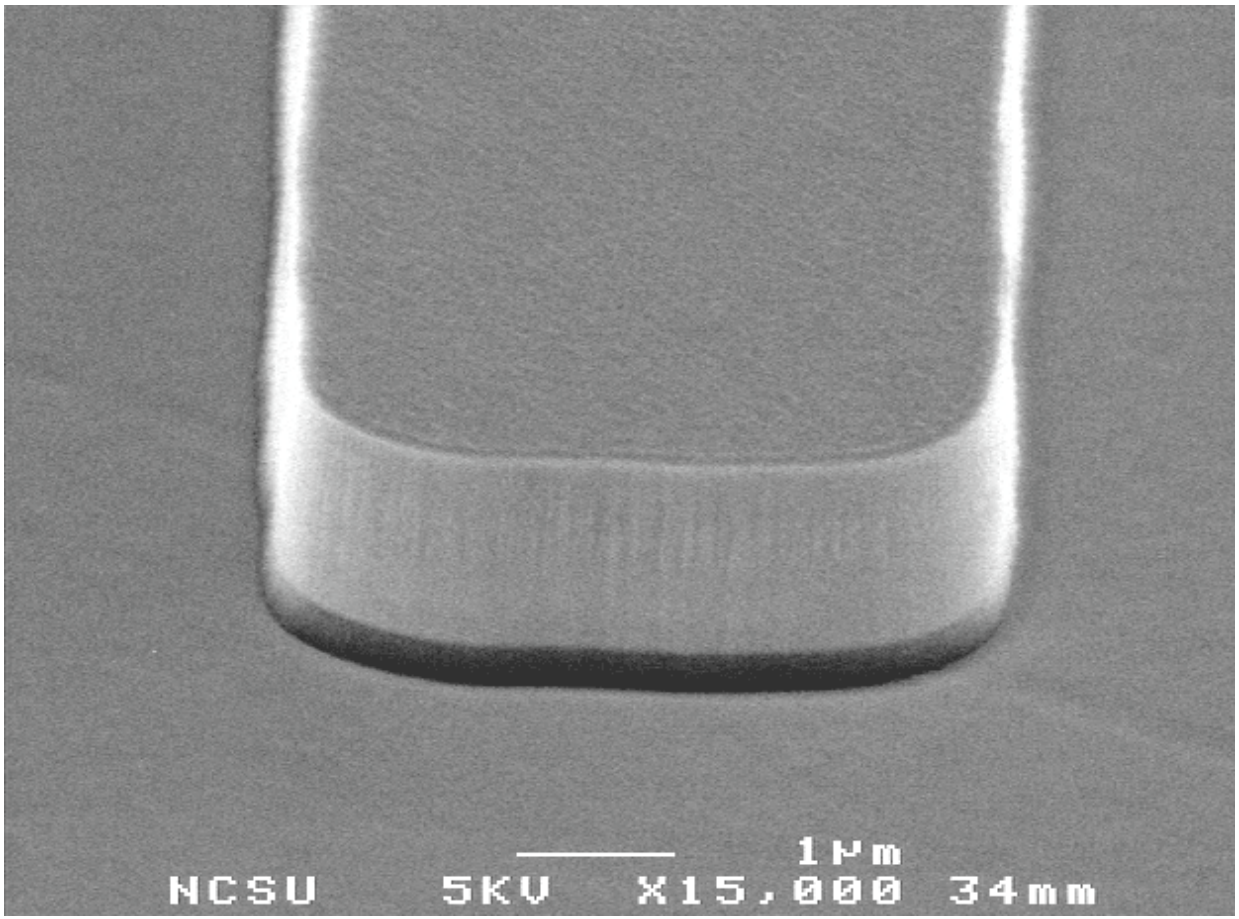

Figure 5. Typical etch microstructure in GaN(0001) achieved using Ni as the etch mask and ICP power = 600 W, DC bias = –150 V, and pressure = 2 mTorr.

CHAPTER 9 PAPER V

Diagnostic studies of GaN etching in a Cl_2/Ar plasma

S. A. Smith and W. V. Lampert
Materials and Manufacturing Directorate, Air Force Research Laboratory, Wright Patterson Air Force Base, OH 45433-7750

C. A. Wolden
Department of Chemical Engineering, Colorado School of Mines, Golden, Colorado 80401-1887

P. Rajagopal, M. D. Bremser, and R. F. Davis
Department of Materials Science and Engineering, North Carolina State University, Raleigh, North Carolina 27695-7919

Optical emission spectroscopy (OES) and Langmuir probe measurements were employed to characterize a Cl_2/Ar inductively coupled plasma used to etch GaN. The ion density and the relative Cl radical density were determined as a function of the ICP power, total pressure, and the percentage of Cl_2 in Ar. Actinometry results suggest that nearly all of the Cl_2 molecules were dissociated under the conditions examined. These parameters were compared with experimental etch rate data to help identify the mechanisms responsible for the etching of GaN. The data indicate that the process is highly dependent upon the ion density, and minimally dependent upon the Cl radical density, which, in turn, suggest that etching is initiated by ion bombardment which cleaves the gallium-nitrogen bond. The resulting nitrogen atoms recombine and desorb, while gallium requires subsequent chlorination before desorption occurs. Ion bombardment appears to be the rate-limiting step for the majority of conditions examined. The etch rate and ion density increase at nearly the same rate with respect to ICP power, while both variables attain a maximum with respect to pressure at approximately 5 mTorr. The results of the experiments in which the Cl_2/Ar fraction was varied suggest that Cl ions are more effective than Ar ions, since they can simultaneously cause bond dissociation and gallium chlorination.

INTRODUCTION

The technological aspects of the etching of GaN continue to advance; however, little has been published regarding the responsible mechanisms. Several plasma chemistries have been employed to etch GaN, including Cl_2/Ar, Cl_2/Ar/H_2, BCl_3/Ar, CH_4/H_2/Ar, BCl_3/Cl_3, and ICl/Cl_2 [1-8]. Most studies have taken a macroscopic approach to characterize and optimize etch rates as a function of power, substrate bias and inlet gas composition. A more fundamental understanding requires the use of either *in-situ* diagnostics and/or detailed modeling. These tools reveal the effects of the operating parameters on the chemical and electrical compositions of the plasma. These results in tandem with etch rates provide information regarding the chemical mechanisms responsible for etching.

In this study optical emission spectroscopy (OES) and Langmuir probe measurements have been applied to characterize an inductively coupled plasma (ICP) employed to etch III-Nitrides [8]. The gas combination of Cl_2/Ar was chosen because of its simplicity and its proven success for etching GaN [8]. Langmuir probe and OES were used, since they are relatively inexpensive diagnostics that complement each other. In this system there are three primary plasma properties that affect etching: ion density, chlorine radical density, and ion energy. The ion energy is independently controlled by the DC bias applied to the sample holder; thus, the radical and ion densities are the critical unknowns. The Langmuir probe measures the ion density of the plasma, and through actinometry, the OES provides a relative measure of radical density as the etching parameters are varied. The results obtained from these diagnostic tools were combined with experimental etch rate measurements to better understand the underlying mechanisms. The experimental etching system and diagnostics design, results, discussions and conclusions regarding potential etching mechanisms are presented in the following sections.

EXPERIMENTAL

ICP Etching System

The ICP system was a custom built, 41 cm diameter by 58 cm tall, loadlocked stainless steel chamber. The RF power was coupled through a 32.4 cm diameter quartz window at the top of the chamber. The inductive source was a planar, 4 turn, 23 cm diameter copper coil which was connected to a RF Power Products 2 kW RF generator operating at 13.56 MHz via an autotuning matching network. Gas was fed into the chamber through a stainless steel shower ring positioned level with the bottom of the quartz window. A water-cooled wafer chuck was mounted on a motor driven vertical translation stage which had 30.5 cm of travel. This allowed samples to be transferred between the loadlock chamber and the processing zone. A second 500 W RF source was connected to the wafer chuck to apply a controllable DC bias to the substrate. The substrate cooling water was maintained at 16°C. The chamber was evacuated by an Alcatel 900 l/s turbomolecular pump which attained a base pressure of 10^{-7} torr.

A magnetic "bucket" containing 240 Nd-Fe-B magnets was mounted on the outside perimeter of the chamber to increase the plasma density by confining the electrons to a central volume within the chamber. This reduced electron losses due to collisions with the chamber walls. The ions were not directly affected by the magnetic field; however, they were also confined to the central volume due to electrostatic coupling with the electrons. Epitaxial GaN thin films grown by chemical vapor deposition on on-axis AlN/6H-SiC(0001) substrates were used for the etching experiments [9].

The etch rate data were taken for each etching parameter while holding the other parameters constant. Unless otherwise stated, the conditions were ICP power = 500 W, pressure = 5 mTorr, DC bias = -150 V, Cl_2 flow = 20 sccm, and Ar flow = 5 sccm. The energy of the impinging ions is directly related to the DC bias and not the RF power; thus, the former was held constant to insure the ion energy did not affect the etch rates. Holding the RF power constant would likely cause the DC bias to vary both with changes in the pressure and the ICP power, and the etch rates would be affected. Etch rates were

determined by measuring the step heights with a Dektak II profilometer on samples that were partially covered with a mask.

Optical Emission Spectroscopy

Optical emission spectroscopy is a line of sight measurement and an excellent diagnostic tool for studying reactive plasmas due to its noninvasive nature. An Ocean Optics SD2000 dual spectrometer was used to quantify the optical emission from the excited chemical species in the plasma. The fiber optics used to gather the emission signal were positioned 5 cm above the substrate.

Emission occurs from atoms when an excited species returns to a lower energy state or when an ionized atom recombines with an electron. In each case, the excess energy is released as a photon. Examples using Ar are presented in Equations 1a and 1b.

$$e + Ar \rightarrow Ar^* + e \rightarrow Ar + e + \hbar\omega \quad \text{(For excited Ar)} \tag{1a}$$

$$e + Ar \rightarrow Ar^+ + 2e \rightarrow Ar + e + \hbar\omega \quad \text{(For ionized Ar)} \tag{1b}$$

The experiments in this research were concerned primarily with emission from atoms. The emission intensity for species x is given in Equation (3) where a_x is a proportionality constant, n_e is the total electron density, n_x is

$$I_x = a_x n_e n_x \int_{\varepsilon}^{\infty} \sigma_x(\varepsilon_x) f(\varepsilon_x) \sqrt{\varepsilon_x} d\varepsilon_x \tag{3}$$

the density of the species x, $\sigma_x(\varepsilon)$ is the excitation cross section for the excitation of x, $f(\varepsilon)$ is the electron energy distribution function, and ε_x is the threshold energy for excitation to the emitting state.

Actinometry provides a means to qualitatively determine the density of the reactive species in the plasma. This technique, originally developed by Coburn *et al.* [10], involves the addition of a small quantity of an inert tracer gas, such as argon or xenon, to the reactive chemistry and the monitoring of the emission of both the inert gas and the

reactive species. The governing principal is that if the excited states of the reactive species and the tracer gas responsible for the emission are similar in energy, then the same group of electrons is responsible for generating emission from both species. Furthermore it was assumed that the excitation cross-section $\sigma_x(\varepsilon)$ is the same or proportional for the reactive species as it is for the tracer gas [10]. When performing actinometry, the intensity of the reactive species is divided by the intensity of the tracer gas, as shown in Equation 4.

$$\frac{I_x}{I_T} = \frac{a_x n_e n_x \int_{\varepsilon_x}^{\infty} \sigma_x(\varepsilon_x) f(\varepsilon_x) \sqrt{\varepsilon_x} d\varepsilon_x}{a_T n_e n_T \int_{\varepsilon_T}^{\infty} \sigma_T(\varepsilon_T) f(\varepsilon_T) \sqrt{\varepsilon_T} d\varepsilon_T} \tag{4}$$

Since $\varepsilon_x = \varepsilon_T$ and $\sigma_x = \sigma_T$, the two integrals cancel leaving with the resultant equation being

$$\frac{I_x}{I_T} = \frac{a_x n_x}{a_T n_T}. \tag{5}$$

For the density of species x one obtains

$$n_x = \frac{a n_T I_x}{I_T} \tag{6}$$

where *a* is a proportionality constant. The number density of the excited species can be determined if the density of the tracer gas, the constant *a*, and the excitation cross section for the excitation of x are known. The relative densities of the reactive species can be determined qualitatively as a function of the plasma parameters without knowledge of the above mentioned properties.

To implement the technique of actinometry within a chlorine-based plasma chemistry, it is necessary to find a tracer gas that has a similar excitation energy to that of the Cl

radical. Donnely [11] reported that the 822.17 nm Cl emission line with an excitation energy of 10.49 eV and the 823.20 nm Xe emission line with an excitation energy of 9.82 eV were compatible. These were the emission lines that were monitored for the experiments in the present research. In the results presented below, the relative density of Cl radicals is represented by the Cl/Xe symbols.

Langmuir Probe Measurements

Langmuir probes, in their simplest form, are a bare wire inserted into a plasma. They allow the determination of the electron density, the electron temperature, the plasma potential, and the ion density by applying a voltage and measuring the current in the wire. It is performed using the ion saturated current region of the voltage sweep. For electropositive plasmas, the electron density measurement is preferred due to the charge neutrality of the plasma. Thus, there should be an approximately equal number of positive ions and electrons in the plasma. Since Cl_2 plasmas tend to be electronegative, the positive ion density measurements were performed for these experiments. With an electronegative plasma, the electron density is less than the positive ion density due to the negative ions that are formed. Since Langmuir probes cannot differentiate between different types of positive ions, only the total positive ion density was measured.

The precision of the direct measurement of the ion density with a Langmuir probe has been questioned [12]. Comparisons among the data for plasma densities measured by microwave techniques, which are thought to be highly accurate [12], and those derived from Langmuir probe plasma studies indicated that the latter technique tends to overestimate this density. However, Hopwood *et al.* [13] obtained excellent agreement between the data obtained using these two techniques. If the ion saturation current is used for ion density measurements, it is thought [12] that the accuracy is dependent upon how close the electron energy distribution approximates a Maxwellian distribution. The electron energy distributions in the present research were examined for all the parameters varied and found to be Maxwellian. This provided additional confidence in the ion density measurements.

The Langmuir probe was a Hiden Analytical ESP series single electrostatic plasma probe consisting of a 0.15 mm diameter and 10 mm long cylindrical tungsten tip. Platinum tips were originally used; however, they melted under high electron current conditions. The probe contained a second electrode for RF compensation. This latter electrode helped to eliminate any RF voltages between the probe and the plasma that distorts the plasma characteristics leading to errors in the measurements of the plasma parameters [14]. The measurements were taken the same 5 cm distance above the surface of the sample holder as used for the position of the fiber optics of the OES.

The governing equation used for these experiments was

$$n_i^{\,2} = -\left(4\pi m_i / 3A^2 e^3\right)\left(\partial I^2 / \partial V\right) \qquad (7)$$

where n_i is the ion density, m_i is the ion mass, and A is the surface area of the probe tip. To determine the ion density, the voltage on the probe was swept from –100 V to a positive value such that the 100 mA maximum current was not exceeded. The data obtained using the negative voltages were plotted as I^2 vs. V. The slope was determined and inserted into Equation 6.

Measurements of chlorine radical density, ion density, and etch rates were acquired in independent experiments as functions of ICP power, total pressure and % Cl_2 in argon. The range of conditions as well as the base conditions are summarized in Table I. The chlorine concentration was only studied between 44% and 100%, because this is typically the range employed for most GaN etching applications. The total flow rate of Ar plus Cl_2 was 25 sccm for all experiments. One sccm of the Xe tracer gas was introduced for the actinometry experiments. The RF power applied to the substrate was automatically varied to maintain a constant DC bias of –150 V.

RESULTS & DISCUSSION

Cl Radical Density

The Cl and Xe emission intensities and the Cl/Xe ratio, which is the relative density of Cl radicals, are shown in Figure 1 as a function of the ICP power. The emission of the Cl and Xe responded similarly to changes in the ICP power with the Xe emission increasing slightly faster. The Cl/Xe ratio increased linearly a minimal 21% as the power was ramped from 300 W to 1100 W.

Changes in total pressure had a more significant affect on the Cl radical density than changes in the ICP power, as shown by a comparison of Figures 1 and 2. The Cl and Xe emission intensities shown in the latter figure again varied similarly as a function of pressure. Equation 6 shows that the density of Cl radicals is dependent on both the intensities of Cl and Xe emission lines and the density of the tracer gas. For the aforementioned study varying the ICP power the density of tracer gas was constant; however, as the pressure was varied, the density of the tracer gas changed. The Cl radical density shown in Figure 2 has been adjusted for the variation in xenon concentration. The increase in Cl radical density with pressure was slightly greater than one-to-one. The 11-fold increase in pressure caused an increase in the chlorine radical density by a factor of 12.5.

The effect of varying the Cl_2/Ar ratio on the Cl and Xe emission intensities and the Cl/Xe ratio was also investigated. The results are displayed in Figure 3. The Cl_2 was increased from 40 to 100 % while maintaining the total flow rate of Cl_2 + Ar at 25 sccm. The relative density of Cl radicals was directly proportional to the chlorine mole fraction. This was expected since the higher the density of Cl_2 atoms in the gas phase, the higher the probability of their dissociation. As with pressure, the increase in the density of chlorine radicals with the increase in the total atomic percentage of chlorine was nearly one-to-one: the former increased 241% in response to a 227% increase in the latter.

A review of the results of the studies of concern in this subsection shows that the Cl radical density was relatively insensitive to the ICP power; however, in the case of both pressure and composition, a positive 1:1 relationship with the total chlorine concentration

was observed. The most plausible explanation for this combined behavior is that for the range of conditions investigated nearly all of the chlorine was dissociated. This is consistent with the minimal change observed with changes in the ICP power. A counter explanation is that a steady-state was achieved wherein the rate of Cl_2 dissociation and the rate of Cl recombination had the same dependence on the ICP power. However, this explanation is not consistent with plasma chemistry. The dissociation rate increases with ICP power due to a higher electron density and increased temperatures. However, the recombination rate should remain essentially constant.

Total Positive Ion Density

Figure 4 shows that the total positive ion density increased linearly with ICP power from $7.7*10^{10}$ ions/cm^3 at 300 W to $3.4*10^{11}$ ions/cm^3 at 1300 W, an increase of 442%, while maintaining the base conditions noted in Table I. Varying the pressure from 1 to 11 mTorr resulted in a curve that increased from an initial value of $1.14*10^{11}$ ions/cm^3 at 1 mTorr to a maximum of $1.49*10^{11}$ ions/cm^3 at 6 mtorr; it then decreased through 11 mTorr, as shown in Figure 5. The latter data suggest that this behavior is the result of two competing effects. The production of ions is directly proportional to the concentration of species in the gas-phase. However, the rate of ion loss due to collisional recombination increases with the square of the pressure. The maxima observed at 6 mTorr reflects a balance between these two processes.

The addition of Ar to the gas chemistry had no significant effect on the total positive ion density. As can be seen in Figure 6, the ion density only varied from $1.41*10^{11}/cm^3$ for 100% Cl_2 to $1.56*10^{11}/cm^3$ for 44% Cl_2. Argon has one of the largest ionization cross-sections; thus, these results are to be expected.

Etch Rates

The results of the etch rate experiments were compared to the previously presented results for the OES and Langmuir probe experiments to provide insight into mechanisms

of the etching process, as the two primary plasma properties that affect the etch rates are ion density and the density of reactive species. The ion energy also affects the etch rate; however, a study of this effect was not included in these experiments, because it was controlled independently of the inductive power and had no effect on the plasma properties when varied.

Figure 7 shows the measured etch rates and a comparison of normalized data among the total positive ion density, the relative chlorine radical density, and the etch rate as a function of ICP power. At low values of power (≤ 700 W) the etch rate and ion density displayed the same dependence, indicating that the ion density was involved in the rate limiting step. The Cl radical density was not responsible for this increase, as it remained nearly constant. At higher values of power the ion density continued to increase while the etch rate appeared to saturate. This suggests that another step such as product desorption or possibly Cl adsorption began to limit the process.

The ion density, relative chlorine radical density, and etch rate are compared as a function of total pressure in Figure 8. All of these parameters increased within the range from 1 to 5 mTorr. Between 5 and 11 mTorr the chlorine radical density continued to increase while the ion density peaked at 6 mTorr and decreased through 11 mTorr. These results again suggest that the etch rate is limited by ion density. However, as shown in Figure 7, the etch rate dropped more sharply than ion density. We attribute this difference to the spatial limitations of the Langmuir probe measurements. As previously mentioned, the ion density was measured approximately 5 cm above the sample surface. As such, these data have a higher value than the ion concentration at the substrate for the following reasons. The ions have to be transported (primarily by diffusion) from the position of the Langmuir probe to the substrate and are subject to recombinational losses along the way. The pressure influences the concentration of ions reaching the substrate in two ways. Firstly, the diffusivity varies with the inverse of total pressure. Secondly, collisional recombination rates increase with pressure. Thus, as the pressure increases the rate of transport decreases, while losses increase. For these reasons we believe that the ion density at the substrate is attenuated more sharply with pressure than indicated by our Langmuir probe measurements. This explanation is consistent with the etch rate data.

In Figure 9 the etch rate is compared to the ion density and the Cl radical density as a function of Cl_2 percentage. To this point we have focused on ion density as the primary rate limiting step. The results in Figure 9 show that the total ion density remained essentially constant while the etch rate increased by more than 50%. These data appear to be inconsist with our hypothesis that ion bombardment is the rate-limiting step. However, though the *total* ion density remained constant, the concentration of chlorine ions increased with an increase in total Cl_2 fraction. We could not distinguish between Ar and Cl ions with our Langmuir probe measurements; however, the total ion density remained nearly constant which suggests that the probability of forming either a Cl or Ar ion must be similar. The data also suggest that the Cl ions are more effective than Ar ions in initiating the etching of GaN. Indeed the etch rate was highest when the gas concentration was 100% Cl_2.

The following mechanism is postulated for the etching of GaN in Cl_2/Ar plasmas.

(s1)	$GaN_{(s)} + ion_{(g)} \rightarrow Ga^*_{(s)} + N^*_{(s)}$	GaN bond dissociation
(s2)	$N^*_{(s)} + N^*_{(s)} \rightarrow N_{2(g)}$	N_2 recombination and desorption
(s3)	$Ga^*_{(s)} + xCl \rightarrow GaCl_x$	Chlorination and desorption of gallium

In the first step an incoming ion ruptures the Ga-N bond creating excited Ga and N atoms on the surface. The nitrogen atoms rapidly combine and desorb as described by step 2. The gallium atom is not volatile and must be chlorinated before desorption can occur. It is suspected that the volatile species in this process are either $GaCl_2$ or $GaCl_3$; thus, the third step may require multiple collisions [15]. Under most of the conditions examined the first step, ion driven dissociation of GaN, is the rate-limiting step. At high ion concentrations the third step begins to attenuate the process. This is consistent with the behavior observed at high ICP powers, as shown in Fig. 8. This also explains the increase in etch rates with an increase in the percentage of Cl_2 in Ar, as shown in Figure 9. If the ion that participates in step 1 above is chlorine, it is likely that it will remain on the surface and bound to the Ga atom. As such, one less chlorine atom is required for step 3 and the etch rates are enhanced.

In summary, plasma diagnostic techniques were employed to aid in the determination of the mechanisms responsible for the etching of GaN in a Cl_2/Ar plasma. The ion denstiy was found to be the rate-limiting factor under most conditions. On the contrary, the etch rates were found to be relatively insensitive to the Cl radical density. The one case where the total ion density was not the rate limiting factor was in the Cl_2 range from 44 to 100%. The total ion density essentially remained constant over this range, while the Cl radical density and the etch rates increased. However, the data do not indicate that the Cl radical density was the rate limiting factor. It is proposed was that the etch rates responded differently to different ions. The Cl ion density rather than the total ion density may have been the rate limiting factor.

This work was supported by the Office of Naval Research under contract No. N00014-96-1-0765. Scott A. Smith wishes to acknowledge the U.S. Air Force PALACE Knight program.

1. S. J. Pearton, C. R. Abernathy, F. Ren, J. R. Lothian, P. W. Wisk, A. Katz, and C. Constantine, Semicond. Sci. Technol. **8**, 310 (1993).

2. S. J. Pearton, C. R. Abernathy, and F. Ren, Appl. Phys. Lett. **64,** 2294 (1994).

3. S. J. Pearton, C. R. Abernathy, and C. B. Vartuli, Electron. Lett. **30**, 1985 (1994).

4. C. B. Vartuli, S. J. Pearton, C. R. Abernathy, R. J. Shul, A. J. Howard, S. P. Kilcoyne, J. E. Parmeter, and M. Hagerott-Crawford, J. Vac. Sci. Technol. A **14**, 1011 (1996).

5. C. B. Vartuli, S. J. Pearton, J. W. Lee, J. Hong, T. D. Mackenzie, C. R. Abernathy, and R. J. Shul, Appl. Phys. Lett. **69** (10), 1426 (1996).

6. R. J. Shul, S. P. Kilcoyne, M. Hagerott, J. E. Parmeter, C. B. Vartuli, C. R. Abernathy, and S. J. Pearton, Appl. Phys. Lett. **66,** 1761 (1995).

7. R. J. Shul, A. J. Howard, S. J. Pearton, C. R. Abernathy, C. B. Vartuli, P. A. Barnes, and M. J. Bozack, J. Vac. Sci. Technol. B **13**, 2016 (1995).

8. S. A. Smith, C. A. Wolden, M. D. Bremser, A. D. Hanser, R. F. Davis, and W. V. Lampert, Appl. Phys. Lett. **71,** 3631 (1997).

9. M. D. Bremser, W. G. Perry, T. Zheleva, N. V. Edwards, O. H. Nam, N. Parikh, D. E. Aspnes, and R. F. Davis, MRS Internet J. Nitride Semicond. Res. **1**, 8 (1996).

10. J. W. Coburn and M. Chen, J. Appl. Phys. **51**, 3134 (1980).

11. V. M. Donnely, J. Vac. Sci. Technol. A **14**, 1076 (1996).

12. M. A. Lieberman and A. J. Lichtenberg (1994), *Principles of Plasma Discharges and Materials Processing*, Wiley-Interscience, New York 173.

13. J. Hopwood, C. R. Guarnieri, S. J. Whitehair, and J. J. Cuomo, J. Vac. Sci. Technol. A **11**, 147 (1993).

14. P. A. Chatterton, J. A. Rees, W. L. Wu, and K. Al-Assadi, Vacuum **42**, 489 (1991).

15. T. Senga, Y. Matsumi, and M. Kawasaki, J. Vac. Sci. Technol. B **14**, 3230 (1996).

Table I - The experimental parameters examined, their ranges, and the base conditions employed in this study.

Parameter	Range	Base Cond.
ICP Power	300-1100 W	500 W
DC Bias	N/A	-150 V
Pressure	1-11 mTorr	5 mTorr
Total Flow Rate	N/A	25 sccm
Cl_2 Percentage	44-100%	80%
Ar Percentage	0-56%	20%

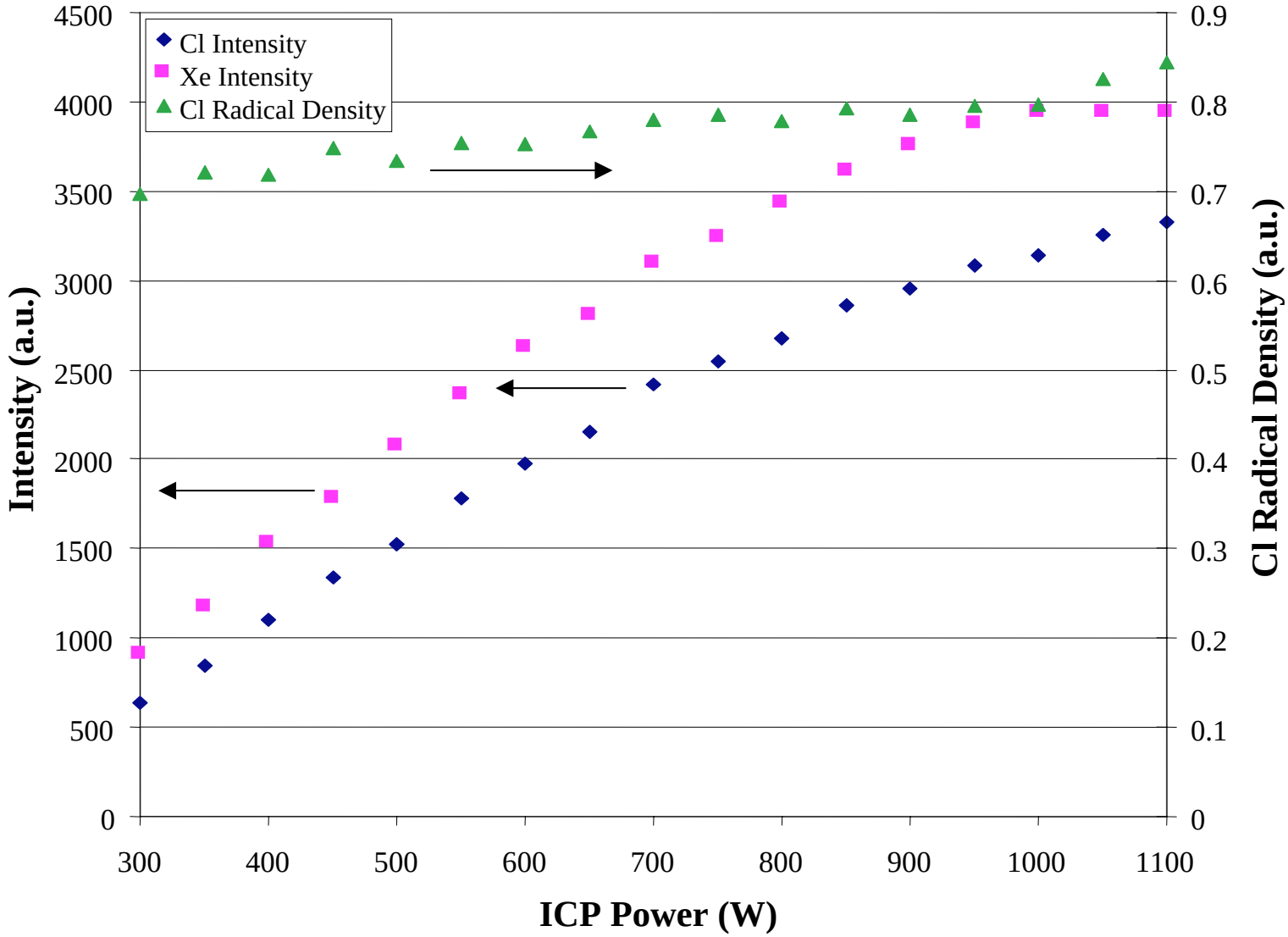

Figure 1. Optical intensity data from the Xe and Cl emission lines and the Cl/Xe ratio, expressed as the Cl radical density as a function of ICP power.

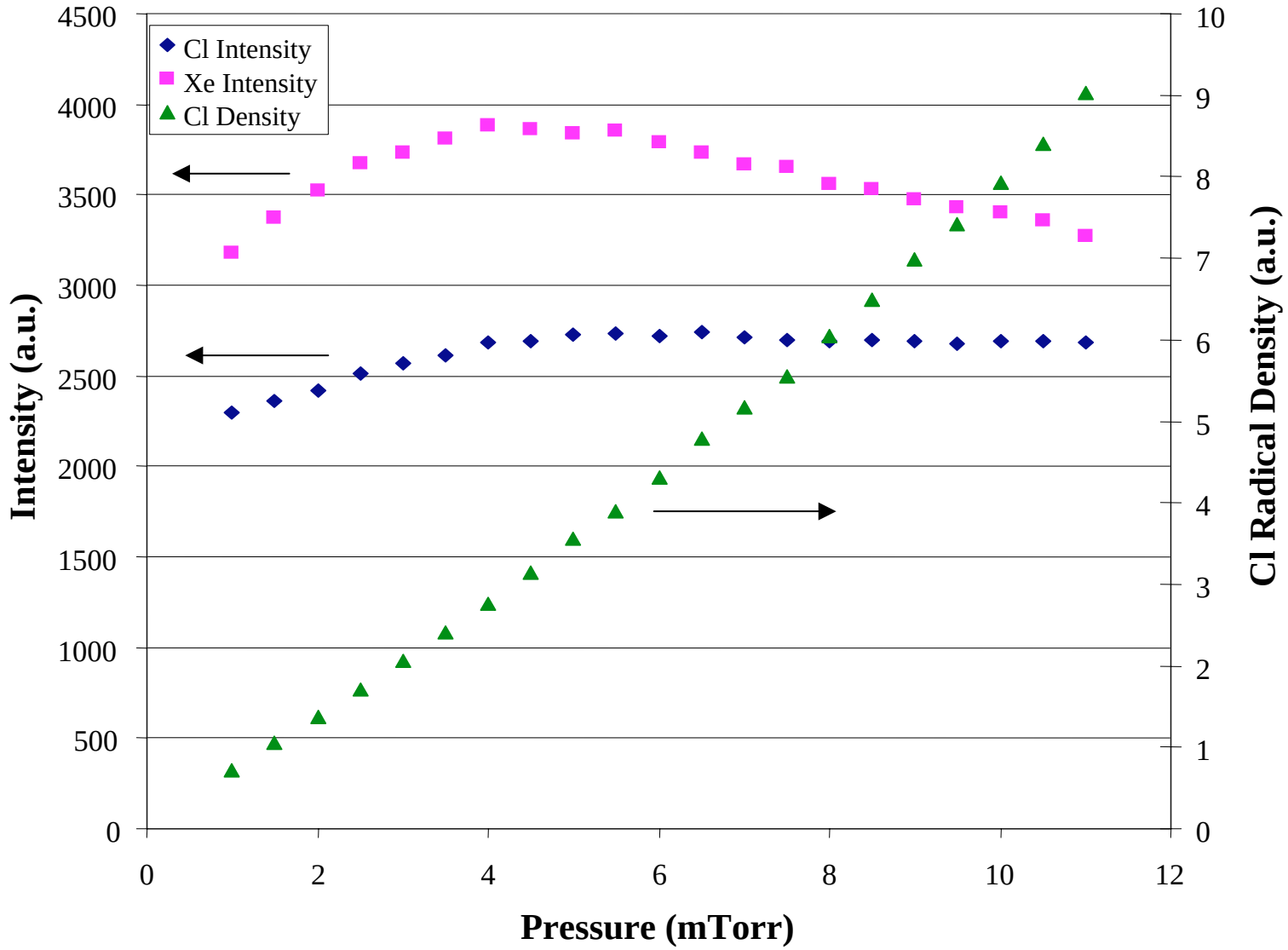

Figure 2. Optical intensity data from the Xe and Cl emission lines and the Cl/Xe ratio, expressed as the Cl radical density as a function of pressure.

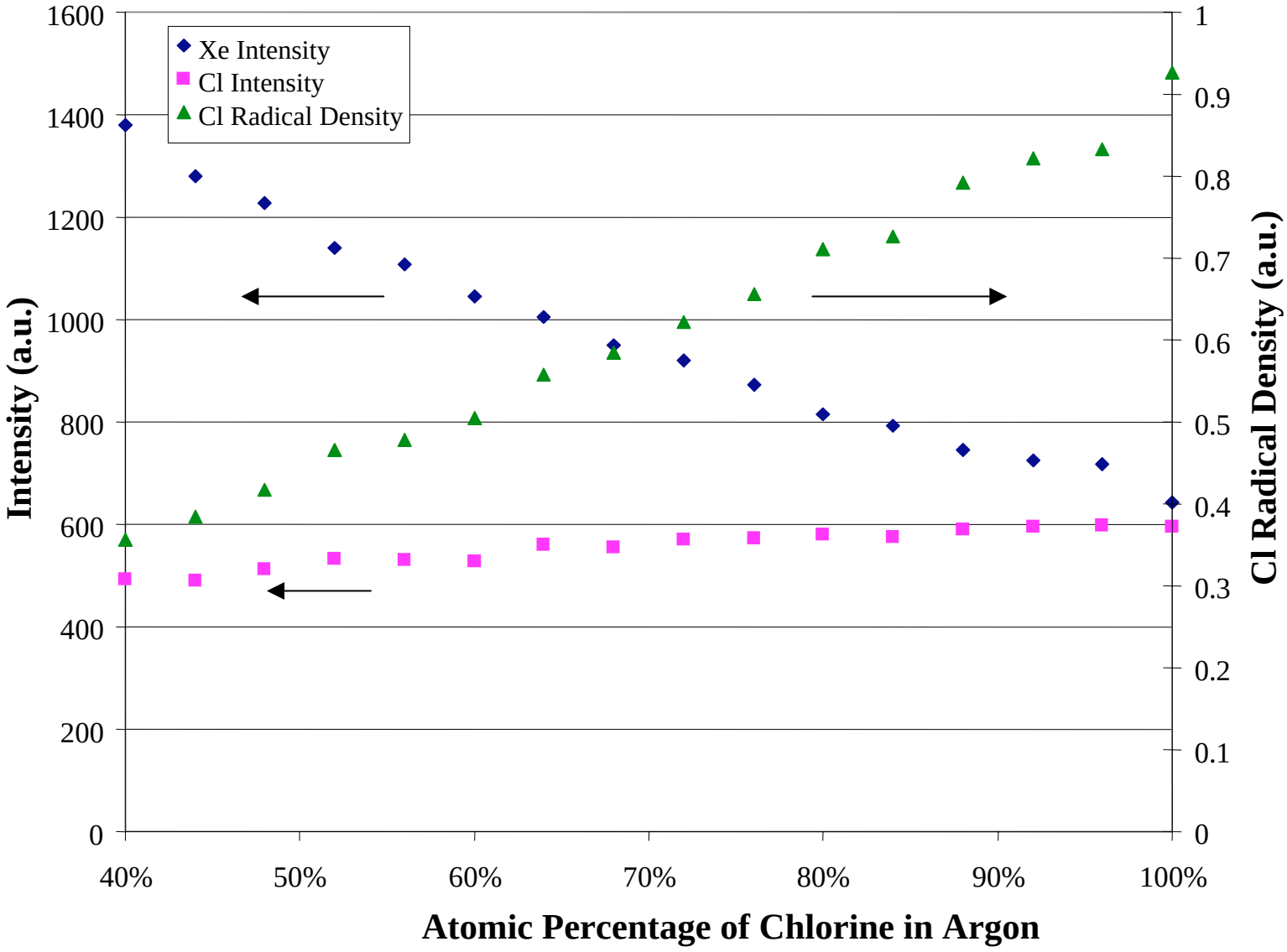

Figure 3. Optical intensity data from the Xe and Cl emission lines and the Cl/Xe ratio, expressed as the Cl radical density as a function of the percentage of Cl_2 in Ar.

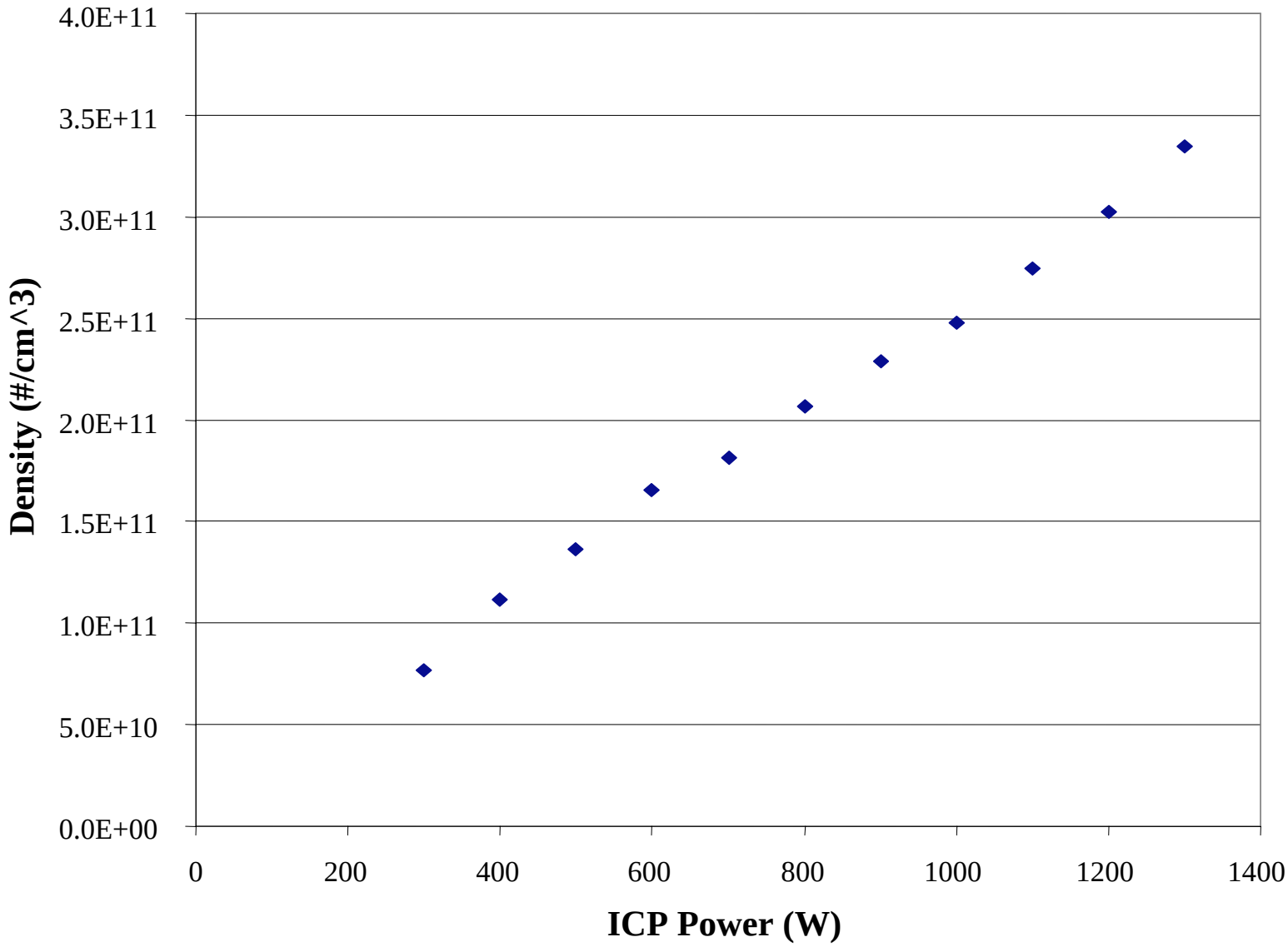

Figure 4. Total positive ion density as a function of ICP power.

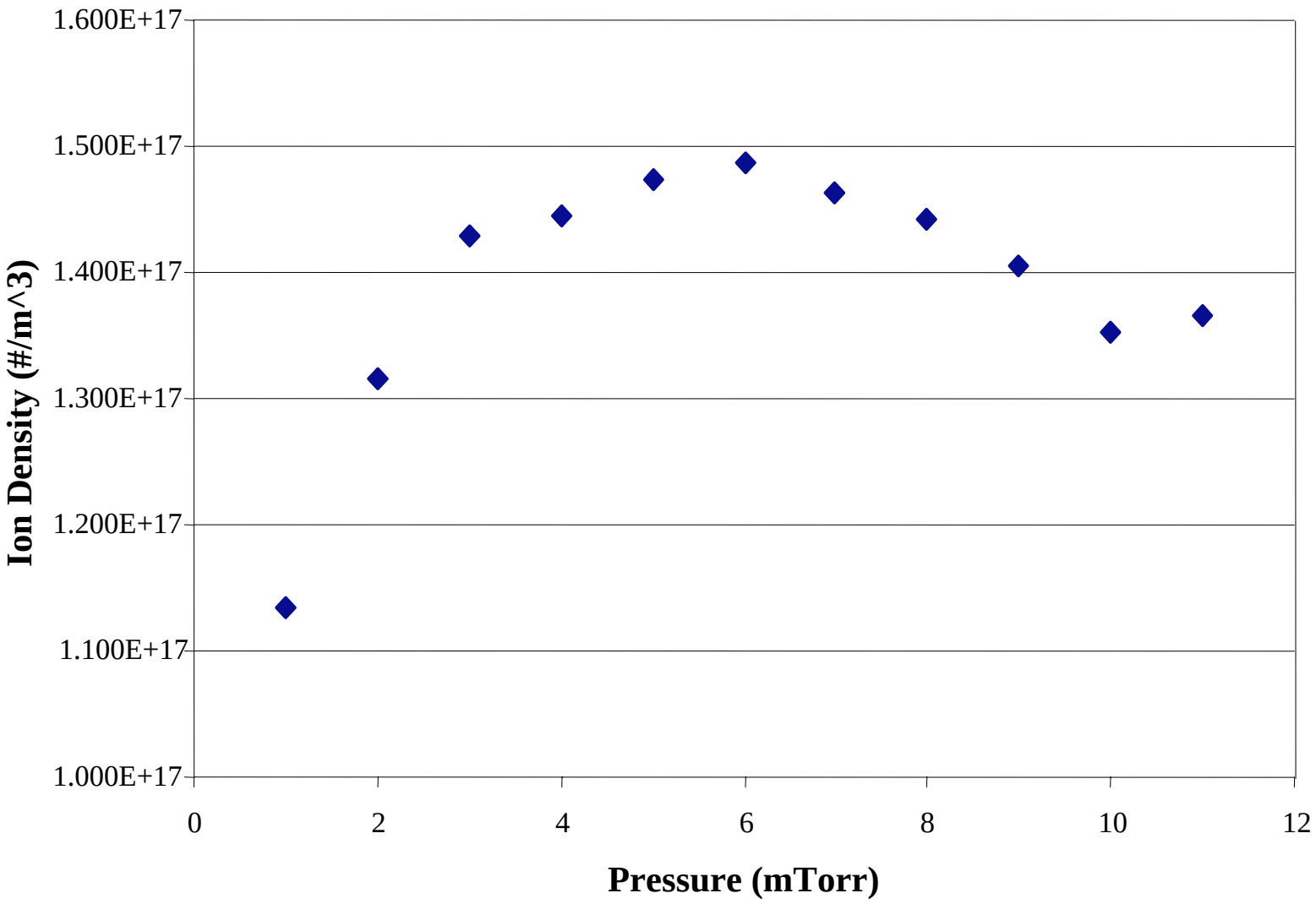

Figure 5. Total positive ion density as a function of pressure.

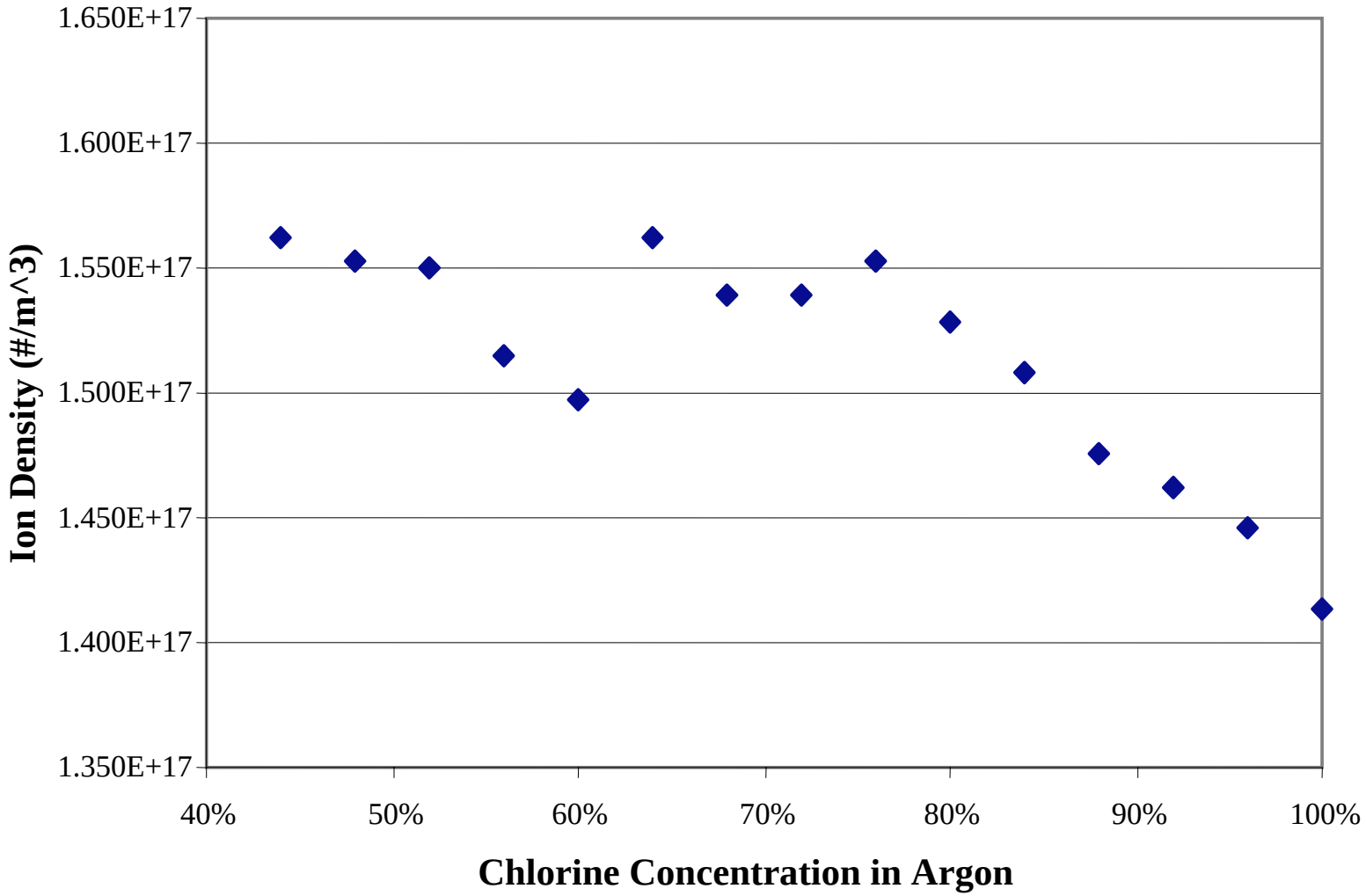

Figure 6. Total positive ion density as a function of Cl_2 concentration in Ar.

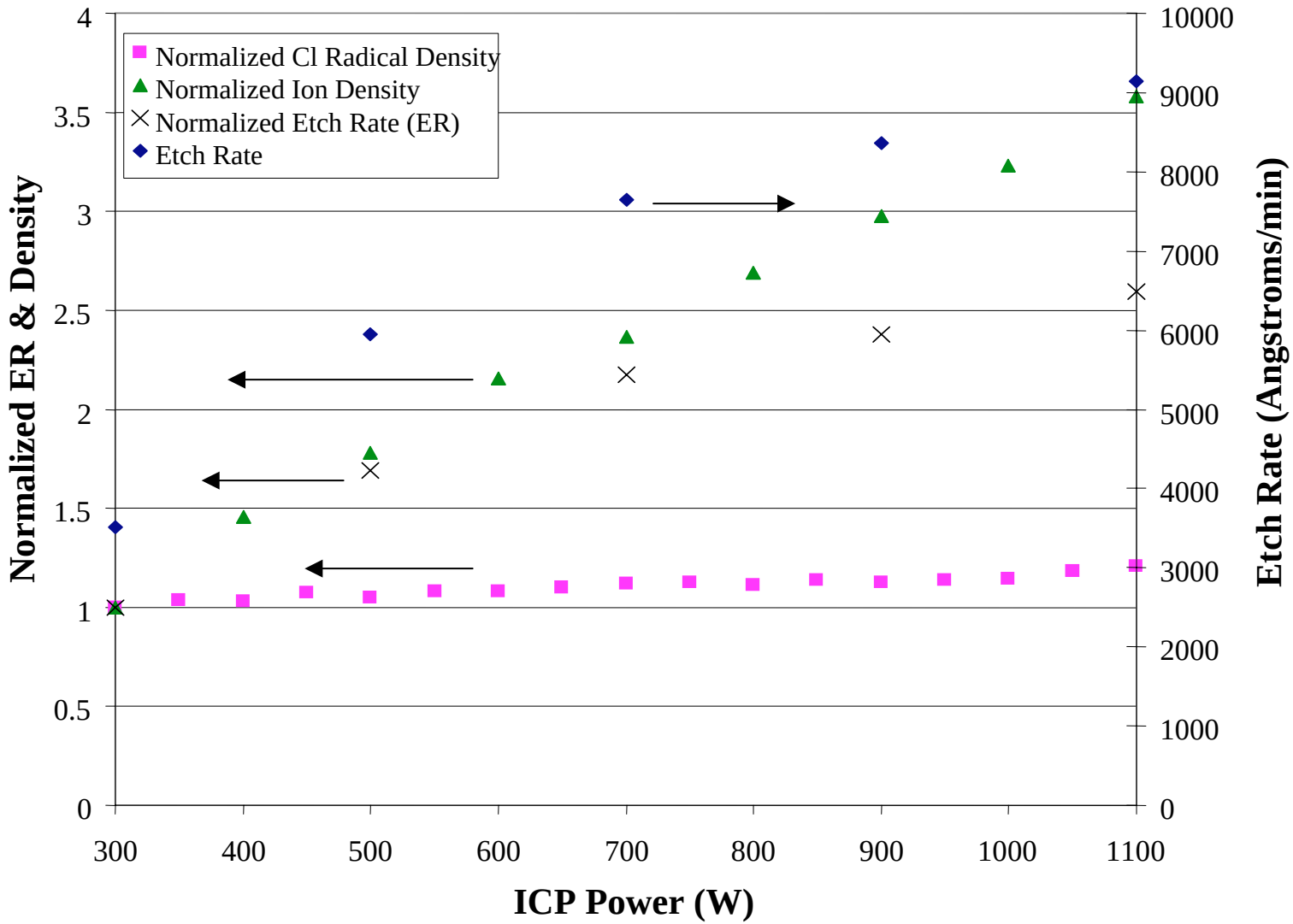

Figure 7. Comparison of the ion density, Cl radical density, and the etch rate (ER) as a function of the ICP power. The data for each of these curves were normalized to 1 for ease of comparison.

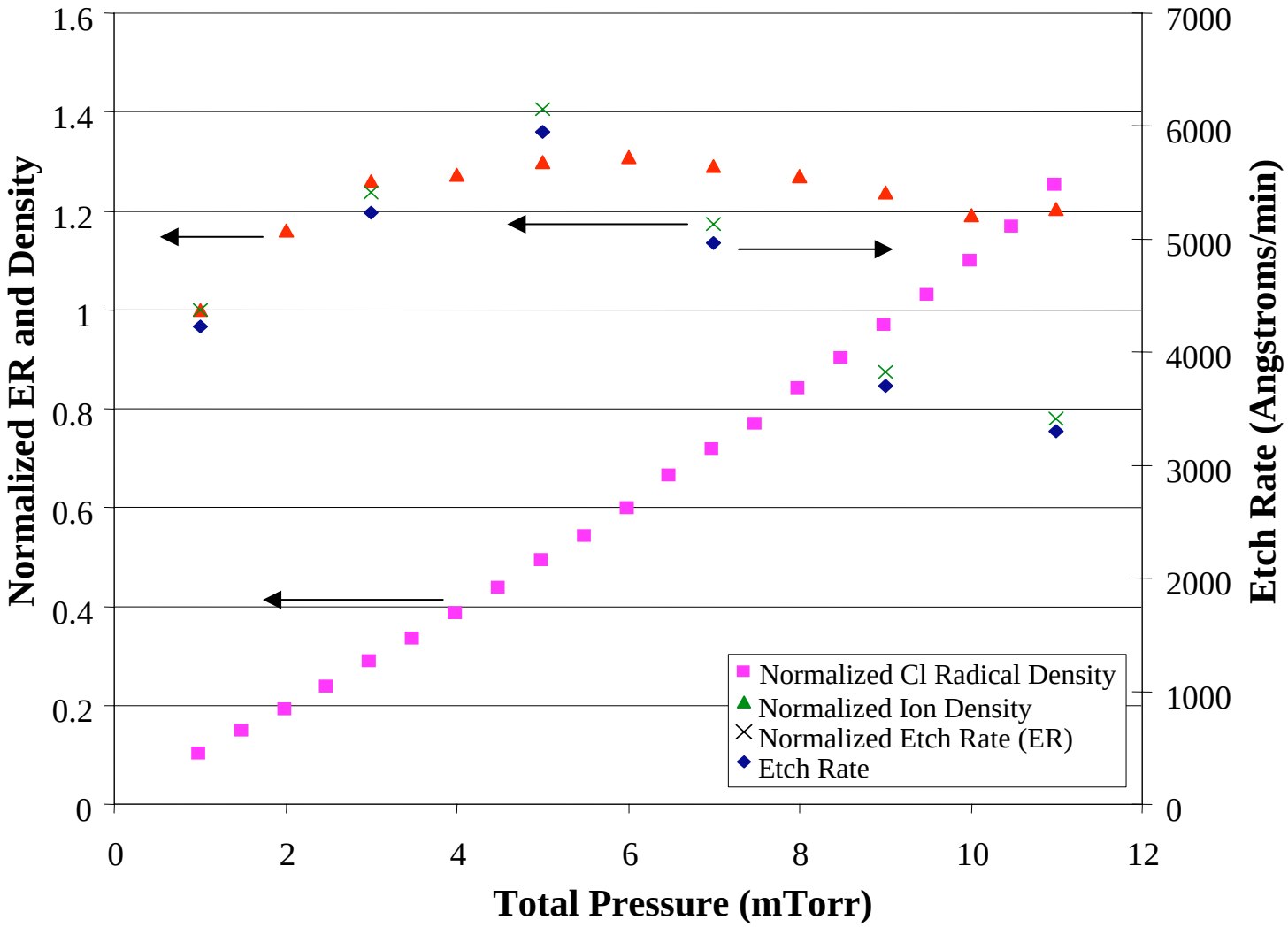

Figure 8. Comparison of the ion density, Cl radical density, and the etch rate (ER) as a function of pressure. The data for each of these curves were normalized to 1 for ease of comparison.

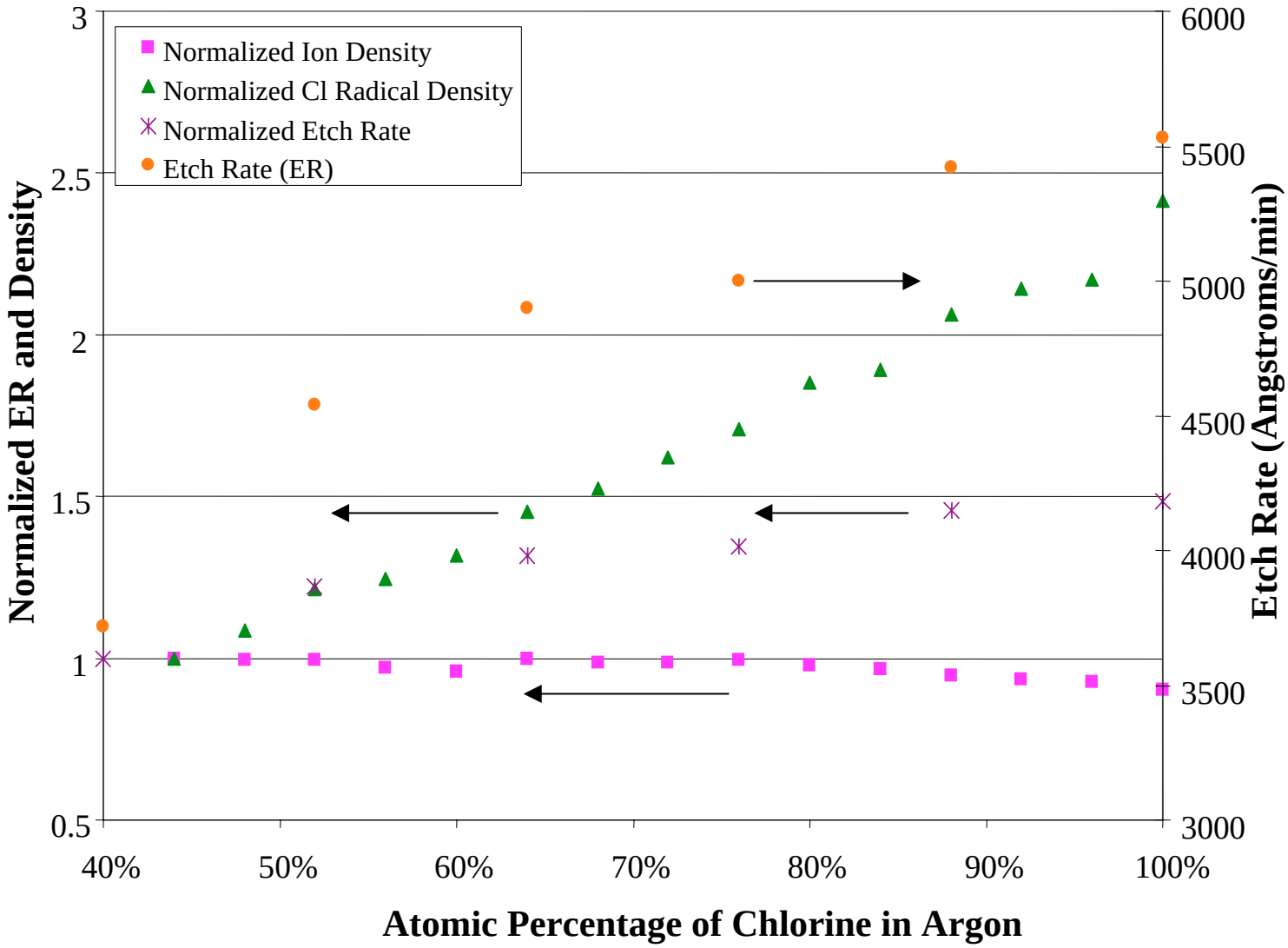

Figure 9. Comparison of the ion density, Cl radical density, and the etch rate (ER) as a function of the percentage of Cl_2 in Ar. The data for each of these curves were normalized to 1 for ease of comparison.

CHAPTER 10 PAPER VI

Optical emission spectrometry as a diagnostic etch stop tool for GaN/AlN heterostructures

S. A. Smith and W. V. Lampert
Materials and Manufacturing Directorate, Air Force Research Laboratory, Wright Patterson Air Force Base, OH 45433-7750

P. Rajagopal, A. D. Banks, and R. F. Davis
Department of Materials Science and Engineering, North Carolina State University, Raleigh, North Carolina 27695-7919

A diagnostic etch stop technique has been demonstrated for the etching of GaN-based heterostructures in a BCl_3/Cl_2-containing inductively coupled plasma (ICP) by monitoring the change in the intensity of the 417 nm Ga emission line with an optical emission spectrometer. A sharp increase or decrease of this Ga emission line indicated the onset or completion, respectively, of the etching of the GaN layer. The detection of the transition from GaN to AlN for AlN layers as thin as 50 Å was achieved using the aforementioned plasma chemistry. Etching in a Cl_2/Ar chemistry was also investigated; however, the results were inferior to those of the BCl_3/Cl_2 chemistry. Substituting BCl_3 for Ar considerably enhanced the Ga emission lines.

The etching technology for III-Nitride planar films has steadily advanced in terms of etch rates, sidewall quality, and selectivity (i.e. the ratio of etch rates between two materials); however, the etching requirements in the fabrication of complex multilayer heterojunction devices are more stringent than the present state-of-the-art can achieve [1-6]. Low etching selectivity between two materials and the etching of a complex structures containing multiple, very thin (<50 nm) layers usually requires the development of a precise etch stop technique. This is especially true when multiple layers of dissimilar materials must be removed before reaching the layer in which the etch must be terminated. Selective etching, where possible between the materials in question, should suffice if only the top layer must be etched through. Selectivities to 48 between GaN and AlN (i.e., the etching rate of GaN was 48 times faster than AlN) have been achieved by the authors [7,8] using Cl_2 and Ar as the feed gases in tandem with low DC biases or the addition of O_2. However, selectivity may fail if multiple layers of similar materials must be etched through prior to stopping at the desired layer. In the GaN, AlGaN, and AlN system this occurs because the mechanism that is causing the GaN to selectively etch relative to the AlN will also cause the GaN to etch selectively relative to the AlGaN.

Etching in combination with the use of a diagnostic tool that monitors gas composition for the desired species, e.g., Ga from GaN, allows one to determine when a given layer has been etched through. Optical emission spectroscopy (OES) is a line of sight measurement and an excellent diagnostic tool for studying the gas phase chemistry of reactive plasmas and the etching process as a function of time due to its noninvasive nature. This technique has been applied to other III-V semiconductor systems with much success [9-12]. Melville *et al.* [9] were able to detect the onset and completion of the etching of 65 Å thick InGaAs quantum wells in InP by monitoring the PH_3^+ in an RIE system. The sample size was 14 mm by 7 mm; the etch rate was not indicated. Thomas III *et al.* [11] examining the etching of a GaInAs/AlInAs heterostructure by monitoring the 417.2 nm Ga signal. They were able to stop the etch 20 Å after entering the AlInAs layer through computer control of the OES and optimization of the residency time through the pressure. The results of Callot and Diallo [12] were similar to those of Melville *et al.* [9] in that they were able to detect the onset and completion of the etching

of AlGaAs quantum wells in GaAs as thin as 50 Å. In our study, an Ocean Optics SD2000 dual spectrometer was employed to quantify the optical emission from the excited chemical species in the plasma. The fiber optics used to gather the emission signal were positioned 10 cm above the substrate. The onset or completion of etching a particular layer was determined by monitoring the predominant emission signals for the respective III-Nitride materials. The 417 and the 403 nm Ga peaks and the 309 and 396 nm Al peaks were monitored for the GaN and the AlN, respectively.

Monitoring the Ga signals with the OES was initially investigated using the Cl_2/Ar plasma chemistry and an approximately 1 cm^2 thin film GaN sample. The intensities from the Ga and Al peaks were low, especially in this small area sample. It was felt that it was important to maximize the Ga signals as to ease the detection of small changes in the signal. Figure 1 shows a typical spectra obtained in this research using Cl_2/Ar as the feed gases. The Ga signals were sufficiently small that they were not considerably higher than the broad Cl_2^+ signal. The normal range of the Cl_2^+ spectrum is from 350 to 550 nm with a peak at 450 nm; however, in this case the signal was attenuated above 400 nm due to the constraints of the spectrometer. The Cl_2/Ar plasma was also examined with the OES while etching an approximately 3 cm diameter pressed circular sample of pure GaN powder [13]. The Ga signals were considerably larger than the Cl_2^+ background signal, which implied that this chemistry may be sufficient for this technique if larger samples were used. The smaller samples dictated the use of a different plasma chemistry.

Similar investigations with a 2 sccm BCl_3 and 18 sccm Cl_2 chemistry revealed that the Ga signals were much larger than in the Cl_2/Ar chemistry for the same sample size. This is illustrated in Figure 2. As such, the BCl_3/Cl_2 chemistry was employed for the remaining experiments, as described below.

There were 2 different sample types used for these experiments, namely, a 1 μm thick GaN(0001) film on a 1000Å AlN(0001) buffer layer previously deposited on a 6H-SiC(0001) substrate and the GaN/AlN multilayer structure shown Figure 3. The decrease in thickness of the AlN layers from 500 Å to 50 Å was used to determine the sensitivity of this technique to the onset and completion of the etching of this material. The surface areas of both samples were approximately 1 cm^2 which were much smaller than would be used in a typical commercial environment. The two Ga signals and the two Al signals

noted above were monitored during etching. Spectra for GaCl and AlCl were also present; however, their intensities were much lower than the Ga and Al signals. The flow rates of BCl_3 and Cl_2 were 2 sccm and 18 sccm, respectively, at a total pressure of 2 mTorr. The plasma power and substrate DC bias were 600 W and –150 V, respectively. The etch rates under these conditions for GaN and AlN were 9500Å/min and 5000 Å/min, respectively.

The initial experiment was performed using the 1 μm GaN/1000Å AlN/SiC sample. The intensities of the 417 and 309 nm wavelengths for Ga and Al, respectively, were monitored as a function of time. The results are shown in Figure 4. The sharp increase of the signals at ~25 seconds was a result of the initiation of the DC bias. The 309 nm Al signal increased upon initiation of the etching due to the use of a partially worn anodized aluminum sample holder. The spectrum in Figure 2 was taken with a new sample holder which resulted in a minimal Al signal. The harsh environment caused a high rate of wear of the holders. The transition from the GaN layer to the AlN layer was easily detected by the OES and was sufficiently sharp to be resolved above the background such that the operator could detect it and react accordingly with minimal hesitation. The 417 nm Ga signal was clearly the preferred indicator, as the intensity of the signal from the Al atoms of the sample holder disallowed the detection of those from the AlN.

The AlN/GaN multilayer structure was subsequently etched. Both the Ga and the Al wavelengths were examined. As shown in Figure 5, the 417 nm and the 309 nm signals were again the most intense for the GaN and the AlN, respectively. As before, the latter was dominated by the signal from the sample holder; the 417 nm signal was used for the diagnostics. The sensitivity setting of the OES was increased due to the thinness of the layers investigated. Thus, the intensities of these spectra were much higher than those of the previous sample as revealed by the comparison of Figures 4 and 5. Increasing the sensitivity increased the integration time of the signal, which, in turn, decreased the number of data points per second. The onset and completion of etching of the 100, 250, and 500 Å layers of AlN were clearly detected. Note the correspondence among the layers illustrated in Figure 3 and those labeled in Figure 5. The 50 Å thick layer was not as easily discerned from the noise as the other AlN layers; however, it was detected.

With further optimization of this technique it should be possible to clearly detect this thin AlN layer.

One aspect that was not examined was the response time of this etch stop technique. Ideally the transition from the GaN to the AlN would occur when the Ga signal begins to decline. Due to the lack of *in situ* surface analysis techniques such as XPS or Auger spectroscopy, it is not known if this was the case. Initiation of the DC bias caused the Ga signal to rise immediately. There was some lag time between the two events; however, it was sufficiently small that detection by the operator was difficult. Similarly, the time interval between switching off the DC bias and the drop in Ga signal was not easily detected. Similar application of the OES may also work when etching between any two of the III-Nitrides.

It may be possible to combine the OES technique with the previously mentioned DC bias selectivity technique to increase the sensitivity of this etch stop method. Significant selectivity between GaN and AlN, using BCl_3/Cl_2 as the process gases, would make the dips in the Ga signal deeper and easier to detect; thus, the time required to stop the process when the desired layer is reached would be reduced. Preliminary observations by the authors have shown that the etch rates of AlN increased significantly with the addition of BCl_3 to the Cl_2; thus, the selectivity between the GaN and AlN was decreased. Additional experiments using the DC bias technique alone and in tandem with the OES must be performed to determine the parameters that produce the highest selectivity.

Assuming high selectivity is not possible when employing the above chemistry, the process must be optimized to enhance the detection of very thin layers. The goal of optimization would be (1) to deepen and widen the dips in the Ga signal that represent the onset of AlN etching, and (2) to make the transitions as sharp as possible. A wider dip allows the operator more time to stop the etch at the beginning of the desired layer without considerable etching into this layer. This could be accomplished by decreasing the etch rate of the GaN and AlN by lowering the DC bias. This may also decrease the depth of the dips; however, this should be minimal in large samples. Increasing the sample size should offset the loss of Ga atoms entering the gas phase resulting from the decrease in the etch rate. Varying the exposure time of the sample to the etching gas via changes in the total gas flow may decrease the time required for the Ga signal to either

decrease into the dip or rise to a maximum. This decrease in time may make it easier to detect the transition from one material to the other.

In summary, the detection of the transition between GaN and AlN during etching has been achieved using an optical emission spectrometer. Monitoring the 417 nm Ga emission line allowed the detection of this transition via the sharp increase or decrease of this signal. The onset of the etching of AlN layers as thin as 50 Å were detected. Optimization of this approach as an etch stop technique may allow the operator to stop the etching at these very thin layers. Optimization studies should include variations in the sample size, etch rates, residency time, and adjustments in the spectrometer sensitivity.

This work was supported by the Office of Naval Research under contract No. N00014-96-1-0765. Scott A. Smith wishes to acknowledge the U.S. Air Force PALACE Knight program.

1. S. J. Pearton, C. Kuo, MRS Bulletin **22**, 17 (1997).

2. M. P. Mack, A. C. Abare, M. Hansen, P. Kozodoy, S. Keller, U. Mishra, L. A. Coldren, and S. P. DenBaars, J. of Crystal Growth **189**, 837 (1998).

3. J. C. Zolper and R. J. Shul, MRS Bulletin **22**, 17 (1997).

4. R. J. Shul, G. B. McClellan, S. A. Casalnuovo, D. J. Rieger, S. J. Pearton, C. Constantine, C. Barratt, R. F. Karlicek, Jr., C. Tran, and M. Shurman, Appl. Phys. Lett. **69,** 1119 (1996).

5. J. W. Lee, C. B. Vartuli, C. R. Abernathy, J. D. MacKenzie, J. R. Mileham, S. J. Pearton, R. J. Shul, J. C. Zolper, M. Hagerott-Crawford, J. M. Zavada, R. G. Wilson, and R. N. Schwartz, J. Vac. Sci. Technol. B **14**, 3637 (1996).

6. H. Cho, S. M. Donovan, J. D. MacKenzie, C. R. Abernathy, S. J. Pearton, J. Han, R. J. Shul, and J. W. Lee, Solid-State Electr., **42**, 1719 (1998).

7. S. A. Smith, C. A. Wolden, M. D. Bremser, A. D. Hanser, R. F. Davis, and W. V. Lampert, Appl. Phys. Lett. **71,** 3631 (1997).

8. S. A. Smith, W. V. Lampert, P. Rajagopal, A. D. Banks, D. Thomson, and R. F. Davis, to be published.

9. D. L. Melville, J. Budinavicius, D. A. Thompson, and J. G. Simmons, Nucl. Instr. And Meth. In Phys. Res. B **106**, 179 (1995).

10. S. J. Pearton, F. Ren, C. R. Abernathy, and C. Constantine, Mater. Sci. and Engr. **B23**, 36 (1994).

11. S. Thomas III, H. H. Chen, C. K. Hanish, J. W. Grizzle, and S. W. Pang, J. Vac. Sci. Technol. B **14**, 2531 (1996).

12. P. Collot, T. Diallo, and J. Canteloup, J. Vac. Sci. Technol. B **9**, 2497 (1991).

13. C. M. Balkas, C. Basceri, and R. F. Davis, Powder Diffraction **10**, 266 (1995).

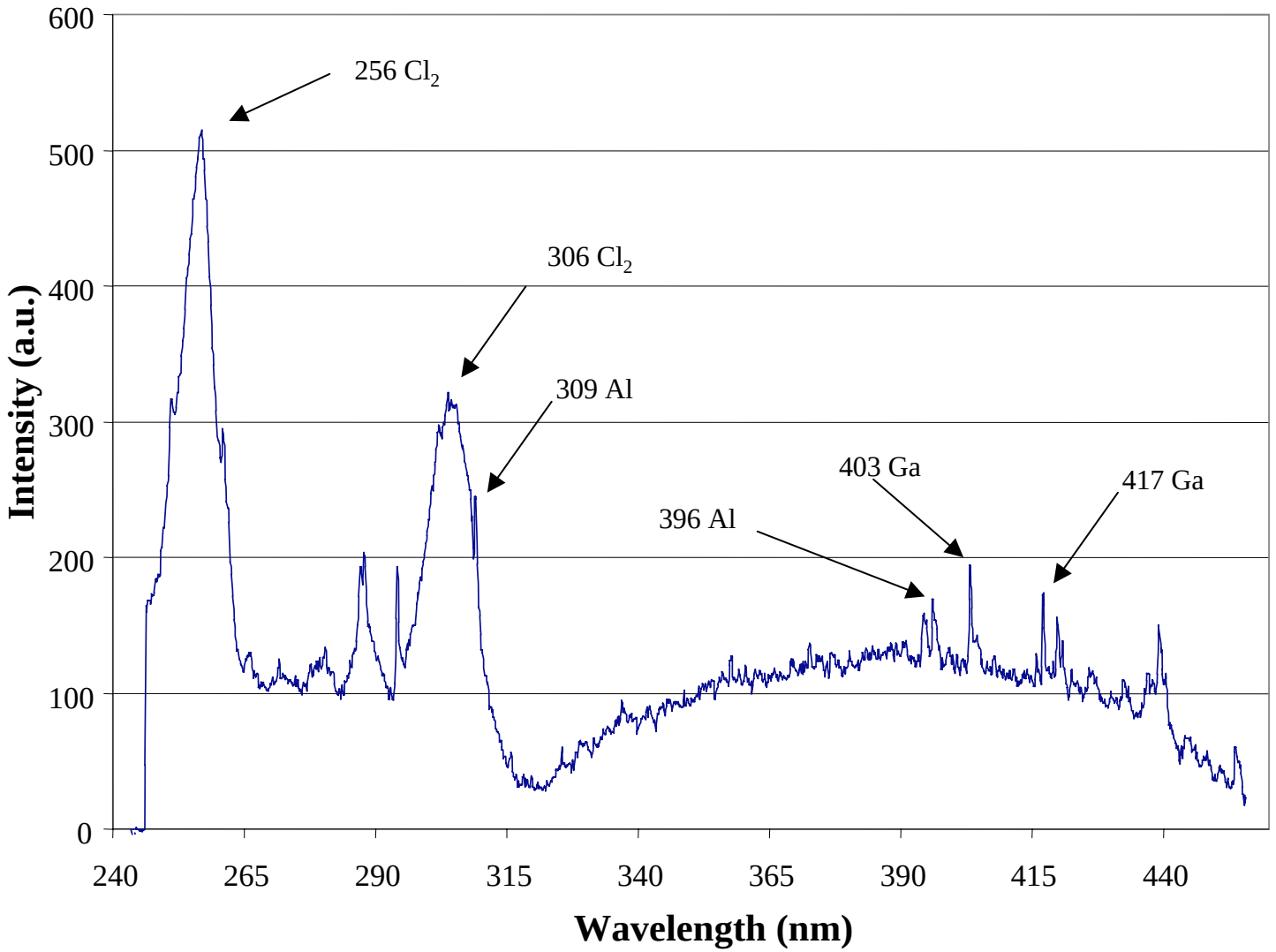

Figure 1. Optical emission spectra obtained during the etching of GaN using a Cl_2/Ar chemistry. The gas flow rates were 20 sccm Cl_2 and 5 sccm Ar.

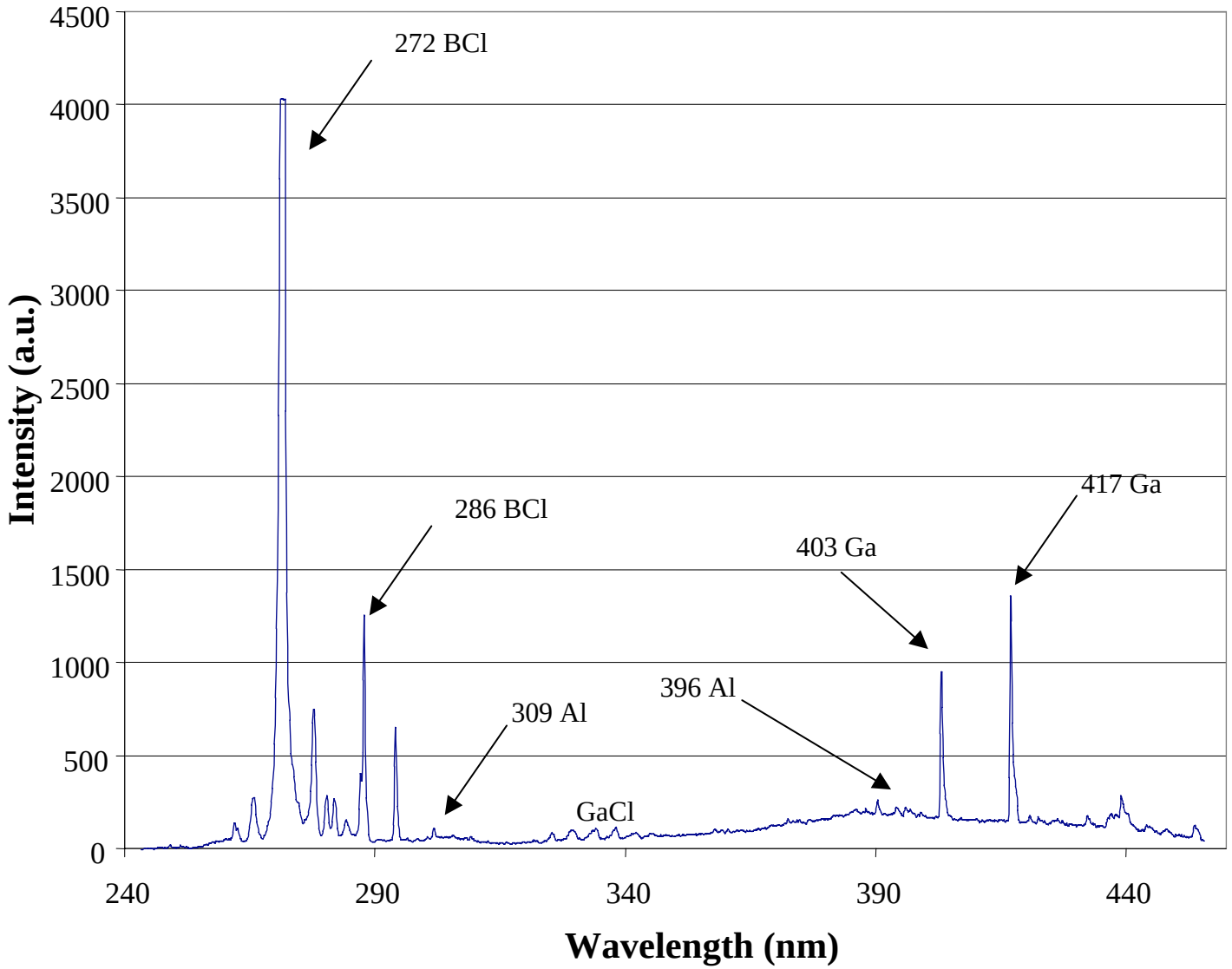

Figure 2. Optical emission spectra obtained during the etching of GaN using a BCl_3/Cl_2chemistry. The gas flows were 2 sccm BCl_3 and 18 sccm Cl_2.

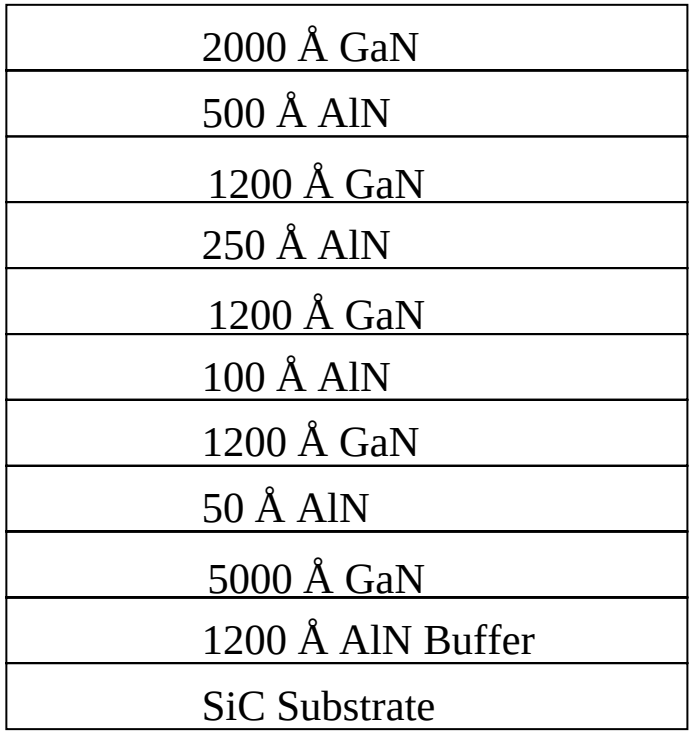

Figure 3. Multilayer structure used to demonstrate the sensitivity of the OES to the onset and completion of etching of thin AlN layers.

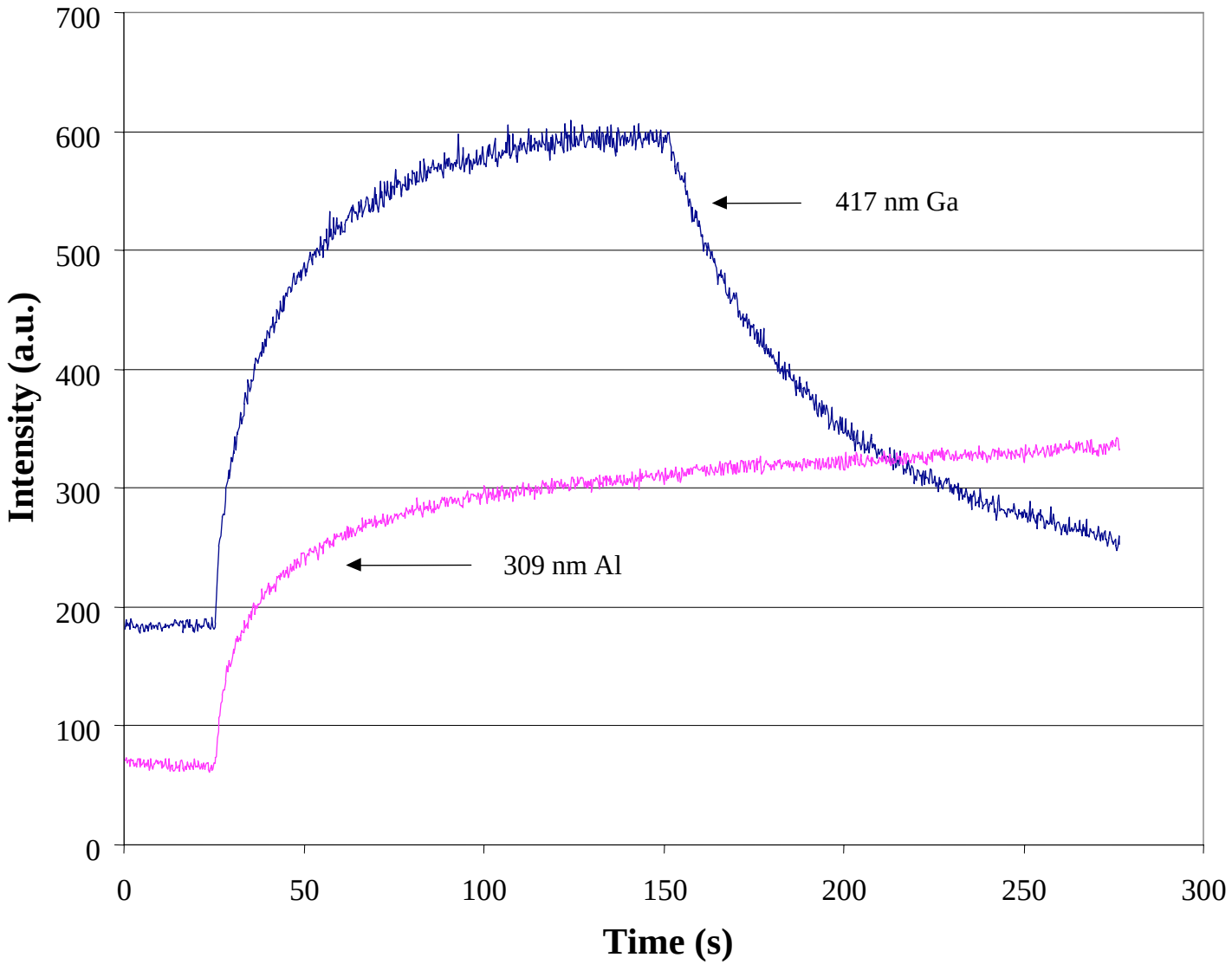

Figure 4. Optical emission spectra showing the transition at ~150 seconds from GaN to AlN during etching using the 417 nm wavelength of Ga. The Al signal is from the anodized Al sample holder.

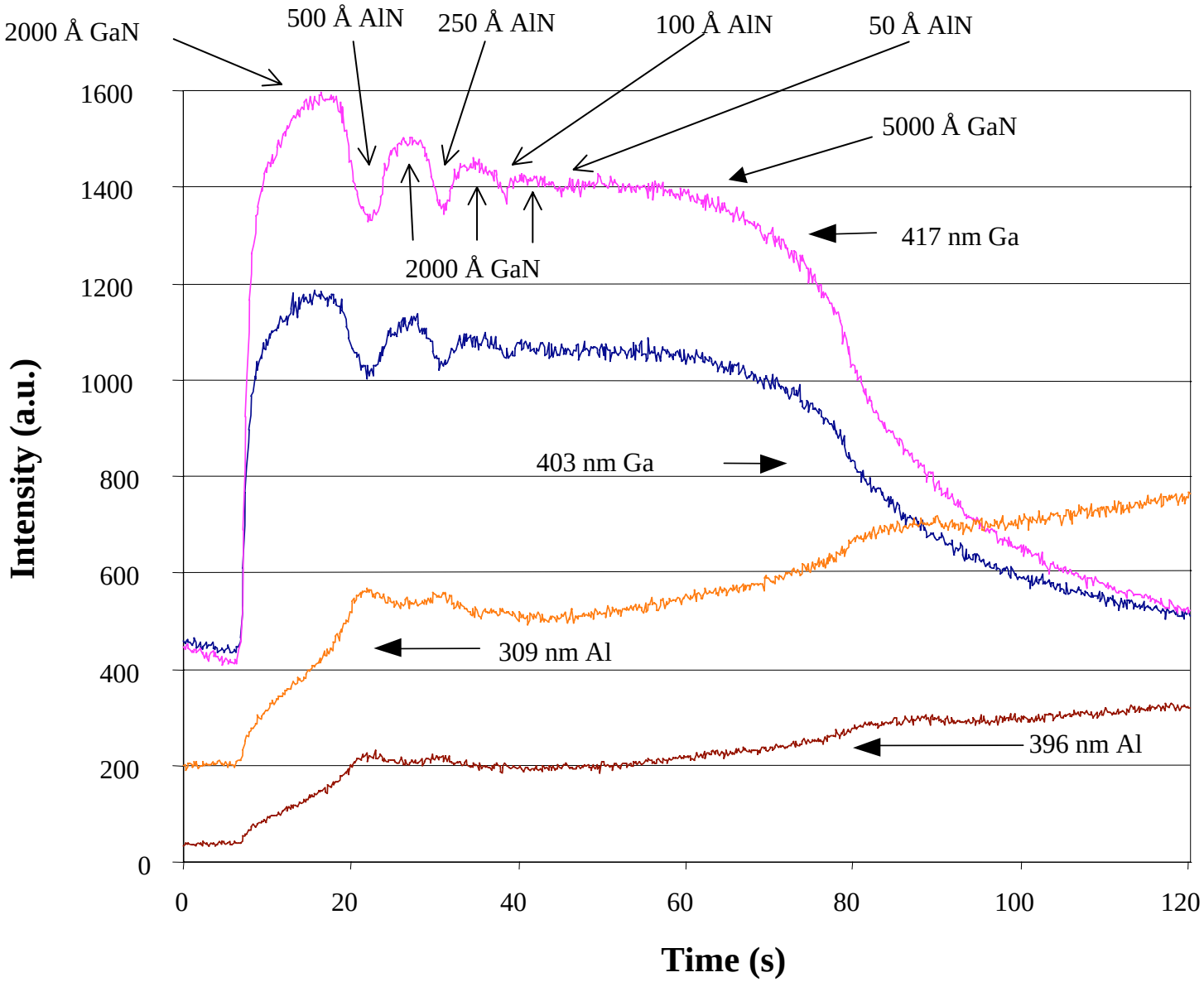

Figure 5. Optical emission spectra of the multilayer structure from Figure 3 during etching. The Al signal is from the anodized Al sample holder.

APPENDICES

APPENDIX 1

ICP Manual

APPENDIX 1

Below is the operation manual for the ICP etching system. It goes through the general procedures and assumes the operator already knows how to use each piece of equipment (MFC controller, RF sources, pressure readouts, etc.). If you do not know how to operate each component then it is strongly advised you read the owners manual for each one.

1. Check water-cooling

1.1. Check to insure water re-circulators are running and full.

1.2. Chillers 1 & 2 should be set to 16 °C. Chiller 2 can be set anywhere between 15 and 25 °C depending on what kind of mask is to be used (e.g.: 25 °C for Ni and 15-20 °C for photoresist mask) or depending on length of the etch run.

1.3. The water level should be approximately 1" from the top of the bath.

1.4. Feel the cooling lines going to the lip in the ICP well and into the ICP matching network. The lines should feel cool. **Do not operate the plasma source if either of these lines feel warm.**

1.5. Chiller 3 does not need to be filled because it uses ethylene glycol.

2. Check exhaust

Check to make sure that the exhaust system is functioning by opening the gas cabinet and feeling the exhaust line. The roughing pump backing the process turbomolecular pump (TMP) and the gas cabinets are vented to the exhaust system. So, if the exhaust system is not working for some reason **do not perform etching until the problem is solved** (as this means that the process gasses will be vented to the lab).

3. Check compressed air supply line

The gauge for the compressed air can be found on top of the gas cabinet. This should read above 60 psi. This is the air supply that is used to operate the pneumatic valves controlling the gas lines.

4. Open gas lines

Open all gas bottles that will be used. The nitrogen bottle by the power lines should also be opened. This bottle is for purging the TMP and the roughing pump during processing. The Cl_2 bottle can be opened to charge the line and then closed. Since the Cl_2 flows are so low, this charge should last all day. Monitor the line pressure in the gas cabinet. If it gets too low (<7 psi) recharge the Cl_2 line. The same is true for the oxygen and BCl_3 lines but these tend to be consumed in lower amounts.

5. Sample cleaning

5.1. Dip the samples in acetone to clean off any grease. Rub with soft cotton swab in the acetone if necessary.

5.2. Remove the sample and spray with methanol while holding over a beaker. The methanol leaves less of a residue than the acetone does when dried.

5.3. Once the sample has been dried, place into beaker of HCl for 5 minutes to remove any oxygen or carbon contaminants.

5.4. The sample can be also be sputter cleaned for 4 seconds at 600W-400V-3mTorr to clean the surface of any debris that could lead to micro-masking.

6. Sample carrier removal

6.1. In order to remove the sample carrier the loadlock must be brought up to atmospheric pressure. Ensure that the valve between the loadlock and the etch chamber is closed, then close the valve between the loadlock and the TMP.

6.2. Unfasten the handle to the loadlock door, and then open the bleed valve from the nitrogen bottle. The door to the loadlock will open when atmospheric pressure is reached.

6.3. Wearing rubber gloves, remove the sample carrier and place on the holder.

7. Mounting the sample on the sample carrier

7.1. Put a *small amount* of vacuum grease on the sample carrier to help hold the sample. Vacuum grease is used because it works fairly well as a thermal conductor and is easily removed with acetone and a cotton swab.

7.2. Mount the sample to the carrier.

8. **Inserting sample carrier into loadlock**

8.1. If the loadlock is under vacuum, follow the procedures in step 6 to bring it up to atmospheric pressure.

8.2. Once at atmospheric pressure, open the loadlock door and insert sample carrier. Align the grooves on the sides of the sample carrier to the fork and slide it on until the carrier touches the base of the fork. The threaded stem of the sample carrier contains a pin going through its diameter. This pin must aligned along the magnetic arm to help fit in the sample stage. Close the door to the loadlock.

9. **Pumping down the loadlock**

9.1. Close the valve between the loadlock roughing pump and TMP.

9.2. Open the valve between the roughing pump and the loadlock for about 10 seconds and close it. This lowers the pressure of the loadlock to about 10^{-3} Torr.

9.3. Open the valve between the loadlock roughing pump and the TMP (for the loadlock) followed by the gate-valve between the TMP and the loadlock. This will reach the desired pressure in about 15 minutes.

10. **Transferring the sample carrier to the etch chamber**

10.1. The sample carrier can be transferred to the etch chamber only when the pressure in the loadlock reaches between 2 and $4*10^{-6}$ Torr or lower. Once the pressure in the loadlock has reached this range of pressure, it is safe to open the gate valve to the chamber.

10.2. Once the gate valve to the chamber is open, slowly slide the transfer arm until the sample carrier is over the sample stage. Make sure the stem on the sample carrier is directly over the hole in the sample stage.

10.3. Raise the sample stage until the stem goes into the hole in the sample stage. The stem should go in far enough so that the pin is down in the hole as well.

10.4. Slide the transfer arm all the way out of the chamber and close the gate valve between the chamber and loadlock.

10.5. Rotate the rotary feed-through on the bottom of the z-stage clockwise until the sample carrier is snug against the sample stage.

11. **Sample level**

The sample stage is currently at the loadlock level. For processing, the sample stage must be raised into the process zone. The counter on the z-stage controller is at 77,500 when at the process level.

12. **Flowing gasses**

12.1. Before flowing any gasses the gate valve in front of the cold cathode gauge must be closed. The capacitance manometer located next to the cold cathode gauge measures the process pressure.

12.2. Open the applicable pneumatic valves using the switches located next to the TMP controllers in the component rack.

12.3. Set the desired operating pressure on the MKS pressure controller.

12.4. Set the appropriate gas flows on the MFC controller.

12.5. Start the gasses.

13. **Starting inductive plasma**

13.1. Before starting the plasma you must insure the chamber pressure $>5*10^{-4}$ Torr. Any less and there may be damage to the matching network and RF source.

13.2. Set the desired power on the RF20S front panel. If it is more than 300 watts, set the ICP power at 300 watts and start the plasma. Allow the ICP matching network to match the impedance of the load to the impedance of the RF source (50 Ohms). Then ramp up the plasma in intervals of not more than 100 watts until the desired power is reached, making sure that the reflected power is always lowered before ramping up any further.

14. **Starting the DC bias**

14.1. The DC bias can be started as soon as the pressure, the rf power and the gas flows are stabilized. The DC bias typically initiates the etching of the sample, so starting the DC bias is also time zero for the etching. Visually check all the other parameters including stopwatch time before starting the DC bias. Also, do not ramp the bias value – set the required value and hit the on button.

14.2. After switching on the dc bias, keep your left hand on the DC bias matching network panel and be ready to adjust the setting to ensure that the reflected power is very low (0-2watts). The rule of thumb is that if the set bias is larger than previous value, then go to the right (and go the left for a lower value). Start the timer only when the actual bias value approaches the set value.

15. **After etching**

15.1 As soon as the etching is completed, switch off the DC bias.

15.2 Ramp down the ICP power until it is around 300 W and then turn it off.

15.3 Turn off the gas flow to the chamber via the MFC controller.

15.4 Set the throttle valve to the open position in the pressure controller. Wait for a few seconds, and turn off the pneumatic valves for all the gasses - leave the purge line on).

15.5 Lower the sample stage to the transfer height (~23,500 units on the z-stage controller).

15.6 Make sure that the pressure in the main chamber is close to the pressure in the loadlock. The purging of the TMP with nitrogen raises the base pressure to around 1.5 e-5 torr or lower. Once this pressure is reached, (preferably lower), the gate valve between the etch chamber and loadlock may be opened.

15.7 Turn the rotary feedthrough counter-clockwise about six or seven times to partially unscrew the sample carrier from the sample stage.

15.8 Slide the magnetic transfer arm to grab the sample carrier using the fork at the end of the arm. Make sure that the fork is fully inserted into the carrier. Do not use unnecessary force.

15.9 Once the carrier is secured by the arm, unscrew the carrier from the stage completely using the rotary feed-through at the bottom. (you will feel the threads slipping when you completely unscrew). Again, do not use force, as not all parts are metal, and most of them are hard to access.

15.10 Lower the stage and wiggle the arm to free it from the stage. Once the carrier clears the stage, slowly and gently slide the arm out of the etch chamber.

15.11 Close the gate valve between the etch chamber and loadlock.

15.12 Now follow section 6 to bring the loadlock up to atmospheric pressure and remove the sample carrier.

15.13 If another sample is not going to be loaded, then insert the carrier and pump down the loadlock as if a sample was loaded. The loadlock pumps down much faster if the carrier has been in vacuum.

16. **Shut Down**

When shutting down for the day the only thing that must be done is to turn off the purge nitrogen. Leaving this on overnight will drain the tank. Everything else gets completed in section 15.

APPENDIX 2

Unpublished Data

APPENDIX 2

This appendix contains data that was taken but not included in this thesis.

Figures 1 and 2 are measurements of the relative Cl radical density, the ion density, and the etch rate of GaN all normalized to 1. These experiments are similar to the ones performed in Paper 5, with the difference being the chemistry was BCl_3/Cl_2 as opposed to Cl_2/Ar. Further studies involving the variation of BCl_3 concentration in Cl_2 need to be performed.

Figures 3 through 5 are OES spectra of GaN etching taken for three different chemistries with and without ion bombardment. The chemistries were Cl_2 alone, BCl_3 alone, and a combination of BCl_3 and Cl_2. The data was taken to observe if any differences in the spectra reveal what role the BCl_3 plays in GaN etching. The BCl_3 appears to have a memory effect because a BCl_3 was seen for the Cl_2 chemistry.

Etch induced damage was also examined using Schottky contacts. Due to cleaning problems the data was no good. The leakage current for the control samples was too high to get any useful data. The cleaning step need to be performed without annealing. Elevating temperatures for cleaning has the potential to anneal out ion induced damage. Cleaning issues need to be resolved before a true measure of the induced damage can be determined.

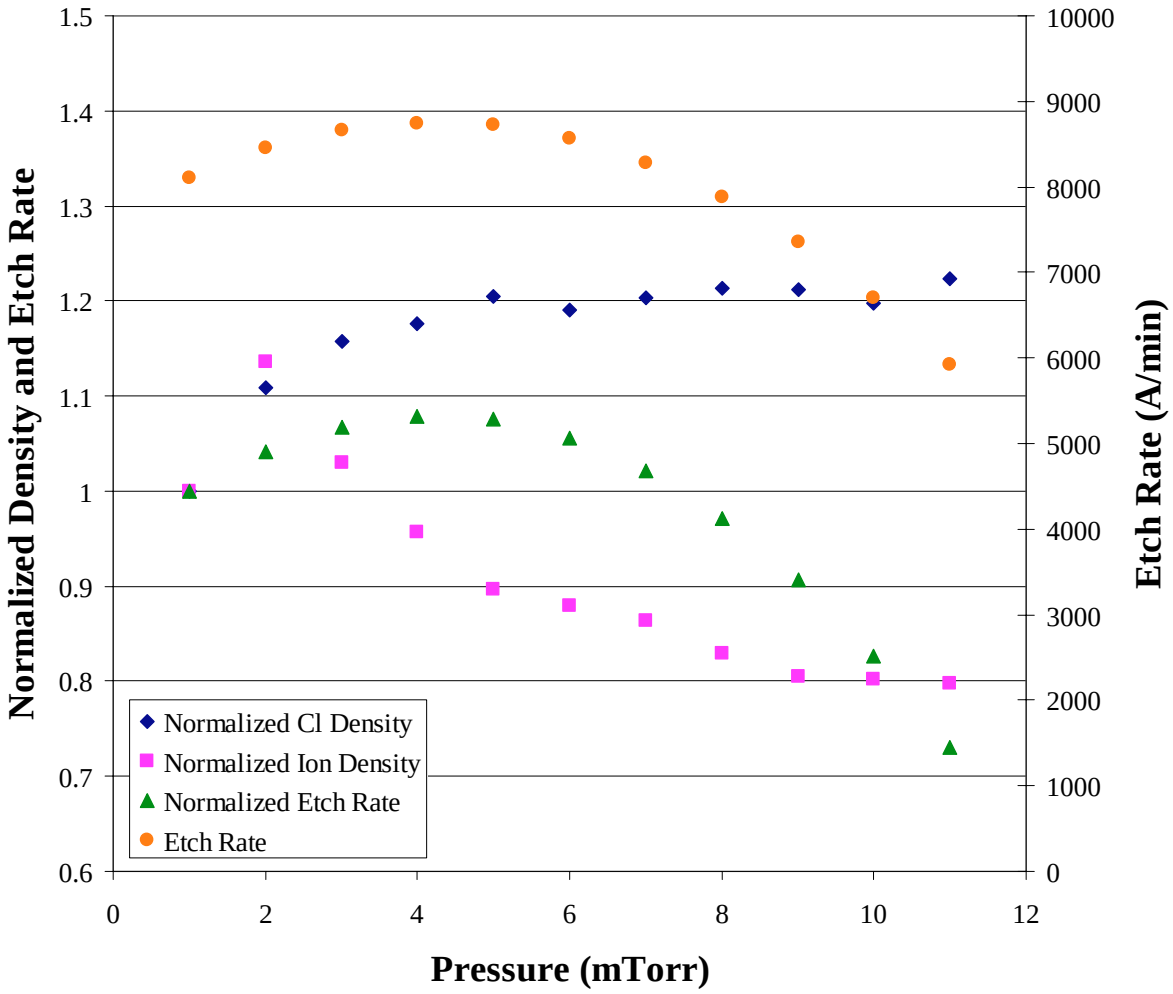

Figure 1. Comparison of the ion density, Cl radical density, and the etch rate as functions of pressure.

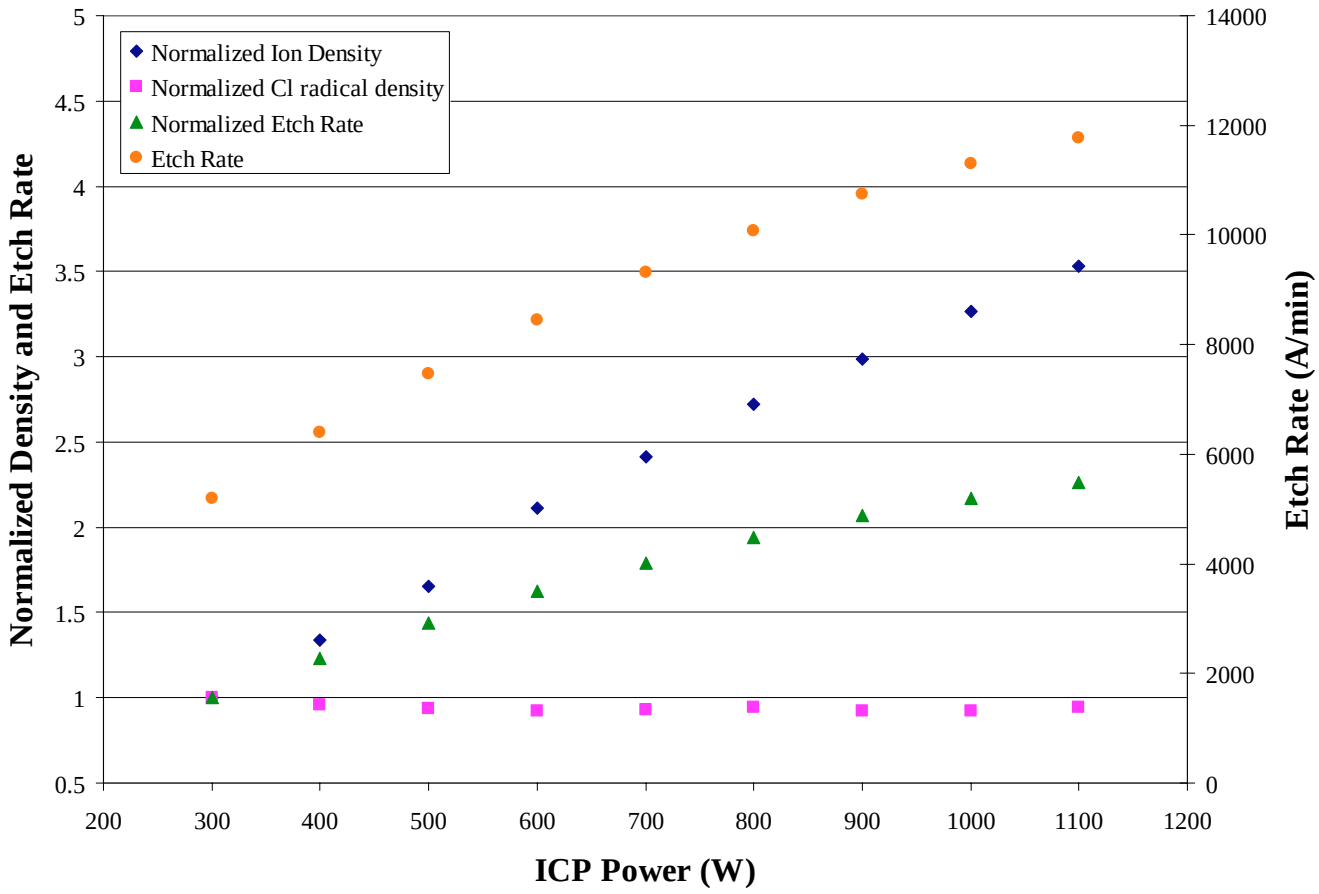

Figure 2. Comparison of the ion density, Cl radical density, and the etch rate as functions of the ICP power.

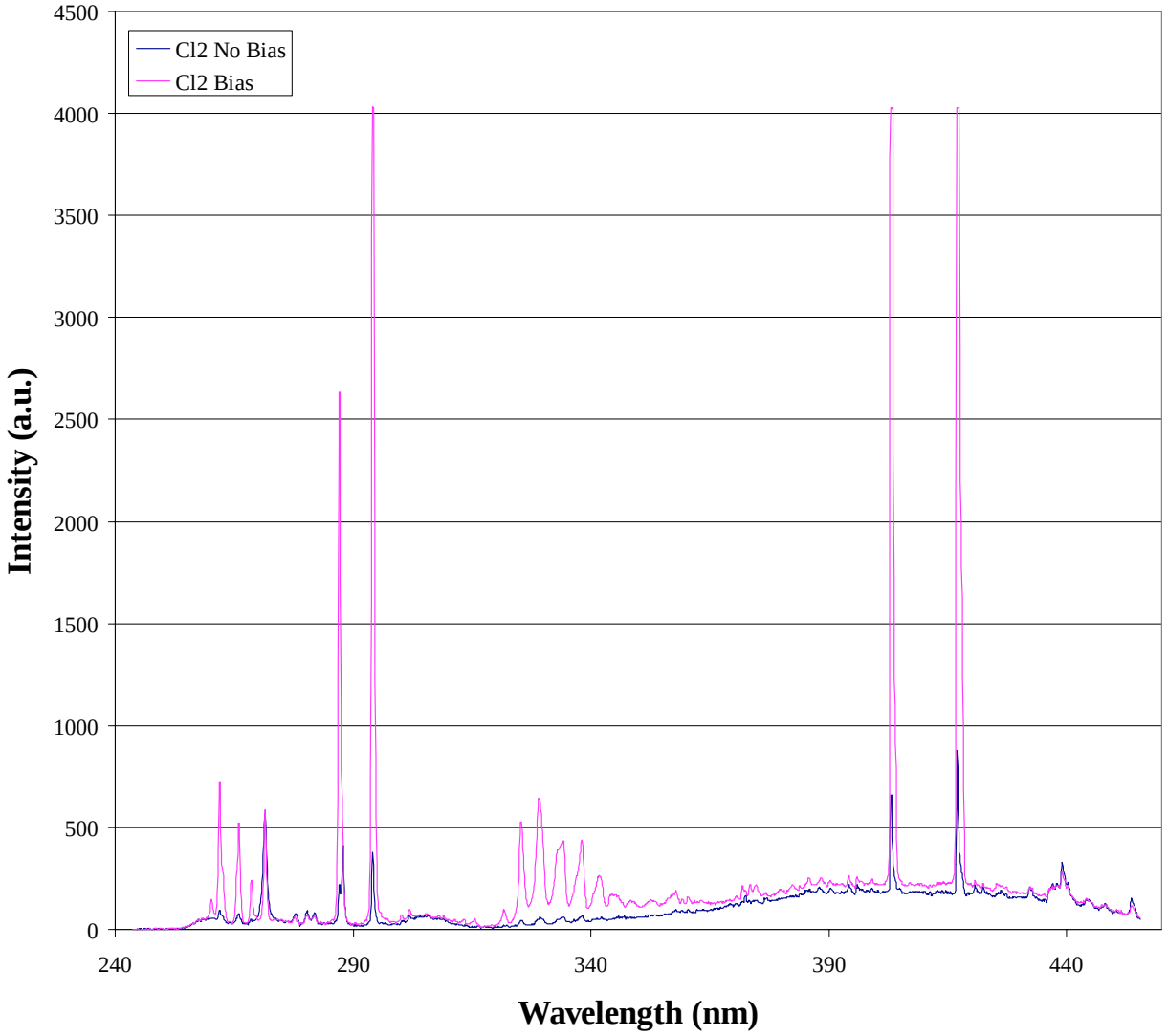

Figure 3. Optical emission spectra of GaN etched in Cl_2.

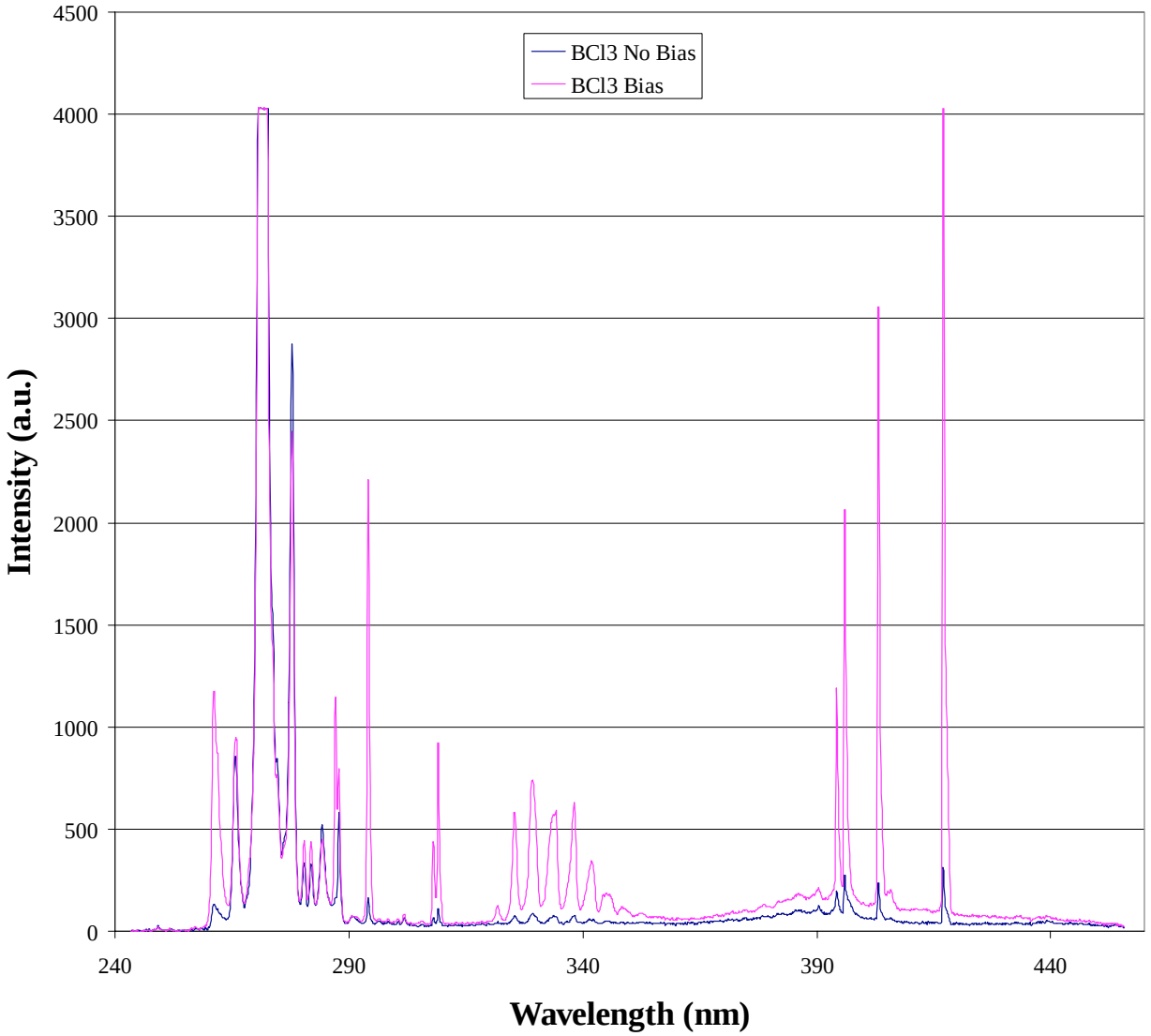

Figure 4. Optical emission spectra of GaN etched in BCl_3.

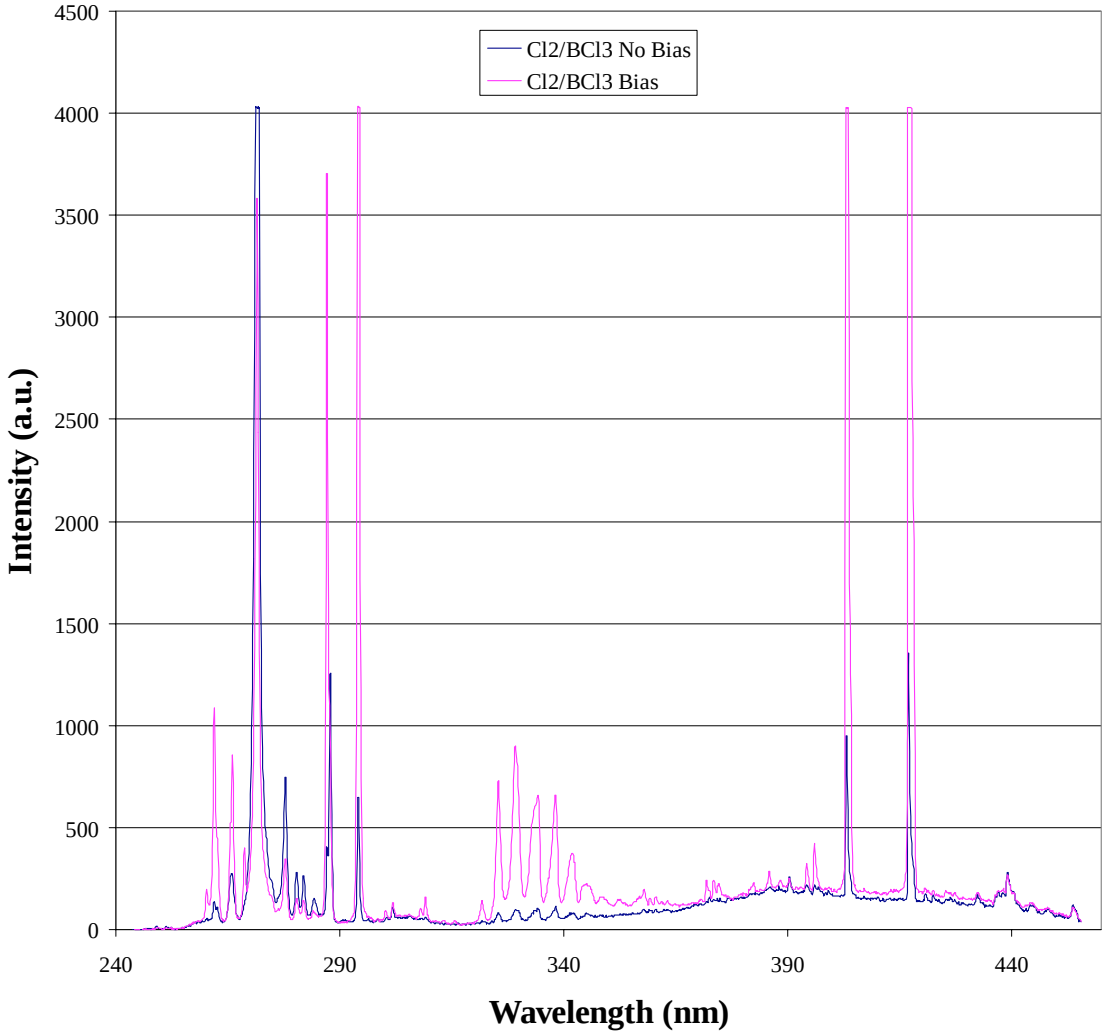

Figure 5. Optical emission spectra of GaN etched in BCl_3/Cl_2.